

**An-Najah National University**

**Faculty of Graduate studies**

**Optimization of Adsorption of  
Tetracycline as Water Contaminant  
onto Solid Supported ZnO Systems  
Using Point of Zero Charge**

**By**

**Rola Fathi Mohammed Tweir**

**Supervisor**

**Prof. Hikmat Hilal**

**Co-Supervisor**

**Dr. Ahed Zyoud**

**This Thesis is Submitted in Partial Fulfillment of the Requirements for  
the Degree of Master of Chemistry, Faculty of Graduate Studies, An-  
Najah National University, Nablus, Palestine.**

**2020**

**Optimization of Adsorption of Tetracycline as Water Contaminant onto Solid Supported ZnO Systems Using Point of Zero Charge**

**By**

**Rola Fathi Mohammed Tweir**

**This Thesis was defended successfully on 3 / 9 /2020, and approved by:**

**Defense Committee Members**

**Signature**

- |   |       |
|---|-------|
| <b>– Prof. Hikmat Hilal / Supervisor</b>      | ..... |
| <b>– Dr. Ahed Zyoud / Co-supervisor</b>       | ..... |
| <b>– Dr. Shaher Zyoud / External Examiner</b> | ..... |
| <b>– Dr. Nidal Zatar / Internal Examiner</b>  | ..... |

### III

## **Dedication**

I dedicate this thesis to everyone who cares about the environment and works to save it.

To everyone who inspires me by his/her science.

To my wonderful parents, my sisters and brothers and my lovely husband for their love, unfailing support and continuous encouragement throughout my life.

## **Acknowledgments**

After thanking Allah, who granted me the ability to finish this work, I would like to express my sincere gratitude to my thesis supervisors: Prof. Hikmat Hilal for all his guidance, understanding, support and sound advice in all aspects of my research work and Dr. Ahed Zyoud for his scientific support, encouragement, guidance and constructive advice. I would like to. I appreciate help and support from members of the Chemistry Department at An-Najah National University especially laboratory technicians, in particular Mr. Nafiz Dweikat. My warm thanks to my dear friends for all their support, motivation and help, especially Dr. Heba Nassar. Parents (Eng. Fathi Tweir and Muna AL-haj Hassan), my sisters (Dr. Hadeel and Eng. Raghad) and brothers (Mohammed, Eng. Moath, Eng. Moatasem and Eng. Mujahed), thank you for being a great source of support, love and encouragement which have always carried me through the way. Finally, my greatest gratitude to my husband Mohammed Foqha for his care and unreserved support which gave me the courage and confidence that I need in my life.

I would like to express my gratitude for everyone who helped me in this research.

Besides my advisor, I would like to show my greatest appreciation to the lab technicians at the Department of Chemistry for their support and skilful technical assistance.

## الإقرار

أنا الموقعة أدناه مقدمة الرسالة التي تحمل العنوان:

### **Optimization of Adsorption of Tetracycline as Water Contaminant onto Solid Supported ZnO Systems Using Point of Zero Charge**

أقر بأن ما اشتملت عليه هذه الرسالة إنما هي من نتاج جهدي الخاص باستثناء ما تمت الإشارة إليه حيثما ورد، وأن هذه الرسالة ككل، أو أي جزء منها لم يقدم من قبل لنيل أية درجة علمية أو بحثية لدى أية مؤسسة تعليمية أو بحثية أخرى.

### **Declaration**

The work provided in this thesis, unless otherwise referenced is my own research work and has not been submitted elsewhere for any other degree or qualification.

**Student's Name:**

اسم الطالبة: رولا فتحي محمد طوير

**Signature:**

التوقيع:

**Date:**

التاريخ: 2020/9/3

## List of contents

No.	Subject	Page
	Dedication	III
	Acknowledgment	IV
	Declaration	V
	List of Contents	VI
	List of Tables	VIII
	List of Figures	IX
	List of Abbreviations	XV
	Abstract	XVI
	<b>Chapter one: Introduction</b>	1
1.1	Overview	1
1.2	Tetracycline	2
1.3	Adsorption	5
1.3.1	Definitions	5
1.3.2	Features of Adsorption	6
1.3.3	Adsorbents used for TC removal from water	6
1.4	Zinc Oxide	7
1.5	Clay	8
1.5.1	Structure of the clay minerals	8
1.5.2	Adsorption on clays	10
1.6	Montmorillonite	11
1.7	Kaolinite	13
1.8	Composite materials	14
1.9	Zero charge point	15
1.10	Objectives	16
1.11	Novelty of this work	17
	<b>Chapter Two: Material and Methods</b>	19
2.1	Chemicals and reagents	19
2.2	Equipment	19
2.3	Preparation of solutions	20
2.3.1	Stock solutions	20
2.3.2	Other solutions	20
2.4	Adsorbent preparation	21
2.4.1	ZnO nanoparticles supported on Montmorillonite or Kaolinite clay	21
2.5	Adsorption experiments	21
2.5.1	Effect of adsorbent type	22
2.5.2	Effect of initial pH	22
2.5.3	Effect of zero charge point	22

2.5.4	Effect of contact time	23
2.5.5	Effect of TC concentration	24
2.5.6	Adsorption isotherm models	24
2.5.6.1	Langmuir adsorption isotherm	25
2.5.6.2	Freundlich adsorption isotherm	26
2.5.7	Adsorption kinetic models	27
2.5.7.1	Pseudo-first-order model	27
2.5.7.2	Pseudo-second-order model	28
2.5.7.3	Intra particle diffusion model	28
2.6	Calibration curve	28
	<b>Chapter Three: Results and Discussion</b>	30
3.1	Catalyst characterization	30
3.1.1	XRD characterization	30
3.1.1.1	XRD pattern for ZnO	30
3.1.1.2	XRD pattern for Montmorillonite	31
3.1.1.3	XRD pattern for Kaolinite	32
3.1.1.4	XRD pattern for ZnO@Montmorillonite	33
3.1.1.5	XRD pattern for ZnO@Kaolinite	34
3.1.2	Scanning Electron Microscopy (SEM)	35
3.1.2.1	SEM result for ZnO	35
3.1.2.2	SEM result for Montmorillonite	36
3.1.2.3	SEM result for Kaolinite	37
3.1.2.4	SEM result for ZnO@Montmorillonite	37
3.1.2.5	SEM result for ZnO@Kaolinite	38
3.2	Tetracycline adsorption experiments	39
3.2.1	Effect of adsorbent type	39
3.2.2	Results of zero charge point	40
3.2.3	Effect of pH	44
3.2.4	Effect of TC concentration	55
3.2.5	Effect of contact time	63
3.2.6	Adsorption isotherm	64
3.2.7	Kinetic of TC adsorption	74
3.3	Adsorption study	83
	Conclusions	85
	Recommendations for future work	87
	References	88
	الملخص	ب

## VIII

**List of Tables**

<b>No.</b>	<b>Subject</b>	<b>Page</b>
2.1	Different concentrations of TC contaminant used for adsorption onto different adsorbents at natural pH.	24
3.1	Zero charge points of different adsorbents measured using pH-drift method	43
3.2	Langmuir and Freundlich isotherm parameters and correlation coefficients for TC adsorption onto different adsorbents.	73
3.3	Pseudo-first-order and pseudo-second-order kinetic model parameters and correlation coefficients for TC adsorption onto different adsorbents	82
3.4	Intra-particle diffusion kinetic model parameters and correlation coefficients for TC adsorption onto different adsorbents	83
3.5	Adsorption capacity of different solid systems in mg/g at different pH values	84

## List of Figures

No.	Figure	Page
1.1	Chemical structures of Tetracyclines: A.Chlorotetracycline, B.Oxytetracycline, C.Tetracycline and D.Demethylchlortetracycline	3
1.2	TC chemical structure with different pKa values	4
1.3	Diagrammatic sketch of the octahedral sheet	10
1.4	Diagrammatic sketch of the tetrahedral sheet	10
2.1	Calibration curve for aqueous TC using UV-Vis spectrophotometry	29
3.1	X-ray diffraction pattern for commercial ZnO powder	31
3.2	X-ray diffraction pattern for Montmorillonite clay	32
3.3	X-ray diffraction pattern for Kaolinite clay	33
3.4	X-ray diffraction pattern for ZnO@Montmorillonite composite	34
3.5	X-ray diffraction pattern for ZnO@Kaolinite composite	35
3.6	Scanning electron micrograph for commercial ZnO	36
3.7	Scanning electron micrograph for Montmorillonite	36
3.8	Scanning electron micrograph for Kaolinite	37
3.9	Scanning electron micrograph for ZnO@Montmorillonite composite	38
3.10	Scanning electron micrograph for ZnO@Kaolinite composite	39
3.11	Effect of adsorbent type on the percentage of TC removal at (initial conc: 100 mg/L, MONT*: 200 mg/L, natl pH, temperature: 25 °C, contact time: 120 min and solid/liquid ratio: 0.1g/ 50 mL)	40
3.12	Plot of $\Delta(pH)$ vs. initial pH for ZnO. Intercept shows value of $pH_{zcp}$ for the solid. Results were made at room temperature	40
3.13	Plot of $\Delta(pH)$ vs. initial pH for MONT. Intercept shows value of $pH_{zcp}$ for the solid. Results were made at room temperature	41
3.14	Plot of $\Delta(pH)$ vs. initial pH for KANT. Intercept shows value of $pH_{zcp}$ for the solid. Results were made at room temperature	41
3.15	Plot of $\Delta(pH)$ vs. initial pH for ZnO@MONT. Intercept shows value of $pH_{zcp}$ for the solid. Results were made at room temperature	42
3.16	Plot of $\Delta(pH)$ vs. initial pH for ZnO@KANT. Intercept shows value of $pH_{zcp}$ for the solid. Results were made at room temperature	42
3.17	Effect of pH on TC structure	44

3.18	Effect of pH on ZnO structure	45
3.19	Effect of pH on TC percentage removal by adsorption onto ZnO adsorbent. Measurements are made using TC at (initial conc: 100 mg/L, pH range from (3-11), temperature: 25 °C, Contact time: 120 min and solid/liquid ratio: 0.1g/50 mL)	45
3.20	Effect of pH on TC % removal by adsorption onto MONT adsorbent. Measurements are made using TC at (initial conc: 100 mg/L, pH range from (3-11), temperature: 25 °C, Contact time: 120 min and solid/liquid ratio: 0.1g/50 mL)	47
3.21	Effect of pH on TC % removal by adsorption onto MONT adsorbent. Measurements are made using TC at (initial conc: 200 mg/L, pH range from (3-11), temperature: 25 °C, Contact time: 120 min and solid/liquid ratio: 0.1g/50 mL)	49
3.22	Effect of pH on TC % removal by adsorption onto ZnO adsorbent. Measurements are made using TC at (initial conc: 100 mg/L, pH range from (3-11), temperature: 25 °C, Contact time: 120 min and solid/liquid ratio: 0.1g/50 mL)	50
3.23	Effect of pH on the percentage removal by adsorption of TC onto ZnO@MONT adsorbent. Measurements are made using TC at (initial conc: 100 mg/L, pH range from (3-11), temperature: 25 °C, Contact time: 120 min and solid/liquid ratio: 0.1g/50 mL)	51
3.24	Effect of pH on the TC % removal onto ZnO@KANT adsorbent. Measurements are made using TC at (initial conc: 100 mg/L, pH range from (3-11), temperature: 25 °C, Contact time: 120 min and solid/liquid ratio: 0.1g/50 mL)	54
3.25	Effect of TC concentration on its % removal by adsorption onto the surface of ZnO adsorbent. Measurements were made using 100, 130, 160, 190 and 210 mg/L initial TC concentrations, natural pH, room temperature, contact time of 120 min and 0.1 g of ZnO in 50 mL of TC	55
3.26	Effect of TC concentration on its removal amount (mg/L) by adsorption onto the surface of ZnO adsorbent. Measurements were made using 100, 130, 160, 190 and 210 mg/L initial TC concentrations, natural pH, room temperature, contact time of 120 min and 0.1 g/50 mL solid/liquid ratio	56
3.27	Effect of TC concentration on its % removal by adsorption onto the surface of MONT adsorbent.	57

	Measurements were made using 150, 250, 300 and 350 mg/L initial TC concentrations, natural pH, room temperature, 120 min contact time and 0.1 g of MONT in 50 mL of TC	
3.28	Effect of TC concentration on amount of adsorption onto the surface of MONT adsorbent. Measurements were made using 150, 250, 300 and 350 mg/L initial TC concentrations, natural pH, room temperature, 120 min contact time and 0.1 g/50 mL solid/liquid ratio	58
3.29	Effect of TC concentration on its % removal by adsorption onto KANT adsorbent surface. Measurements were made using 20, 40, 60 and 80 mg/L initial TC concentrations, natural pH, room temperature, 120 min contact time and 0.1 g of KANT in 50 mL of TC	59
3.30	Effect of TC concentration on its removal by adsorption onto KANT adsorbent. Measurements were made using 20, 40, 60 and 80 mg/L initial concentrations, natural pH, room temperature, 120 min contact time and solid/liquid ratio of 0.1g/50 mL	60
3.31	Effect of TC concentration on its % removal by adsorption onto the surface of ZnO@MONT adsorbent. Measurements were made using 130, 160, 190 and 210 mg/L initial TC concentrations, natural pH, room temperature, 120 min contact time and 0.1 g of ZnO@MONT in 50 mL of TC	60
3.32	Effect of TC concentration on amount of adsorption onto the surface of ZnO@MONT adsorbent. Measurements were made using 130, 160, 190 and 210 mg/L initial TC concentrations, natural pH, room temperature, 120 min contact time and 0.1 g/50 mL solid/liquid ratio	61
3.33	Effect of TC concentration on its % removal onto the ZnO@KANT adsorbent surface. Measurements were made using 70, 130, 160 and 190 mg/L initial TC concentrations, natural pH, room temperature, 120 min contact time and 0.1 g/50 mL solid/liquid ratio	62
3.34	Effect of TC concentration on its removal amount by adsorption onto the surface of ZnO@KANT adsorbent. Measurements were made using 70, 130, 160 and 190 mg/L initial concentrations, natural pH, room temperature, 120 min contact time and 0.1 g ZnO@KANT in 50 mL TC	63
3.35	Effect of contact time on the % removal of TC by adsorption onto different adsorbents. Measurements were made using initial TC concentration: 100 mg/L, natural pH, room temperature and solid/liquid ratio: 0.1 g/50 mL. For	63

## XII

	MONT, 200 mg/L TC was used	
3.36	Equilibrium adsorption isotherm of TC onto ZnO. Measurements were made using 100, 130, 190 and 210 mg/L initial TC concentrations, room temperature, natural pH, contact time: 120 min and solid/liquid ratio: 0.1 g/50 mL	64
3.37	Equilibrium adsorption isotherm of TC onto MONT. Measurements were made using 150, 250, 300 and 350 mg/L initial TC concentrations, natural pH, contact time: 120 min and solid/liquid ratio: 0.1 g/50 mL	65
3.38	Equilibrium adsorption isotherm of TC onto KANT. Measurements were made using 20, 60 and 80 mg/L initial TC concentrations, room temperature, natural pH, contact time: 120 min and solid/liquid ratio: 0.1 g/50 mL	65
3.39	Equilibrium adsorption isotherm of TC onto ZnO@MONT. Measurements were made using 130, 190 and 210 mg/L initial TC concentrations, room temperature, natural pH, contact time: 120 min and solid/liquid ratio: 0.1 g/50 mL	66
3.40	Equilibrium adsorption isotherm of TC onto ZnO@KANT. Measurements were made using 130, 160 and 190 mg/L initial TC concentrations, room temperature, natural pH, 120 min and solid/liquid ratio: 0.1 g/50 mL	66
3.41	Langmuir plot for TC adsorption onto ZnO. Measurements were made using 100, 130, 190 and 210 mg/L initial TC concentrations, room temperature, natural pH, contact time: 120 min and solid/liquid ratio 0.1 g/50 mL	67
3.42	Langmuir plot for TC adsorption onto MONT. Measurements were made using 150, 250, 300 and 350 mg/L initial TC concentrations, room temperature, natural pH, contact time: 120 min and solid/liquid ratio 0.1 g/50 mL	68
3.43	Langmuir plot for TC adsorption onto KANT. Measurements were made using 20, 60 and 80 mg/L initial TC concentrations, room temperature, natural pH, contact time: 120 min and solid/liquid ratio 0.1 g/50 mL	68
3.44	Langmuir plot for TC adsorption onto ZnO@MONT. Measurements were made using 130, 190 and 210 mg/L initial TC concentrations, room temperature, natural pH, contact time: 120 min and solid/liquid ratio 0.1 g/50 mL	69
3.45	Langmuir plot for TC adsorption onto ZnO@KANT. Measurements were made using 130, 160 and 190 mg/L initial TC concentrations, room temperature, natural pH,	69

## XIII

	contact time: 120 min and solid/liquid ratio 0.1 g/50 mL	
3.46	Freundlich plot for TC adsorption onto ZnO. Measurements were made using 100, 130, 190 and 210 mg/L initial TC concentrations, room temperature, natural pH, contact time: 120 min and solid/liquid ratio 0.1 g/50 mL	70
3.47	Freundlich plot for TC adsorption onto MONT. Measurements were made using 150, 250, 300 and 350 mg/L initial TC concentrations, room temperature, natural pH, contact time: 120 min and solid/liquid ratio 0.1 g/50 mL	70
3.48	Freundlich plot for TC adsorption onto KANT. Measurements were made using 20, 60 and 80 mg/L initial TC concentrations, room temperature, natural pH, contact time: 120 min and solid/liquid ratio 0.1 g/50 mL	71
3.49	Freundlich plot for TC adsorption onto ZnO@MONT. Measurements were made using 130, 190 and 210 mg/L initial TC concentrations, room temperature, natural pH, contact time: 120 min and solid/liquid ratio 0.1 g/50 mL	71
3.50	Freundlich plot for TC adsorption onto ZnO@KANT. Measurements were made using 130, 160 and 190 mg/L initial TC concentrations, room temperature, natural pH, contact time: 120 min and solid/liquid ratio 0.1 g/50 mL	72
3.51	Kinetics of TC adsorption onto ZnO adsorbent according to pseudo-first-order model at (initial concentration: 100 mg/L, contact time: 150 min, natural pH, room temperature and solid/liquid ratio: 0.1g/50 mL)	75
3.52	Kinetics of TC adsorption onto MONT adsorbent according to pseudo-first-order model at (initial concentration: 200 mg/L, contact time: 180 min, natural pH, room temperature and solid/liquid ratio: 0.1g/50 mL)	75
3.53	Kinetics of TC adsorption onto KANT adsorbent according to pseudo-first-order model at (initial concentration: 100 mg/L, contact time: 150 min, natural pH, room temperature and solid/liquid ratio: 0.1g/50 mL)	76
3.54	Kinetics of TC adsorption onto ZnO@MONT adsorbent according to pseudo-first-order model at (initial concentration: 100 mg/L, contact time: 180 min, natural pH, room temperature and solid/liquid ratio: 0.1g/50 mL)	76
3.55	Kinetics of TC adsorption onto ZnO@KANT adsorbent according to pseudo-first-order model at (initial concentration: 100 mg/L, contact time: 180 min, natural pH, room temperature and solid/liquid ratio: 0.1g/50 mL)	77
3.56	Kinetics of TC adsorption onto ZnO adsorbent according to pseudo-second-order model at (initial concentration:	77

	100 mg/L, contact time: 150 min, natural pH, room temperature and solid/liquid ratio: 0.1g/50 mL)	
3.57	Kinetics of TC adsorption onto MONT adsorbent according to pseudo-second-order model at (initial concentration: 200 mg/L, contact time: 180 min, natural pH, room temperature and solid/liquid ratio: 0.1g/50 mL)	78
3.58	Kinetics of TC adsorption onto KANT adsorbent according to pseudo-second-order model at (initial concentration: 100 mg/L, contact time: 180 min, natural pH, room temperature and solid/liquid ratio: 0.1g/50 mL)	78
3.59	Kinetics of TC adsorption onto ZnO@MONT adsorbent according to pseudo-second-order model at (initial concentration: 100 mg/L, contact time: 180 min, natural pH, room temperature and solid/liquid ratio: 0.1g/50 mL)	79
3.60	Kinetics of TC adsorption onto ZnO@KANT adsorbent according to pseudo-second-order model at (initial concentration: 100 mg/L, contact time: 180 min, natural pH, room temperature and solid/liquid ratio: 0.1g/50 mL)	79
3.61	Kinetics of TC adsorption by ZnO adsorbent according to the intra-particle diffusion model at (initial concentration: 100 mg/L, contact time: 150 min, natural pH, room temperature and solid/liquid ratio: 0.1g/50 mL)	80
3.62	Kinetics of TC adsorption by MONT adsorbent according to the intra-particle diffusion model at (initial concentration: 200 mg/L, contact time: 180 min, natural pH, room temperature and solid/liquid ratio: 0.1g/50 mL)	80
3.63	Kinetics of TC removal by KANT adsorbent according to the intra-particle diffusion model at (initial concentration: 100 mg/L, contact time: 150 min, natural pH, room temperature and solid/liquid ratio: 0.1g/50 mL)	81
3.64	Kinetics of TC adsorption by ZnO@MONT adsorbent according to the intra-particle diffusion model at (initial concentration: 100 mg/L, contact time: 180 min, natural pH, room temperature and solid/liquid ratio: 0.1g/50 mL)	81
3.65	Kinetics of TC adsorption onto ZnO@KANT composite adsorbent according to the intra-particle diffusion model at (initial concentration: 100 mg/L, contact time: 180 min, natural pH, room temperature and solid/liquid ratio: 0.1g/50 mL)	82

### List of Abbreviations

<b>Symbol</b>	<b>Abbreviation</b>
<b>MONT</b>	Montmorillonite
<b>KANT</b>	Kaolinite
<b>TC</b>	Tetracycline
<b>XRD</b>	X-Ray Diffraction
<b>SEM</b>	Scanning Electron Microscopy
<b>UV-Vis</b>	Ultraviolet-Visible
<b>ZCP</b>	Zero charge point
<b>rpm</b>	Round per minute
<b>NPs</b>	Nanoparticles
<b>R<sup>2</sup></b>	Correlation coefficient
<b>C<sub>e</sub></b>	Equilibrium concentration of the adsorbate (mg/L)
<b>C<sub>0</sub></b>	Initial concentration of the adsorbate (mg/L)
<b>q<sub>t</sub></b>	Mass of adsorbate per unit mass of adsorbent at time t (mg/g)
<b>Q<sub>0</sub></b>	Adsorption capacity at equilibrium from Langmuir isotherm (mg/g).
<b>q<sub>e</sub></b>	Mass of adsorbate per unit mass of adsorbent at equilibrium (mg/g).
<b>K<sub>F</sub></b>	Freundlich constant related to adsorption capacity (mg/g)
<b>b</b>	Langmuir affinity constant (L/mg)
<b>k<sub>1</sub></b>	Rate constant of the pseudo-first-order model (min <sup>-1</sup> )
<b>k<sub>2</sub></b>	Rate constant of the pseudo-second-order model (min <sup>-1</sup> )
<b>k<sub>p</sub></b>	Rate constant of the intra particle diffusion model (mg/g min <sup>0.5</sup> )
<b>CTC</b>	Chlortetracycline
<b>OTC</b>	Oxytetracycline
<b>DMCTC</b>	Demethylchlorotetracycline

**Optimization of Adsorption of Tetracycline as Water Contaminant  
onto Solid Supported ZnO Systems Using Point of Zero Charge**

**By**

**Rola Fathi Mohammed Tweir**

**Supervisor**

**Prof. Dr. Hikmat S.Hilal**

**Co- Supervisor**

**Dr. Ahed Zyoud**

**Abstract**

Water pollution is a difficult challenge that faces the world nowadays. Pollutions may be caused by pesticides, fertilizers, industrial discharge, domestic waste and pharmaceutical residue. Contamination of surface water by pharmaceuticals is considered a serious environmental threat, which makes their treatment from water a vital issue in researches. Adsorption, a simple, economic, safe and efficient process, is one method used in water treatment. In this work, adsorption of a widely used antibiotic, Tetracycline (TC), was studied using commercial ZnO, Montmorillonite (MONT), Kaolinite (KANT), prepared ZnO@MONT and ZnO@KANT as low-cost, environmentally friendly and effective adsorbents. ZnO nano-sized adsorbent was supported on MONT (a clay with high surface area) and KANT (a clay with good stability) to improve TC adsorption capacity and to facilitate adsorbent recovery from water. Characterization of commercial ZnO, MONT, KANT, prepared ZnO@MONT and ZnO@KANT was made using X-ray diffraction (XRD) and scanning electron microscopy (SEM) equipment. Zero charge point (ZCP) was determined for each adsorbent using pH drift method. Effects of different parameters on the TC adsorption process were studied, such as:

solution pH (3-11 pH range), adsorbent type, contact time and TC concentration. ZCP values were 9.8, 4.5 and 7.5 for commercial ZnO, MONT and KANT, respectively, and 7.2 for the prepared composites (ZnO@MONT and ZnO@KANT). The experimental data showed that MONT is the best adsorbent with maximum adsorption capacity of 125 mg/g at neutral pH following the Freundlich isotherm. KANT and ZnO@MONT also followed the Freundlich isotherm. ZnO and ZnO@KANT followed the Langmuir isotherm. Kinetic study showed that the pseudo-second order model is the most representing model for each adsorbent. Equilibrium adsorption time was ~120 min. The optimum pH range was between (5-7) that gives the best adsorption, affected by the ZCP of each adsorbent and the surface charge of TC at this pH. The opposite charges between adsorbent and adsorbate cause an electrostatic attraction which increase the adsorption capacity. Increasing of TC concentration causes an increase in adsorption.

# Chapter One

## Introduction

### 1.1 Overview

Antibiotics are antimicrobial medicines that are widely used to kill or inhibit the bacterial growth (Danner, Robertson, Behrends, & Reiss, 2019). Antibiotics can be classified into two types depending on their action against bacteria. The first type is called the bacteriostatic antibiotics which cause an inhibition in the bacterial growth. The other type is called the bactericidal antibiotics which can kill the bacteria (Lv et al., 2019). Antibiotics have been used to treat and control the bacterial infections with selective toxicity for bacteria (Han et al., 2019; Lv et al., 2019).

Antibiotics can also be used as a growth foster as they can activate the vitamin production by the microorganisms of the digestive system. In addition to that, they can improve the absorption of the nutrients in intestine (Lv et al., 2019). On the other hand, large use of these drugs may induce an antibiotic resistance by bacteria, which resulted in decreasing of their performance (Han et al., 2019). This increase in antibiotics results in transition of antibiotic to the environment. This is due to compound stability (Danner et al., 2019).

Contamination of the environment (such as soils and natural water) by antibiotics can cause problems. Humans and plants are affected by

antibiotics. For example, Children's hearing is affected. Wheat growth can also be negatively influenced (Han et al., 2019).

Antibiotics may reach water by different paths: Firstly by the waste water remediation factories. Secondly ones are the manufacturers of chemicals. Thirdly, animal cultivation and the rearing of aquatic animals or the husbandry of aquatic plants (Danner et al., 2019). One commonly used antibiotic is Tetracycline.

## **1.2 Tetracycline**

The Tetracyclines, which were made in 1940s, are a family of antibiotics with various compounds (Chopra & Roberts, 2001; Nguyen et al., 2014). Tetracyclines are classified into four types: Chlortetracycline (CTC), Tetracycline (TC), Oxytetracycline (OTC)

("https://www.scripps.edu/baran/images/grpmtgpdf/Lin\_Mar\_05revised.pdf," ; X. Liu et al., 2018) and Demethylchlorotetracycline (DMCTC) ("https://www.scripps.edu/baran/images/grpmtgpdf/Lin\_Mar\_05revised.pdf,"), Figure 1.1.

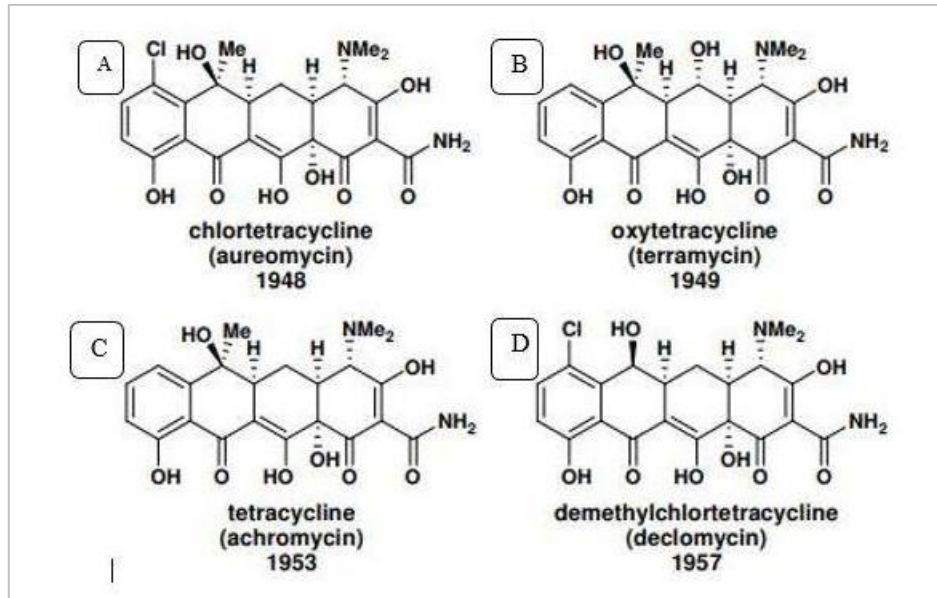


**Figure 1.1:** Chemical structures of Tetracyclines: A.Chlorotetracycline, B.Oxytetracycline, C.Tetracycline and D.Demethylchlorotetracycline

("https://www.scripps.edu/baran/images/grpmtgpdf/Lin\_Mar\_05revised.pdf,").

TC inhibits protein synthesis by preventing the connection of aminoacyl-tRNA with the ribosomal acceptor (A) site (Nguyen et al., 2014). TC has been used globally in human and animal infection therapies due to its good adsorption and low cost (Uriarte et al., 2019). Moreover, TC has an antimicrobial and nonantimicrobial effects, which encourage its activity in medicine (Pasquale & Tan, 2005). It is active against both Gram-positive and Gram-negative bacteria. Examples of infections treated by TC are *rickettsiae*, *mycoplasmas*, *chlamydiae* and *protozoan parasites* (Nguyen et al., 2014).

TC molecular formula is  $C_{22}H_{24}N_2O_8$ . It is not highly water-soluble. TC is biologically active and stable (Parsa et al., 2019).

TC ionic form depends on the solution pH. TC has three values of pKa in the pH range (2-10.5), Figure 1.2. At acidic pH (<3), TC molecules are fully protonated ( $\text{TCH}^{3+}$ ). At higher pH, deprotonation occurs at different pKa values. At the first pKa (3.3), TC has a Zwitterion form, which results from the deprotonation of the hydroxyl group on  $\text{C}_3$ . At pKa 7.7, TC has negatively charged molecules ( $\text{TCH}^-$ ), that gain from the deprotonation of the diketone system (consists of  $\text{O}_{11}$  and  $\text{O}_{12}$ ). At the third pKa (9.7), TC has two negatively charged ions ( $\text{TC}^{2-}$ ), generated from the deprotonation of the dimethylamino group (Parolo et al., 2010).

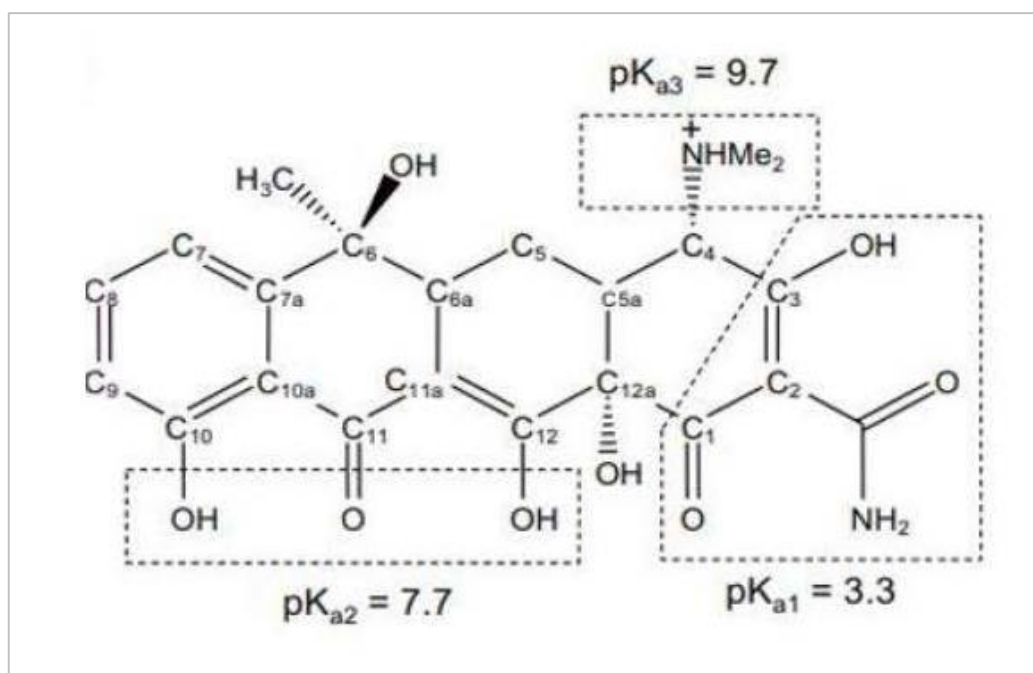


**Figure 1.2:** TC chemical structure with different pKa values .

("https://www.researchgate.net/figure/Structure-of-graphene-oxide-a-Structure-of-tetracycline-and-pKa-values-b\_fig22\_259155862,").

TCs are crystalline amphoteric materials. They themselves have low solubility in water, but their hydrochloride form is more soluble. Hydrochloride solutions are acidic and completely stable, except the

Chlortetracycline solution (Dr. Nguta, 2014). TCs have high ability for chelation with divalent and trivalent ionic species (Turner & Merriman, 2005). This chelation action weakens the absorption of TC in the body (C.-X. Liu et al., 2020; Song et al., 2020), and causes transfer of most dosage to the environment. TC contaminates aquatic environment (ground water, surface water and drinking water) at different concentrations (ng/L to mg/L) (C.-X. Liu et al., 2020). As TCs are widely used, they inhibit the microorganism's growth and metabolism. They also encourage the generation of antibiotic resistance genes and raise the resistance of bacteria, which are not welcome (C.-X. Liu et al., 2020). Therefore, purification of aquatic environment from TC contaminants is necessary. Among the different purification processes are: photolysis, oxidation and adsorption. Adsorption is used in this work, as it is cheap, simple and effective method for TC removal.

### **1.3 Adsorption**

#### **1.3.1 Definitions**

Adsorption is a very vital surface process. This process can be defined as the adhesion or accumulation of substance molecules (gas, liquid or dissolved solid) onto the surface of another solid substance ([https://shodhganga.inflibnet.ac.in/bitstream/10603/22665/8/08\\_chapter3.pdf](https://shodhganga.inflibnet.ac.in/bitstream/10603/22665/8/08_chapter3.pdf)). Adsorption is a very vital surface process. The material that accumulates at the surface of a solid is called the adsorbate, while the solid on which the adsorption occurs is called adsorbent. Adsorbent type affects

adsorption efficiency. Adsorbent should have a high surface area, which causes a higher capacity of adsorption.

The forces between adsorbent and adsorbate define the type of adsorption. Chemical bonds forming means that there is a **Chemisorption process**, whereas, if there are no chemical bonds but only weak van der Waals forces, the process is named **Physisorption**

([https://nptel.ac.in/content/storage2/courses/103104045/pdf\\_version/lecture25.pdf](https://nptel.ac.in/content/storage2/courses/103104045/pdf_version/lecture25.pdf)).

### **1.3.2 Features of Adsorption**

Adsorption process is a technique with significant importance in many applications such as technology, environment, industry and separation processes (Dąbrowski & science, 2001). Among the applications is waste water treatment. This is due to its flexibility, simplicity, efficiency and safety as it produces a fewer toxic and harmful by-product. Moreover, adsorption has the ability of recycling and reusing the adsorbent (Jemutai-Kimosop, Orata, Shikuku, Okello, & Getenga, 2020; Tu et al., 2020; Vikrant, Kim, Peng, Ge, & Ok, 2020).

### **1.3.3 Adsorbents used for TC removal from water**

Variety of adsorbents were used for TC removal from water such as: Cu-immobilized alginate (Zhang et al., 2019), *Myriophyllum aquaticum* under water (Guo et al., 2019), alginate-graphene-ZIF67 aerogel (Kong et al., 2020), Phenolic hydroxyl (bayberry tannin), Functionalized copper

alginate microspheres (Zhang, Lin, He, & Luo, 2019), Biochar modified by Chitosan-Fe/S (J. Liu et al., 2019), boron nitride nanosheets (Bangari & Sinha, 2019), synthesized silica-composited biochars (Zhao et al., 2019), activated 2:1 layered clay mineral (Maged et al., 2020), montmorillonite (Wu et al., 2019), Kaolinite (Li et al., 2010), Pistachio shell coated with ZnO nanoparticles (Mohammed & Kareem, 2019), ZnO@Montmorillonite (Zyoud et al., 2017) and ZnO@Kaolinite (Zyoud et al., 2019).

#### **1.4 Zinc Oxide**

Zinc Oxide (ZnO) is an n-type semiconductor, with a wide band gap value (3.3 eV). ZnO may have wurtzite crystal structure, and piezoelectric properties (Bhatia & Nath, 2020; Djurišić, Chen, Leung, & Ng, 2012; Kamaraj et al., 2020). ZnO nano particles (ZnO-NPs) have many advantages that make them a useful and multifunctional material. Such as having a higher specific area (especially when mixed with other metal oxide, and when its size is in nano scale) (Bhatia & Nath, 2020; Hu et al., 2019), which improve the adsorption capacity, and so better environment purification from contaminants, especially pollutants with negative surface charge, as it preserves a positive surface charge. Moreover, ZnO-NP owns a high stability and symmetry, which facilitates its embedding ability to other materials for improvement process (Hu et al., 2019).

Furthermore, ZnO-NP is an effective photosensitive, catalytically active (Bhatia & Nath, 2020), safe and low-cost material. These properties make it a favorable substance for photocatalytic degradation applications

(Kamaraj et al., 2020). ZnO are also used as sensors, laser diodes, solar cells and active material in sunscreens (Djurišić et al., 2012).

## **1.5 Clay**

Natural Clay minerals are useful in many applications ( Murray, 1991). One of the most common uses is adsorption of different pollutants (organic and inorganic) including heavy metals (Kumar & Lingfa, 2019; Lazaratou, Vayenas, & Papoulis, 2019). Ability of clays in adsorption comes from their high surface areas, which increase the adsorption capacity. Also chemical and mechanical stability improve their efficiency. Clay minerals are also naturally abundant with low cost (Choi et al., 2017; Kumar & Lingfa, 2019; Lazaratou et al., 2019).

### **1.5.1 Structure of the clay minerals**

Clay minerals structure involves two stacked sheets: Octahedral and Tetrahedral ones.

The octahedral sheet involves oxygen and atoms hydroxyl groups. In octahedral coordination, the aluminum, iron, and magnesium atoms are organized, Fig 1.3. Minerals can be termed as: dioctahedral or trioctahedral depending on the number of the filled positions. The term (dioctahedral) is used when the cation present is aluminum with a three positively valence (two-third of the probable locations are filled). While the expression (trioctahedral) is termed when magnesium with a two positive charge is exist (the three positions are filled).

The other layer is tetrahedral layer in the clay structure. In this layer, the silicon atom is centered on the tetrahedron and the four oxygens or hydroxyls are present around it with equal distances. The tetrahedral sheet is resulted from repeating a hexagonal network, on which the tetrahedrons are coordinate, infinitely in two horizontal directions, Figure 1.4 (Murray, 2006). Classification of clay minerals depends on the number and arrangement of the clay sheets: octahedral and tetrahedral, 1:1 clay mineral layer and 2:1 clay mineral layer

([https://www.srs.fs.usda.gov/pubs/ja/ja\\_barton002.pdf](https://www.srs.fs.usda.gov/pubs/ja/ja_barton002.pdf); Murray, 2006) and 2:1:1 clay mineral layer. In the first type (1:1 clay), the basic structure unit consists of one tetrahedral and one octahedral sheet. Example of this type is Kaolin group, in which the kaolinite is the most common mineral. In the second type (2:1 clay), a three sheet mineral is produced by joining two tetrahedral sheets with one octahedral sheet. Examples of this type are the mica, smectite, and vermiculite groups. The most common mineral in the smectite group is the Montmorillonite. The third type (2:1:1 clay) is represented by the chlorite group, which consist of 2:1 layer structure with interlayer of brucite (magnesium hydroxide) or gibbsitel (aluminum hydroxide) like sheet

([https://www.srs.fs.usda.gov/pubs/ja/ja\\_barton002.pdf](https://www.srs.fs.usda.gov/pubs/ja/ja_barton002.pdf)).

Differences between the industrial clays result from the different arrangement and composition of the octahedral and tetrahedral sheets (Murray, 2006).

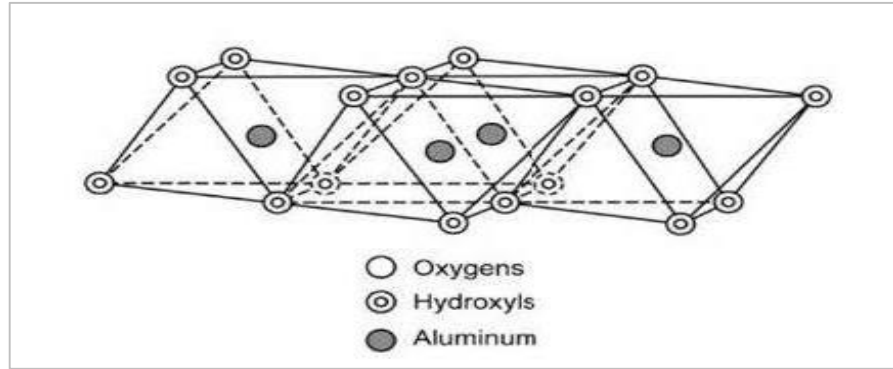


**Fig 1.3:** Diagrammatic sketch of the octahedral sheet (Haydn H Murray, 2006).

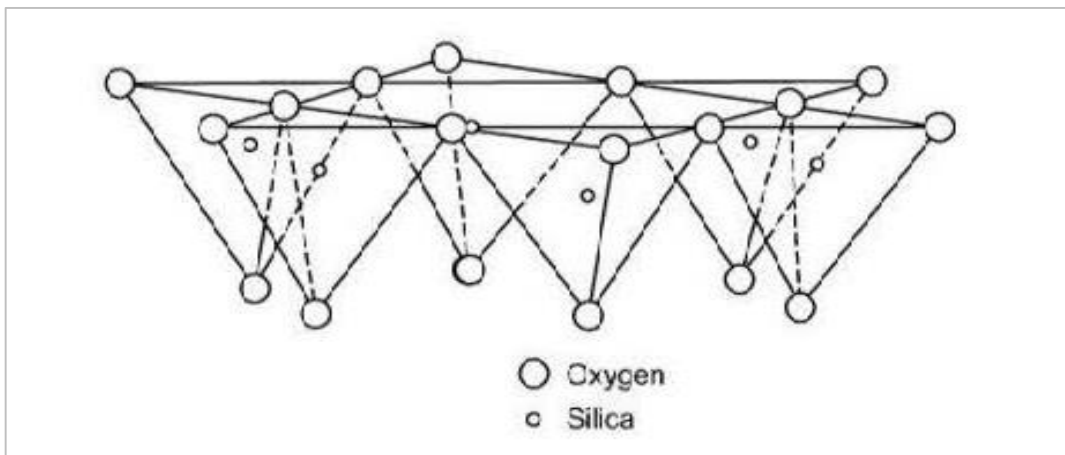


**Fig 1.4:** Diagrammatic sketch of the tetrahedral sheet (Haydn H Murray, 2006).

### 1.5.2 Adsorption on clays

Clays can be used for adsorption of cationic and anionic pollutants. In general, the adsorption of cationic pollutants, organic (e.g., dyes) or inorganic (e.g., ammonium), on the clay surface is more efficient than the anionic ones. However, the anionic contaminant adsorption is considered to be good using natural clays, because of their large surface areas and ion exchange capacities. This helps in surface property modification, resulting in increase of the adsorption capacity of anionic pollutants.

Due to their negative charges, clay surfaces adsorb cations, and balance of the negative charge occurs. The Anion Exchange Capacity (AEC) of clays is affected by the pH and temperature by protonation of hydroxyl groups on the metal oxide surfaces and the silica clays edges (Lazaratou et al., 2019).

### **1.6 Montmorillonite**

Montmorillonite (MONT) is a 2:1 Clay (Kenane et al., 2020; Zhou et al., 2019; R. Zhu et al., 2016) with octahedral sheet placed between two tetrahedral layers (Zhou et al., 2019; R. Zhu et al., 2016). It belongs to the smectites group (Lazaratou et al., 2019). This aluminum silicate clay (Kenane et al., 2020; Wang et al., 2018) (nano layer structure: 1 nm thickness and 200-300 nm lateral dimension) (Kenane et al., 2020) has a permanent negative charge on its layer surfaces (Silva et al., 2020; Wang et al., 2018; Zhou et al., 2019; Zhu et al., 2016), resulted from the isomorphous substitution of the ions in the Octahedral ( $\text{Al}^{3+}$  by  $\text{Mg}^{2+}$ ) (Silva et al., 2020; Zhou et al., 2019; Zhu et al., 2016) and Tetrahedral ( $\text{Si}^{4+}$  by  $\text{Al}^{3+}$ ) sheets (Silva et al., 2020; Zhou et al., 2019). The edge faces have amphoteric nature (Zhou et al., 2019). Between layers, there are cations. These cations counterbalance the permanent negative charge. They can be replaced by other aqueous cations (Silva et al., 2020). This causes adsorption of cations (Silva et al., 2020; Zhu et al., 2016). MONT also adsorbs other chemicals by: hydrogen bonding, van der Waals forces and electrostatic interactions. This causes intercalation of compounds (Silva et al., 2020).

MONT clay is an adsorbent with many advantages, such as:

1. High cation exchange capacity (ability to adsorb cationic pollutants)(Kang et al., 2018; Kenane et al., 2020; R. Zhu et al., 2016).
2. Large surface area (Kenane et al., 2020).
3. Swelling ability (Zhu et al., 2016).
4. Enhanced surface acidity (Kang et al., 2018).
5. High adsorptive properties (Kenane et al., 2020).
6. Low-cost (Silva et al., 2020; R. Zhu et al., 2016).
7. Rich in reserve.
8. Ability to use as a basic clay for other adsorbents, and increase their adsorption capacity on various and wide range of contaminants (R. Zhu et al., 2016).
9. Natural occurrence and biocompatibility (Silva et al., 2020).

MONT is suitable for polar contaminant removal (e.g. aflatoxines) by adsorption. Conversely, the low polar compounds (e.g. mycotoxins) may not adsorb onto the hydrophilic surface of MONT (Wang et al., 2018). This problem can be solved by modifying the clay's polarity by replacing the exchangeable ions with emulsifying agents (organic/inorganic), which make the MONT clay more comparable with organic species (Kenane et al., 2020).

## 1.7 Kaolinite

Kaolinite (KANT), one type of natural 1:1 clays (Guo et al., 2019; Isah et al., 2019; Khan et al., 2012; Kumar & Lingfa, 2019), is an aluminum silicate mineral (Prasad et al., 1991; B.-L. Zhu et al., 2019). It has two layers: the silica tetrahedral (Duarte-Silva, Villa-García, Rendueles, & Díaz, 2014; Isah et al., 2019; Khan et al., 2012; Prasad et al., 1991), with inert  $-\text{Si}-\text{O}-\text{Si}-$  links to form six membered ring (Prasad et al., 1991), and the alumina octahedral (Duarte-Silva et al., 2014; Isah et al., 2019; Khan et al., 2012; Prasad et al., 1991) (gibbsite) layer, on which the aluminum links with oxygens or hydroxyls to form six fold coordination (Prasad et al., 1991), (with layer thickness of  $\sim 7 \text{ \AA}$  (Khan et al., 2012)). The two layers are bonded by hydrogen bonds (Khan et al., 2012) to form a neutral solid structure. The negative charges on the KANT edges result from the protonation/ deprotonation of the hydroxyl groups. These groups affect the solution pH (Silva et al., 2014).

KANT, belongs to Kaolin group. It is chemically inert with low conductivity (Prasad et al., 1991). KANT is a multifunctional material. It is used in catalyst supports, coating materials, filler and adsorbent in: oil, cosmetics, ceramics, paper and rubber industries (Prasad et al., 1991). KANT ability for coating (i.e.: paper) and filling (i.e.: in plastic or paint industry) results from their covering power, its dispersive nature in solution, softness and whiteness (Kumar & Lingfa, 2019; Prasad et al., 1991). KANT is used in paints, wine purifiers, cracking catalysts and carrier material for insecticides (Kumar & Lingfa, 2019). Kaolinite

nanocomposites are also used as gas barriers, sensors and flames retardants (Zhu et al., 2019). KANT is adsorbent for cationic contaminants due to its low cost (Khan et al., 2012; Prasad et al., 1991) and fast adsorption (Khan et al., 2012). KANT is hydrophilic and can be modified using organic molecules. Modification may convert KANT surface to hydrophobic type (Silva et al., 2014).

### **1.8 Composite material**

Composite materials are combinations of two or more materials to yield better properties, (electrical, mechanical or thermal) (Rocky et al., 2020). Nanoparticles can be improved by mixing with others (Hocaoglu et al., 2019; Kutláková et al., 2015). Despite their advantages (Hocaoglu et al., 2019), their small particles make their recovery and separation from the solution difficult. ZnO metal oxide is useful for adsorption and photodegradation applications. It is stable, abundant and safe (Li & Yang, 2014). However, ZnO may aggregate. It also dissolves in acids (Fatimah et al., 2011). To improve ZnO properties and enhance its photocatalytic efficiency, it can be supported into stable solid inorganic substrates (as silica, zeolites, activated carbon, graphene oxide, montmorillonite and kaolinite). Among these solids, montmorillonite and kaolinite, are good choice due to their natural availability, safety, chemical stability and low-cost (Kutláková et al., 2015). Montmorillonite clay, as described above, has many features that increase the adsorption capacity and make it a good support for other inorganic nanoparticles, e.g., ZnO and TiO<sub>2</sub> (Fatimah et

al., 2011; Sani et al., 2017). Impregnating ZnO into MONT clay may affect its properties (Fatimah et al., 2011).

Kaolinite clay ( $\text{Al}_2\text{Si}_2\text{O}_5(\text{OH})_4$ ) is also used as a support for ZnO (KutlÁková et al., 2015; Li & Yang, 2014; Zyoud et al., 2019). It improves ZnO adsorption and photocatalysis action by blocking aggregation of its nanoparticles. Moreover, KANT surface has a special structure containing aluminum cations coordinated with OH groups which increases specific surface area and adsorption capacity (Li & Yang, 2014).

### 1.9 Zero charge point

Zero charge point (ZCP) is defined as the pH value at which the negatively charged species are equal to the positively charged ones, which means that the total surface charge is zero. The ZCP is useful in describing the surface charge of the material under study. At pH higher than its ZCP, the solid surface is negatively charged, and positively charged at pH lower than the ZCP (Appel et al., 2003; Dumont et al., 1990; Gatabi, et al., 2016; Kragović et al., 2019; Sarma et al., 2014). For metal oxides, with surface OH groups at metal ions, the protonation/deprotonation of OH groups causes the change of surface charge, depending on the solution pH, as shown in equations:



The sign of the solid surface is similar to the sign of the most abundant species ( $\text{OH}^-$  or  $\text{H}^+$ ) (Dumont et al., 1990). Surface charge is affected by the solution pH. To reach the optimum adsorption, pH should be controlled (Gatabi et al., 2016; Kragović et al., 2019). Maximum adsorption occurs with opposite charges of adsorbent and adsorbate (Zyoud et al., 2019). ZCP value surface charge are affected by material preparation method and its size. Heat treatment and modification also affect ZCP (Gatabi et al., 2016).

ZCP is measured by various methods, such as: solid surface titration (Silvy et al., 1995), potentiometric titration (where the  $\text{H}^+$  and  $\text{OH}^-$  adsorption is measured in solutions with changing ionic strength (I)), direct measurement of surface charges, electroacoustic mobility (Appel et al., 2003), and pH drift method (Gatabi et al., 2016; Kragović et al., 2019; Villanueva et al., 2014; Zyoud et al., 2019). pH-drift method is preferred as it is economic, accurate and needs basic equipment (Gatabi et al., 2016).

### **1.10 Objectives**

The main objective of this research is to study the surface charge of Zinc Oxide (ZnO), Montmorillonite (MONT), Kaolinite (KANT), ZnO@MONT and ZnO@KANT, which are economic and safe adsorbents. This is to find the optimal pH conditions for maximum adsorption capacity of different water organic contaminants. In this work, the adsorption of a widely encountered pharmaceutical pollutant, TC will be investigated. With higher adsorption, it

is assumed that future ZnO photocatalytic efficiency becomes higher for contaminant degradation.

While achieving this purpose, the following technical objectives will be achieved:

1. Preparation of nano-sized composite materials (ZnO@MONT and ZnO@KANT) by thermal precipitation method.
2. Characterization of the commercial (ZnO, MONT, KANT ) and prepared ZnO@MONT and ZnO@KANT adsorbents using X-ray diffractometer (XRD) and scanning electron microscopy (SEM) equipment.
3. Using the commercial adsorbents (ZnO, MONT and KANT) and the prepared composites (ZnO@MONT and ZnO@KANT) in TC adsorption from water.
4. Determination of zero charge point (ZCP) for the adsorbents (ZnO, MONT, KANT, ZnO@MONT and ZnO@KANT), and studying the effect of their surface charge on TC adsorption efficiency.
5. Studying effects of pH, TC concentration, adsorbent type and contact time on adsorption capacity.
6. Studying the kinetics and adsorption isotherms for each adsorbent.

### **1.11 Novelty of this work**

Adsorption is a very common and useful technique that has been used to remove water pollutants by different adsorbents. In this work, ZnO, a

common and efficient substance, have been used for adsorption process. On earlier studies, ZnO has been used for adsorption and degradation of different organic pollutants, such as pharmaceutical antibiotics like Tetracycline. In this research, commercial ZnO in nano-sized powder form was used for adsorption of Tetracycline. Also, other solids were used to support ZnO and enhance its adsorption ability: Montmorillonite and Kaolinite clays, a common and efficient adsorbents that were used in other researches (Duarte-Silva et al., 2014; Wu et al., 2019). In this study, Tetracycline adsorption onto the surface of ZnO, naked Montmorillonite, naked Kaolinite, ZnO@Montmorillonite and ZnO@Kaolinite composites, was studied and compared, for the first time. Adsorption was applied under several conditions to determine the optimum conditions for each adsorbent.

In addition, the surface charge of the adsorbents was studied by determination of zero charge point value (the pH at which the surface charge equals zero) and compared with the Tetracycline surface charge (pH dependent), to determine the best pH for good adsorption.

These novel results can be used as reference values when performing future water treatment studies, such as photo-catalysis.

## Chapter Two

### Materials and Methods

#### 2.1 Chemicals and Reagents

Commercial ZnO was purchased from Sigma-Aldrich, Cat.NO. (11439.), Montmorillonite (MONT) clay was purchased from Aldrich, Cat.NO. (69866), Kaolinite (KANT) clay was purchased from Sigma-Aldrich, Cat.NO. (03584), NaCl, NaOH and HCl were all purchased from Frutarom. Tetracycline hydrochloride (TC) was thankfully donated from Birziet-Palestine Pharmaceutical Company in pure form.

#### 2.2 Equipment

A Shimadzu UV-3101 spectrophotometer was used to measure UV/Visible spectra. Centrifugation was made using a centrifuge (Centrion, scientific Ltd). A Jenway-3510 pH-meter was used to adjustment the pH values. A four degenerate balance (Radwag-200/2000C/2) was used for measuring the masses of chemicals. A Labtech shaker and water bath was used for shaking the solutions.

XRD, A PANalytical X'Pert PRO X-ray diffractometer (XRD), with Cu Ka ( $\lambda = 1.5418 \text{ \AA}$ ), available in the laboratories of UAEU, was used for X-ray diffraction (XRD) patterns for ZnO, Kaolinite, and ZnO/Kaolinite.

SEM, A Jeol-EO Scanning Electronic Microscope, available in the laboratories of United Arab Emirates University (UAEU), was used for

scanning electron microscopy (SEM) measurements (A. H. Zyoud et al., 2019).

## **2.3 Preparation of solutions**

### **2.3.1 Stock solutions**

1. A 100 mg/L of TC stock solution was prepared by weighing 0.1g of TC and dissolving it in distilled water and then diluting to 1000 mL (using 1000 mL volumetric flask).

From this stock solution, different diluted concentrations were prepared; such as: 20, 40, 60 and 80 mg/L.

2. Another stock solution of TC (1000 mg/L) was prepared by weighing and dissolving 1g of TC in distilled water, and then diluting to 1000 mL.

Different concentrations of TC, 130, 150, 160, 190, 200, 210, 250, 300, and 350 mg/L, are then prepared from this stock solution.

### **2.3.2 Other solutions**

1. A 1L of 0.01 M NaCl was prepared by dissolving 0.5844 g of NaCl in distilled water and then diluting to 1000 mL.
2. Diluted sodium hydroxide NaOH and hydrochloride HCl solutions were prepared by dissolving 2 g of NaOH solid , and 2 mL of conc. HCl solution in 100 mL distilled water for each.
3. A 250 mL of 200 mg/L TC solution was prepared by dissolving 0.05 g of TC solid in 250 mL distilled water.

4. A 100 mL of 200 mg/L TC solution was prepared by dissolving 0.02 g of TC solid in 100 mL distilled water.

## **2.4 Adsorbent preparation**

### **2.4.1 ZnO nanoparticles supported on Montmorillonite or Kaolinite clay**

In a 250-ml conical flask, a 20 g of ZnO, 30 g of the clay (Montmorillonite or Kaolinite), and 200 ml of distilled water were mixed. In order to make this mixture more homogenous, it was sonicated for 10 hours at 25 °C. The solution was left for 1 week. After that, it was decanted, and then magnetically stirred and heated until the total amount of water was evaporated (for approximately 1 hour). The resulting solid was dried and annealed in the oven at 450 °C for 90 minutes. Then, it was stored in a desiccator.

## **2.5 Adsorption experiments**

Batch experiments were performed to study the TC adsorption onto the surfaces of ZnO, MONT, KANT, ZnO@MONT and ZnO@KANT. In each experiment, a 0.1 g of the adsorbent was added to 50 mL of TC solution (100 mg/L for each, 200 mg/L for MONT, and different concentrations for studying effect of concentration) in a covered Erlenmeyer flask. The pH of the solution was then adjusted to the desired value, solution were placed in a shaker. Temperature and speed were fixed at 25 °C and 199 rpm, respectively, until reaching equilibrium. After that, a portion of each solution was taken and centrifuged (155 rpm, 6 minutes). To find the final concentration of TC, the

absorbance of the liquid phase was measured spectrophotometrically. The concentration was then determined using a calibration curve. The amount of the TC adsorbed on the solid surface was calculated using the following equation:

$$Q_e = \frac{(C_0 - C_e)V}{W} \quad (2.1)$$

Where  $C_0$  and  $C_e$  (mg/L) are the concentrations of TC solution initially and at equilibrium, respectively.  $V$  is the solution volume (L) and  $W$  is the adsorbent mass (g).

### **2.5.1 Effect of adsorbent type**

TC adsorption on different adsorbents, ZnO, MONT, KANT, ZnO@MONT and ZnO@KANT, was studied. For each adsorbent, a 0.1 g was added to a TC solution (50 mL, 100 mg/L), which was previously prepared, pH of solution was adjusted to ~3. The flasks were then covered and shaken for 2 h at 25 °C.

### **2.5.2 Effect of initial pH**

Effect of initial pH adsorption for different adsorbents, ZnO, MONT, KANT, ZnO@MONT and ZnO@KANT, was investigated in the pH range 3-11. The pH was adjusted as desired, by adding drops of diluted sodium hydroxide or hydrochloric acid solutions, as explained earlier. Adsorbent samples (0.1g) were placed into the adjusted pH Tetracycline solutions (50 mL, 100 mg/L for each adsorbent, and 200 mg/L for MONT). The mixtures were then shaken for 2 hours at room temperature.

### **2.5.3 Effect of zero charge point**

The zero charge point of the different adsorbents (ZnO, MONT, KANT, ZnO@MONT, and ZnO@KANT) were determined using pH-drift method. A series of NaCl (0.01 M) solutions were boiled to remove dissolved CO<sub>2</sub> and then cooled to room temperature. Six vials (for each adsorbent) were filled with 50 mL of the pre-boiled NaCl solution. The initial pH were adjusted to different values between ~2 and ~12 using diluted HCl or diluted NaOH. The six vials were exposed to N<sub>2</sub> gas for a few minutes (1 to 3 min), and then the initial pH was measured and recorded. A 0.1 g adsorbent was then added to each adjusted pH solution (50 mL for each) in a capped vial. The solutions were then shaken and equilibrated for 24 h. The final pH was measured after settling of the mixtures. The pH change was plotted against the initial pH. The pH at which the curve crosses initial pH axis was taken as zero charge point pH. This procedure was carried out for each adsorbent used in this work. The ZCP measurement procedure was repeated three times for each sample. The average value of the three measurements was calculated and used in this work.

### **2.5.4 Effect of contact time**

The effect of time on adsorption for different adsorbents, ZnO, MONT, KANT, ZnO@MONT and ZnO@KANT, was investigated.

Adsorbent sample (0.1 g) was placed into TC solution (50 mL, 100 mg/L for each adsorbent, except for MONT: 50 mL, 200 mg/L) at pH~6.

The mixtures were shaken at 25 °C. After centrifuge, aliquots (2 ml each) of the clear solution were taken at various time intervals until equilibrium was reached after ~150 min. This process was performed for the five adsorbents (ZnO, MONT, KANT, ZnO@MONT, ZnO@KANT).

### 2.5.5 Effect of TC concentration

Effect of contaminant concentration was studied. For each adsorbent, different concentrations were used depending on their ability to adsorption, as summarized in Table 2.1.

**Table 2.1: Different Concentrations of TC contaminant used for adsorption onto different adsorbents at natural pH.**

<b>Adsorbent(amount)</b>	<b>Contaminant TC Concentration (mg/L)</b>			
<b>ZnO (0.1g)</b>	100	130	160	190
<b>MONT (0.1g)</b>	150	250	300	350
<b>KANT (0.1g)</b>	20	40	60	80
<b>ZnO@MONT (0.1g)</b>	130	160	190	210
<b>ZnO@KANT (0.1g)</b>	70	130	160	190

A 0.1 g adsorbent for each was added to these solutions, with natural pH.

The mixtures were shaken at room temperature (25 °C) until reaching equilibrium (~2 h). After centrifuge, the final concentration was measured. The amount of adsorption at equilibrium,  $q_e$  (mg/g), was calculated using equation (2.1). The data were then checked for Langmuir and Freundlich isotherms to assess the adsorption parameters.

## 2.5.6 Adsorption isotherm models

Knowing surface properties of the solid adsorbent surface is important to know the best operating procedures. Therefore, the adsorption isotherm was studied as described (Mohammed et al., 2019). Langmuir and Freundlich isotherms are the most commonly used isotherms in solid adsorbents for waste water remediation (Sahu & Singh, 2019).

### 2.5.6.1 Langmuir adsorption isotherm

Langmuir assumes monolayer adsorption at equilibrium. It is good for systems having low coverage. It may also be used to describe the binary adsorption systems.

The linear form of the Langmuir equation is:

$$\frac{C_e}{q_e} = \frac{1}{Q_0 b} + \frac{1}{Q_0} C_e \quad (2.2)$$

Where  $C_e$  is the concentration of the adsorbate at equilibrium (mg/L),  $q_e$  is the equilibrium amount of the adsorbate per unit mass of adsorbent (mg/g),  $Q_0$  is adsorption capacity constant at equilibrium (mg/g) and  $b$  is the Langmuir constant related to the affinity of adsorption (L/mg) (Liu et al., 2019).

The major assumptions of Langmuir model are:

1. Adsorbent surface involves similar specific binding sites.
2. Adsorption sites on a given adsorbent surface are the same and adsorb only one adsorbed molecule each.

3. At complete coverage, only one layer of molecules cover with the adsorbent surface.
4. Heat of adsorption is independent of the coverage because there is no interaction between the adsorbed molecules on the adsorbent surface (surface of the adsorbent is homogenous) (Bushra et al., 2016; "<http://www.zzm.umcs.lublin.pl/Wyklad/FGF-Ang/4A.F.G.F.Ads.S-G.%20Interface.pdf>,").
5. There is direct proportional relation between the fractional surface coverage and the desorption rate.
6. At equilibrium, adsorption and desorption rates are equal (L. Liu et al., 2019).

### 2.5.6.2 Freundlich adsorption isotherm

The first isotherm model for sorption process was the Freundlich isotherm. This isotherm describes the non-ideal adsorptions on heterogeneous surfaces with different types and affinities. In Freundlich isotherm the multilayer adsorption is assumed.

Freundlich isotherm is represented by equation (2.3).

$$\log q_e = \log K_F + \left(\frac{1}{n}\right) \log C_e \quad (2.3)$$

where  $q_e$  is the adsorbate mass per adsorbent mass unit (mg/g),  $C_e$  is the remaining equilibrium concentration of the adsorbate (mg/L),  $K_F$  is the Freundlich constant that depends on the adsorption capacity of the adsorbent ((mg/g)(mg/L)<sup>1/n</sup>))(de Sá et al., 2017; Mu & Sun, 2019). The

slope ( $1/n$ ) indicates the heterogeneity of the surface. As the slope goes near to zero, the surface becomes more heterogeneous (Lu, 1998). The value of ( $1/n$ ) indicates if the adsorption process is favorable or not; if ( $1/n$ ) is lower than 1, Langmuir adsorption is favorable. Freundlich adsorption occurs if ( $1/n$ ) is higher than 1 (Fytianos, 2000).

### **2.5.7 Adsorption kinetic models**

Kinetics are important in adsorption study. They give detailed description about adsorption mechanisms and adsorbent performance, which is vital application. Kinetics determine the adsorption rate on adsorbent, and time needed to reach adsorption completion (Qiu et al., 2009). Various kinetic models are used to determine adsorption mechanism and rate limiting step. Examples are pseudo-first and second-order rate model, Adam-Bohart-Thomas relation, intra particle diffusion model, Weber and Morris sorption, first-order equation of Bhattacharya and Venkobachar, external mass transfer model and first-order reversible reaction model (sridev, 2009). In this work, pseudo-first order, pseudo-second order, and intra particle diffusion models will be used to test the experimental data of tetracycline adsorption on the five adsorbents used in this study.

#### **2.5.7.1 Pseudo-first-order model**

The pseudo-first-order model was proposed by Lagergren. The relation for this model is shown in equation (2.4) (Mohammed et al., 2019):

$$\log(q_e - q_t) = \log q_e - \frac{k_1}{2.303} t \quad (2.4)$$

Where  $q_e$  and  $q_t$  (mg/g) are the masses of adsorbate per unit mass of adsorbent at equilibrium and at time  $t$  (min), respectively, and  $k_1$  ( $\text{min}^{-1}$ ) is the rate constant of the pseudo-first-order model.

### 2.5.7.2 Pseudo-second-order model

Ho and McKay described the pseudo-second-order model (Mohammed et al., 2019). The model assumes that the rate limiting step can be chemical adsorption of adsorbate on adsorbent.

The model can be expressed in equation (2.5):

$$\frac{t}{q_t} = \frac{1}{k_2 q_e^2} + \frac{1}{q_e} t \quad (2.5)$$

Where  $q_e$  and  $q_t$  (mg/g) are the masses of adsorbate per unit mass of adsorbent at equilibrium and at time  $t$  (min), respectively.  $k_2$  (g/mg min) is the pseudo-second-order rate constant of adsorption

### 2.5.7.3 Intra particle diffusion model

The intra-particle diffusion model was proposed by Weber and Morris (Mohammed et al., 2019). Equation (2.6) describes this model:

$$q_t = k_p t^{0.5} + b \quad (2.6)$$

Where  $q_t$  (mg/g) is the mass of adsorbate per unit mass of adsorbent at time  $t$  (min),  $k_p$  ( $\text{mg/g min}^{0.5}$ ) is the rate constant of intra-particle diffusion and ( $b$ ) is a constant that indicates the thickness of the boundary layer.

## 2.6 Calibration curve

UV-visible spectrophotometry was used to determine the concentration of the TC in aqueous solutions during the study of its adsorption studies. The absorbance of TC was measured at ~360 nm wavelength. For each solution, a blank was prepared and its absorbance was measured.

Calibration curve for TC was made by plotting the concentration of the standard solutions against their measured absorbance using the UV-Vis spectrophotometry. The standard solutions of different concentrations ranging from (0-100 mg/L) were prepared from the stock solution (100 mg/L). The concentration of the unknown solution can be determined by measuring its absorbance. The calibration curve of TC solution is shown in Figure 2.1.

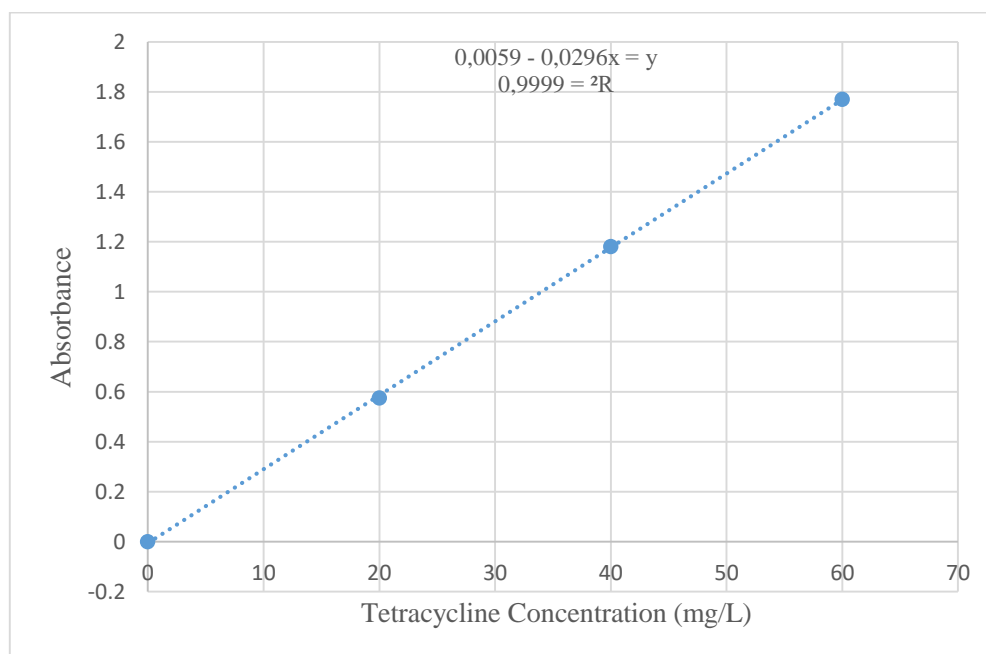


**Figure 2.1:** Calibration curve for aqueous TC using UV-Vis spectrophotometry.

## Chapter Three

### Results and discussion

#### 3.1 Catalyst characterization

##### 3.1.1 XRD characterization

###### 3.1.1.1 XRD pattern for ZnO

XRD pattern of commercial ZnO powder is shown in Figure 3.1. The diffraction peaks are positioned at  $31.7^\circ$ ,  $34.41^\circ$ ,  $36.24^\circ$ ,  $47.52^\circ$ ,  $56.57^\circ$ ,  $62.84^\circ$ ,  $66.35^\circ$ ,  $67.93^\circ$  and  $76.94^\circ$  ( $2\theta$ ). These peaks can be correspond to reflections of (100), (002), (101), (102), (110), (103), (200), (112), (201) and (202) bragg's planes, respectively (Arefi & Rezaei-Zarchi, 2012). Agreement between the XRD pattern of the commercial ZnO in this work and that in the literature (Arefi & Rezaei-Zarchi, 2012; X. Li & Yang, 2014; A. Zyoud et al., 2017; A. H. Zyoud et al., 2019) confirms the identity of ZnO compound that has been used.

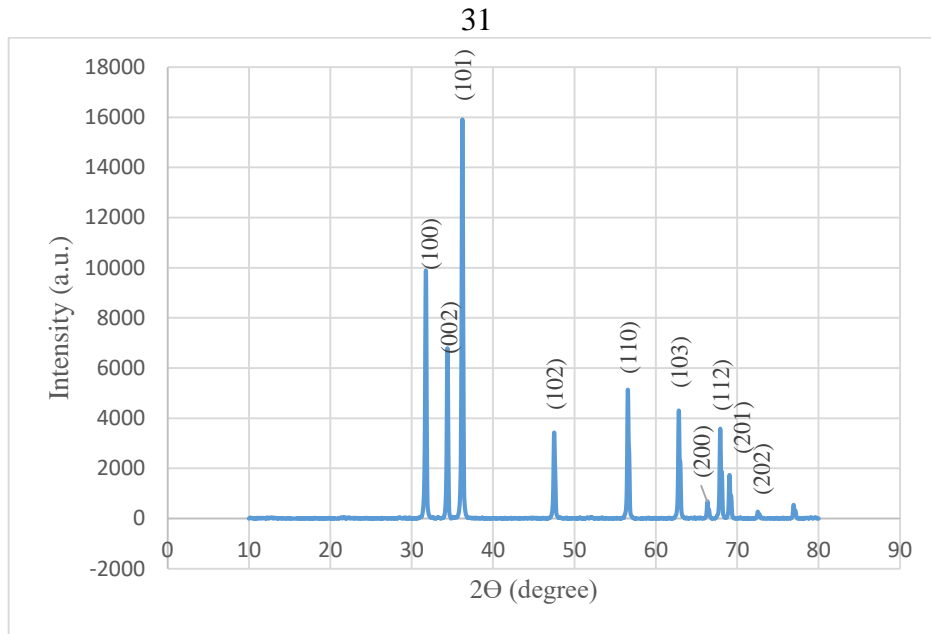


**Figure 3.1:** X-ray diffraction pattern for commercial ZnO powder.

The particle size of ZnO was calculated using Scherrer equation (Fatimah et al., 2011):

$$D = K \lambda / \beta \cos\theta \quad (3.1)$$

Where D is the particle diameter (nm), K is the shape factor ( $\sim 0.9$ ),  $\lambda$  is the wavelength of X-ray (0.154 nm) and  $\beta$  is full width at half maximum (FWHM) of the reflection at  $2\theta$  (in radian).

ZnO size in diameter (nm) was calculated using  $31.7^\circ$  (100),  $34.41^\circ$  (002) and  $36.24^\circ$  (101). The values are close to other (51.45, 54.79 and 49.29 nm, respectively). The average size is 51.89 nm.

### 3.1.1.2 XRD pattern for Montmorillonite

Montmorillonite (MONT) XRD pattern is represented in Figure 3.2. Reflections of (110), (200) and (060) occurs at  $(2\theta) = 20.8^\circ$ ,  $36.5^\circ$  and  $62.2^\circ$ ,

respectively, which corresponds to the results in literature (Zyoud et al., 2017).

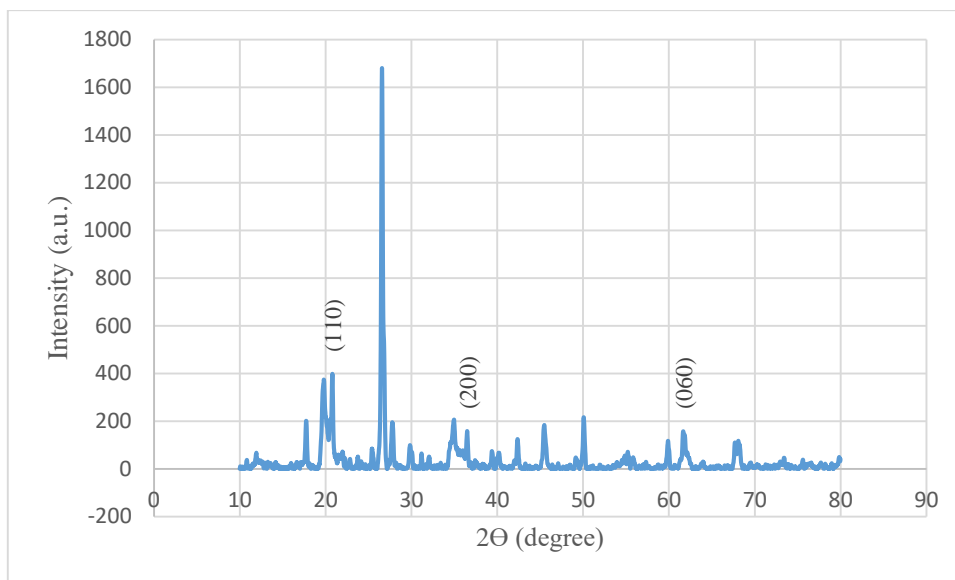


**Figure 3.2:** X-ray diffraction pattern for Montmorillonite clay.

Based on Scherer equation, particle size of MONT was calculated at the three characteristic peaks ( $2\Theta = 20.8^\circ$ ,  $36.5^\circ$  and  $62.2^\circ$ ). Results are precise and close to other: 39.42, 43.64 and 41.25 nm, respectively. The mean size was found to be 41.45 nm.

### 3.1.1.3 XRD pattern for Kaolinite

XRD pattern for Kaolinite (KANT) is presented in Figure 3.3. The Figure shows the diffraction peaks of KANT where the characteristic ones positioned at  $2\Theta = 12.36^\circ$  (001),  $25.2^\circ$  and  $29.8^\circ$  (002). Results agree with literature (Wawrzyn et al., 2013; Kutlakova et al., 2015; Zyoud et al., 2019).

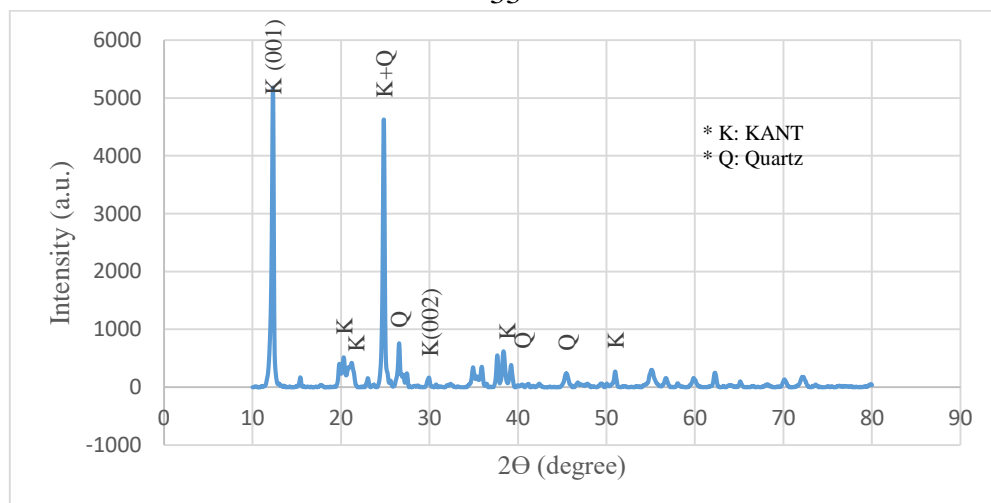


**Figure 3.3:** X-ray diffraction for Kaolinite clay.

KANT particle size was determined using Scherer equation. The three diffraction peaks' positions ( $2\theta = 12.36^\circ$ ,  $25.2^\circ$  and  $29.8^\circ$ ) were used to find the average size of KANT. Results are very close: 35.17, 37.91 and 38.82 nm, respectively. Mean size of KANT was 37.3 nm.

#### 3.1.1.4 XRD pattern for ZnO@Montmorillonite

XRD pattern of ZnO@Montmorillonite (ZnO@MONT) is shown in Figure 3.4. The Figure confirms that ZnO is supported by MONT. The basic diffraction peaks of ZnO ( $31.74^\circ$ ,  $34.41^\circ$  and  $36.22^\circ$ ) and for MONT ( $20.8^\circ$  and  $62.2^\circ$ ) appear without shift in position, which confirms that ZnO is located at the surface of MONT without intercalation between layers. This result corresponds with earlier researchs (Zyoud et al., 2017).

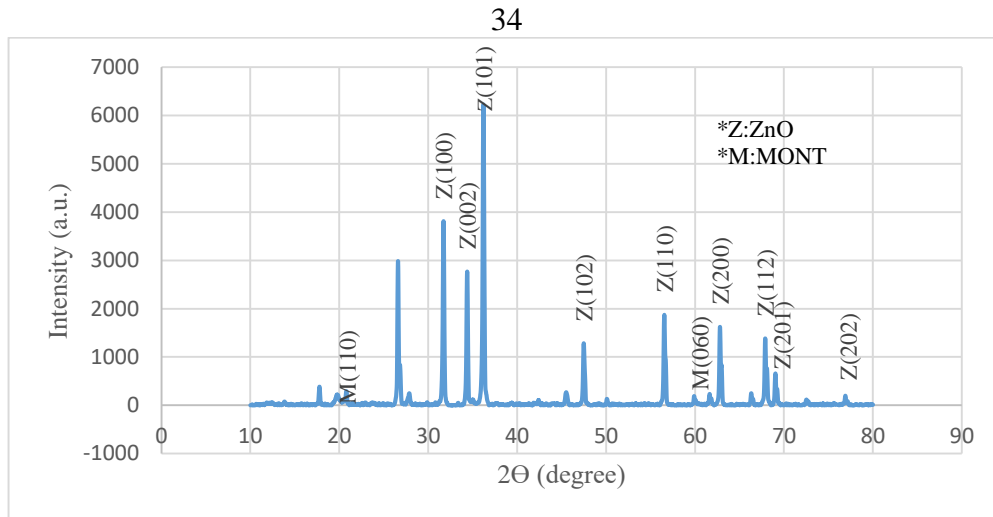


**Figure 3.4:** X-ray diffraction pattern for ZnO@Montmorillonite composite.

Particle size of the ZnO and MONT in the composite was measured using Scherrer equation at ( $2\Theta = 31.74^\circ$  and  $20.8^\circ$ , respectively). Results showed that the particle size have no significant change after supporting of ZnO on MONT (56.7 and 50.3 nm, respectively). The particle size of pristine ZnO and MONT, as shown above, are: 51.89 and 41.45 nm, respectively.

### 3.1.1.5 XRD pattern for ZnO@Kaolinite

XRD pattern for ZnO@Kaolinite is presented in Figure 3.5. Peaks of ZnO ( $2\Theta = 31.74^\circ$ ,  $34.41^\circ$  and  $36.22^\circ$ ) and Kaolinite ( $2\Theta = 12.4^\circ$  and  $24.9^\circ$ ) (Kutlakova et al., 2015; Li & Yang, 2014; Zyoud et al., 2019) are appeared in the Figure. This confirms the presence of ZnO at the surface of Kaolinite without intercalation.

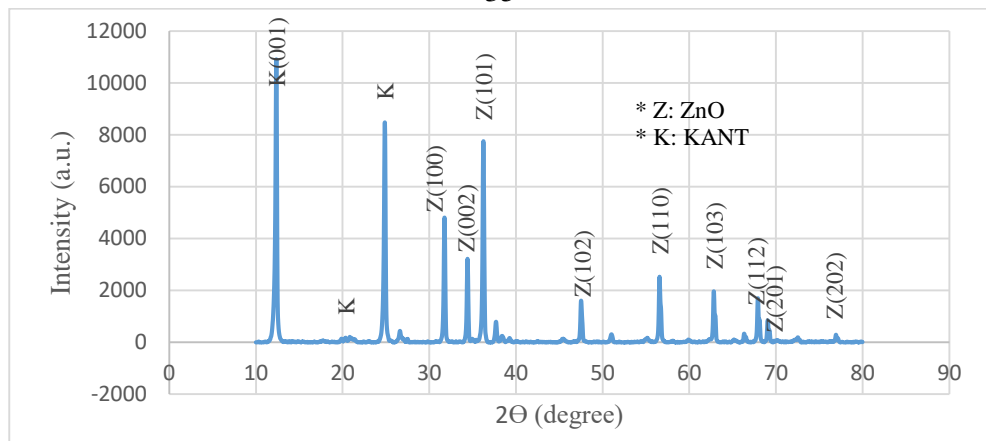


**Figure 3.5:** X-ray-diffraction of ZnO@Kaolinite composite.

Using Scherer equation, the ZnO and Kaolinite particle size in their composite was calculated. Results confirmed that the particle size of each component have no significant change after composition process. The size of ZnO and Kaolinite have measured at ( $2\theta = 36.2^\circ$  and  $12.4^\circ$ , respectively) to give a size of 52.55 and 42.87 nm, respectively.

Pristine ZnO as shown above, has a size of 51.89 nm and pristine Kaolinite particle size is 37.3 nm.

### 3.1.2 Scanning electron microscopy (SEM)

#### 3.1.2.1 SEM result for ZnO

SEM micrograph of ZnO is shown in Figure 3.6. The Figure shows that ZnO is exist as agglomerates of  $\sim 787.65$  nm diameter (the average of different values ranging from  $\sim 400$ - $1100$  nm agglomerate diameter) that contain smaller nanoparticles of ( $\sim 51.84$  nm) calculated from XRD pattern of pristine ZnO.

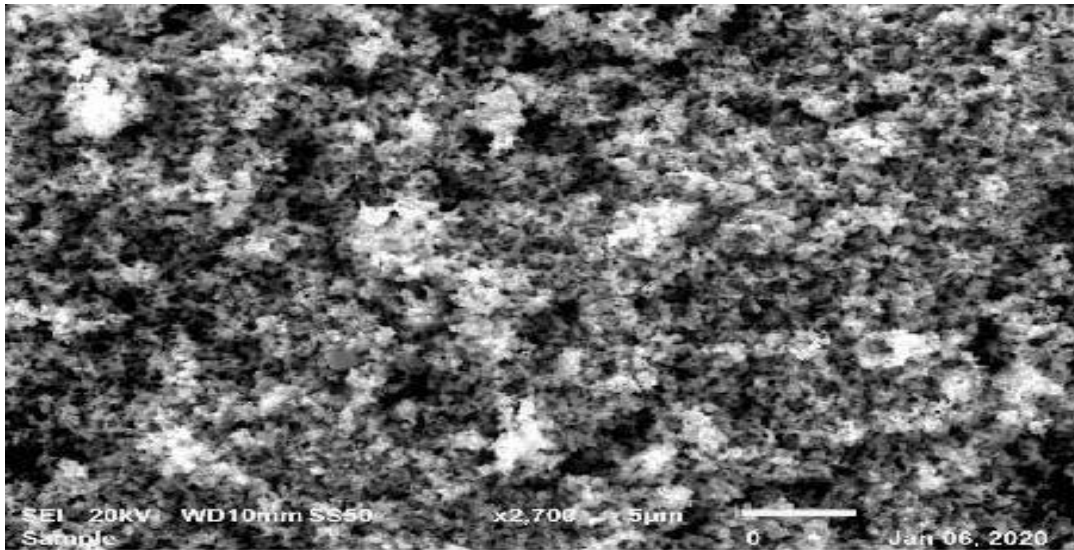


**Figure 3.6:** Scanning electron micrograph for commercial ZnO.

### 3.1.2.2 SEM result for Montmorillonite

SEM micrograph of Montmorillonite (MONT) is shown in Figure 3.7. Agglomerates of MONT can be seen in the Figure with particle size in diameter of  $\sim 2720.7$  nm (The average of different values ranging from  $\sim 1800$ - $4090$  nm agglomerate diameter), which contain smaller nanoparticles of MONT ( $\sim 41.27$  nm) calculated from XRD of MONT.

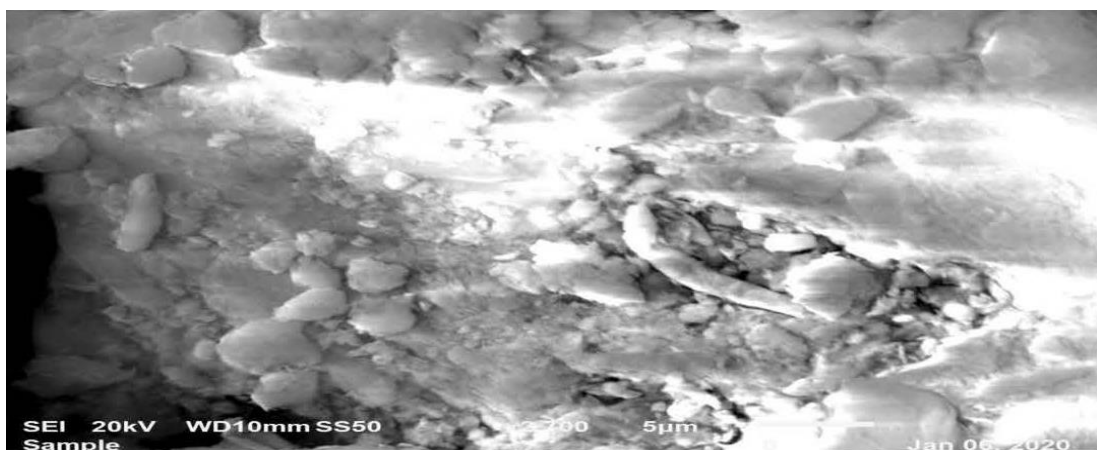


**Figure 3.7:** Scanning electron micrograph for Montmorillonite.

### 3.1.2.3 SEM result for Kaolinite

Kaolinite (KANT) morphology can be seen by SEM in Figure 3.8. SEM and XRD results confirm that KANT is present in agglomerates of 5499.4 nm average size (the mean value of different sizes ranging from ~1100-14000 nm) containing smaller nanoparticles (~37.2 nm) measured from XRD pattern.

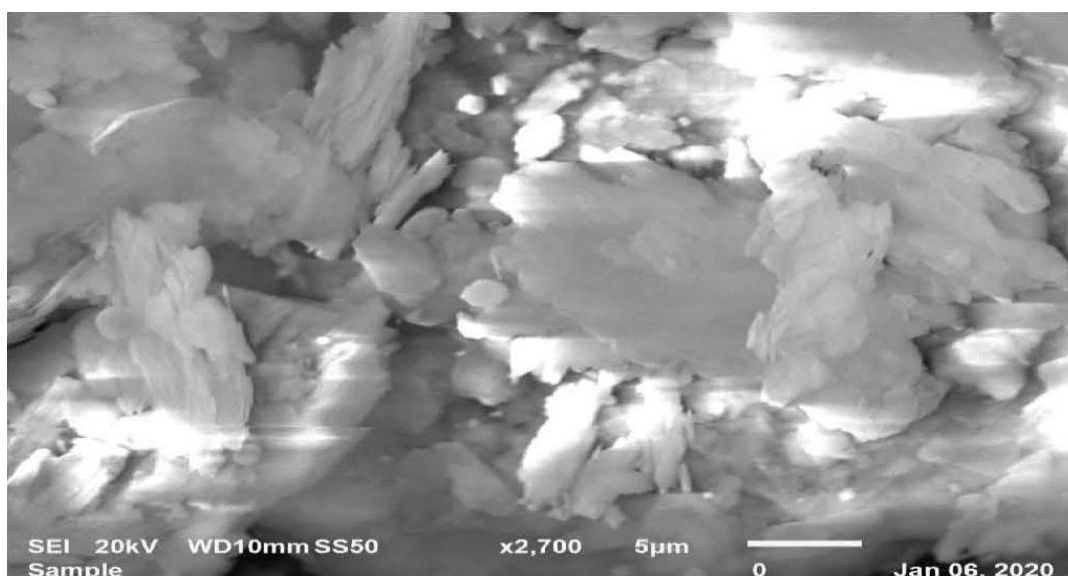


**Figure 3.8:** Scanning electron micrograph for Kaolinite.

### 3.1.2.4 SEM result for ZnO@Montmorillonite

SEM micrograph for ZnO@MONT composite is presented in Figure 3.9. The Figure shows that the morphology of MONT in the composite (like-flower shape) differs from that for the naked MONT (flaky shape), which confirms the existence of ZnO@MONT composite.

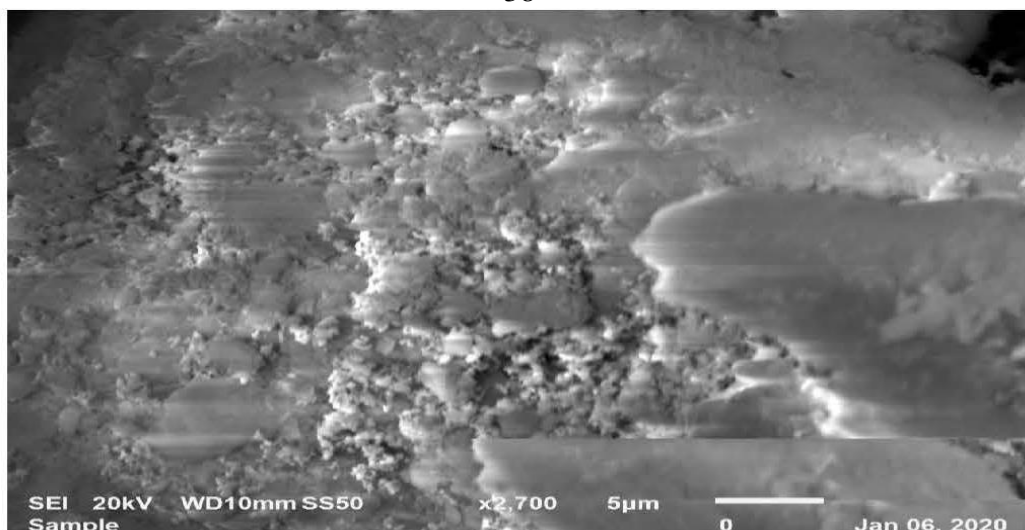


**Figure 3.9:** Scanning electron micrograph for ZnO@Montmorillonite.

Agglomerates of MONT and ZnO have an average size of  $\sim 1110.66$  nm (values are ranging between  $\sim 800$ - $2700$  nm) that contain nanoparticles of ZnO ( $\sim 56.7$  nm) and MONT ( $\sim 50.3$  nm), measured from the composite XRD pattern.

### **3.1.2.5 SEM result for ZnO@Kaolinite**

SEM micrograph of ZnO@KANT is presented in Figure 3.10. The change in the KANT is clear in the Figure (from flaky to flower-like shape). The micrograph, also, showed the ZnO agglomerates of  $\sim 694$  nm average size in diameter (the value are ranging between  $\sim 500$ - $1000$  nm) involving nanoparticles of ZnO ( $\sim 52.55$  nm, measured from XRD pattern of ZnO@KANT), which distribute on the KANT agglomerates' surfaces.

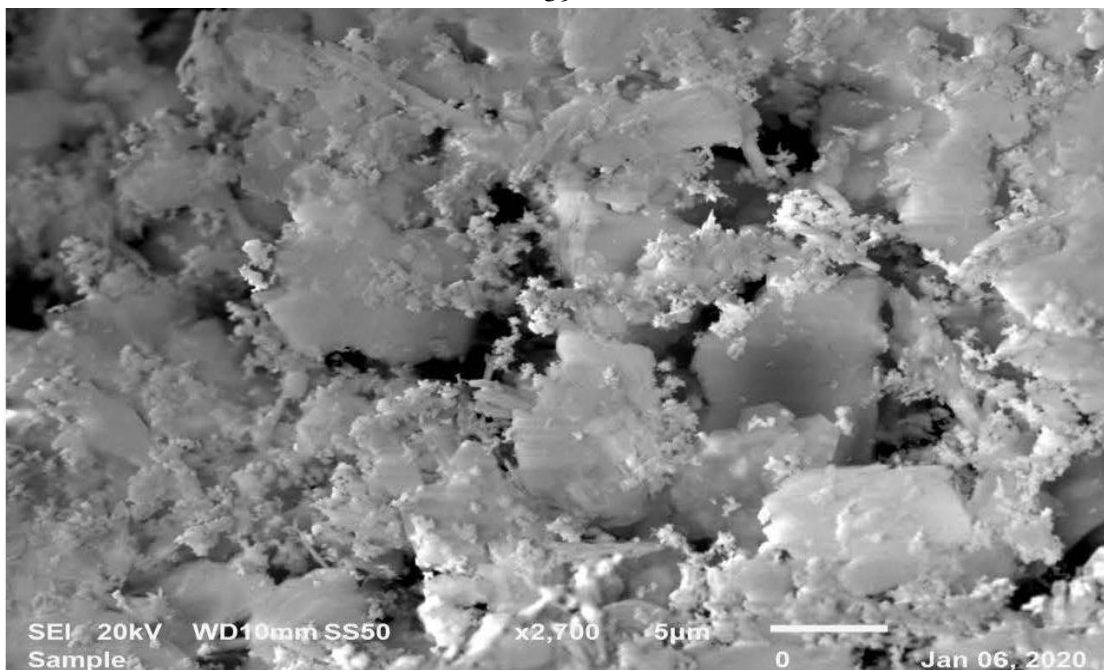


**Figure 3.10:** Scanning electron micrograph for ZnO@Kaolinite

## 3.2 Tetracycline adsorption experiments

### 3.2.1 Effect of adsorbent type

The percentages of Tetracycline (TC) removal on different adsorbents are shown in Figure 3.11. Surface area was measured based on BET manual lab, prepared, analyzed and found to be 27, 330, 34, 310 and 35 m<sup>2</sup>/g for ZnO, MONT, KANT, ZnO@MONT and ZnO@KANT, respectively.

Figure 3.11 shows that MONT has the highest adsorption capacity compared to the other adsorbents. This can be due to its large surface area.

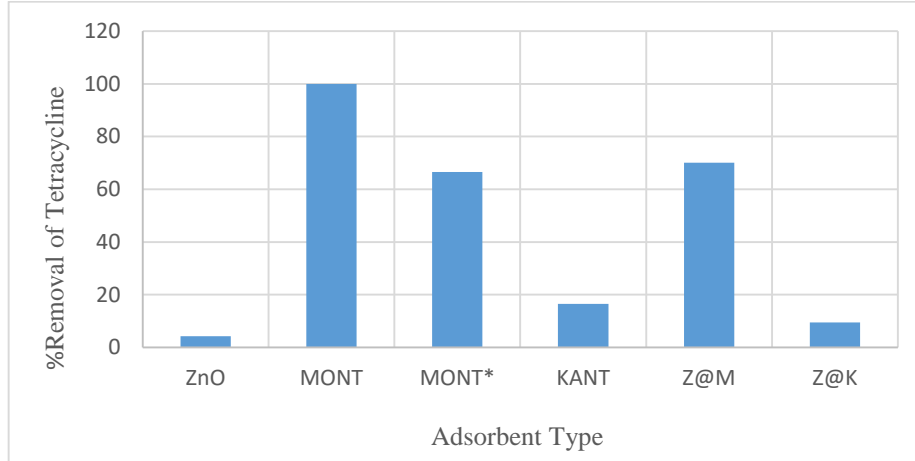


**Figure 3.11:** Effect of adsorbent type on the percentage of TC removal at (initial conc.: 100 mg/L, MONT\*: 200 mg/L, pH ~3, temperature: 25 °C, contact time: 120 min and solid/liquid ratio: 0.1g/50mL).

### 3.2.2 Results of zero charge point

Plots and values of zero charge points of unsupported ZnO, MONT, KANT, ZnO@MONT and ZnO@KANT are described and summarized in Figures (3.12-3.16) and table (3.1), respectively.

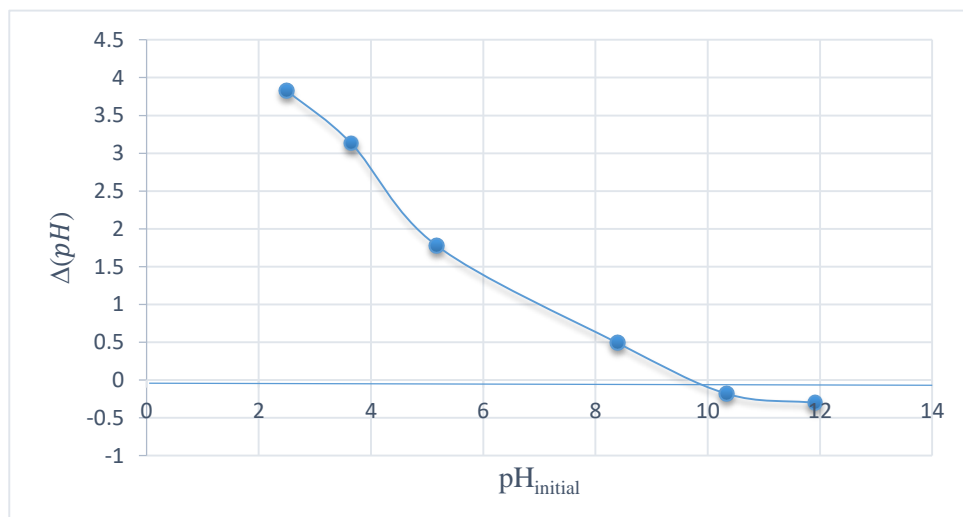


**Figure 3.12:** Plot of  $\Delta(pH)$  vs. initial pH for ZnO. Intercept shows value of  $pH_{zcp}$  for the solid. Results were made at room temperature.

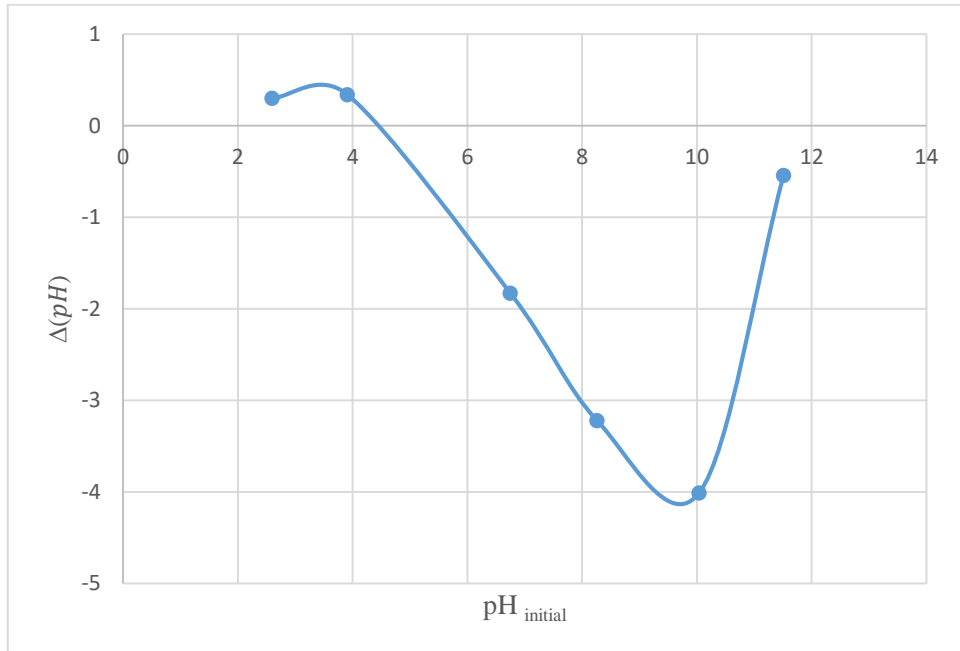


**Figure 3.13:** Plot of  $\Delta(\text{pH})$  vs.  $\text{pH}_{\text{initial}}$  for MONT. Intercept shows value of  $\text{pH}_{\text{zcp}}$  for the solid. Results were taken at room temperature.

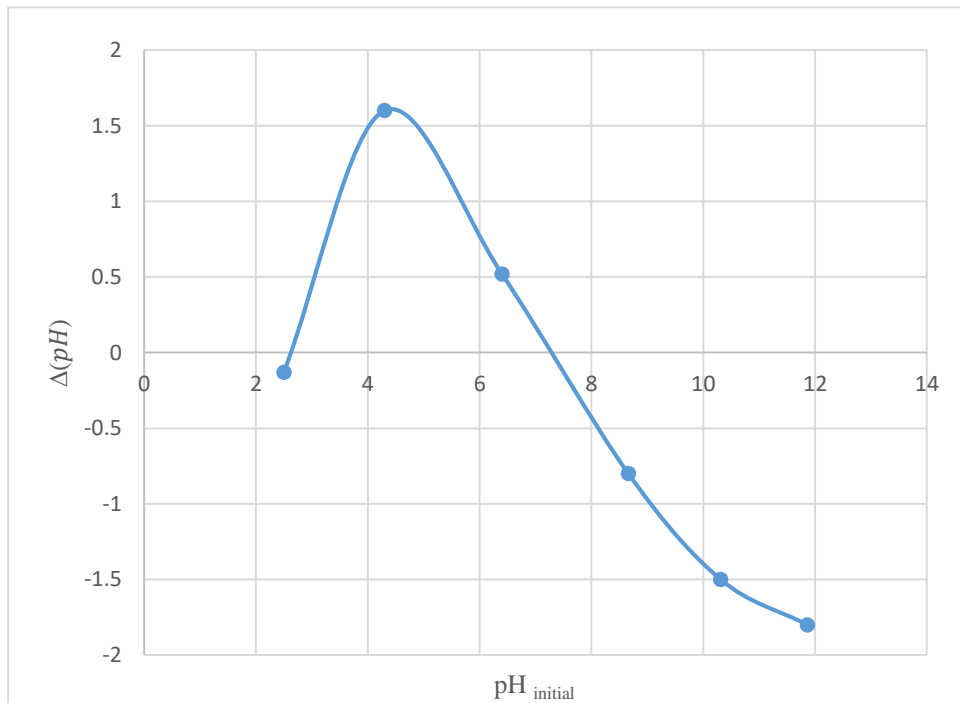


**Figure 3.14:** Plot of  $\Delta(\text{pH})$  vs.  $\text{pH}_{\text{initial}}$  for KANT. Intercept shows value of  $\text{pH}_{\text{zcp}}$  for the solid. Results were taken at room temperature.

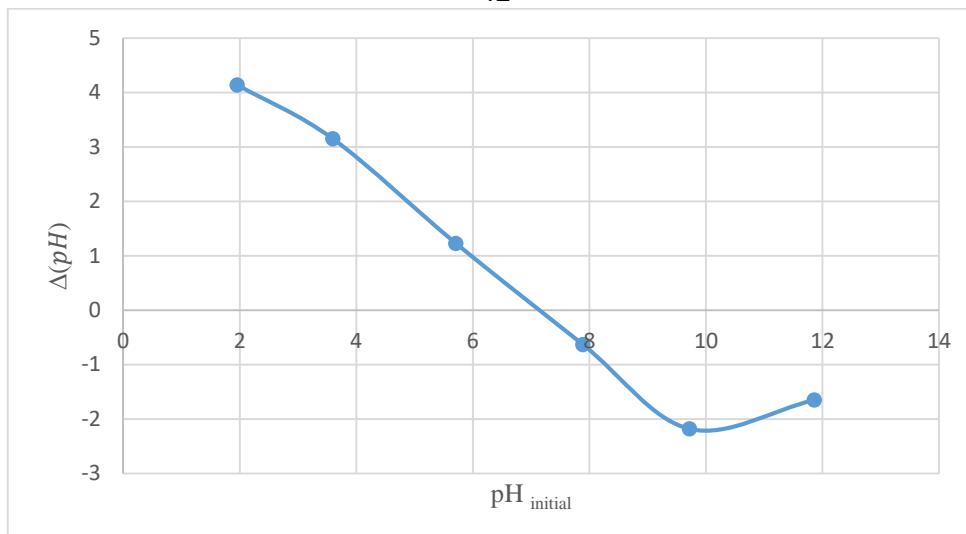


**Figure 3.15:** Plot of  $\Delta(\text{pH})$  vs.  $\text{pH}_{\text{initial}}$  for ZnO@MONT. Intercept shows value of  $\text{pH}_{\text{zcp}}$  for the solid. Results were taken at room temperature.

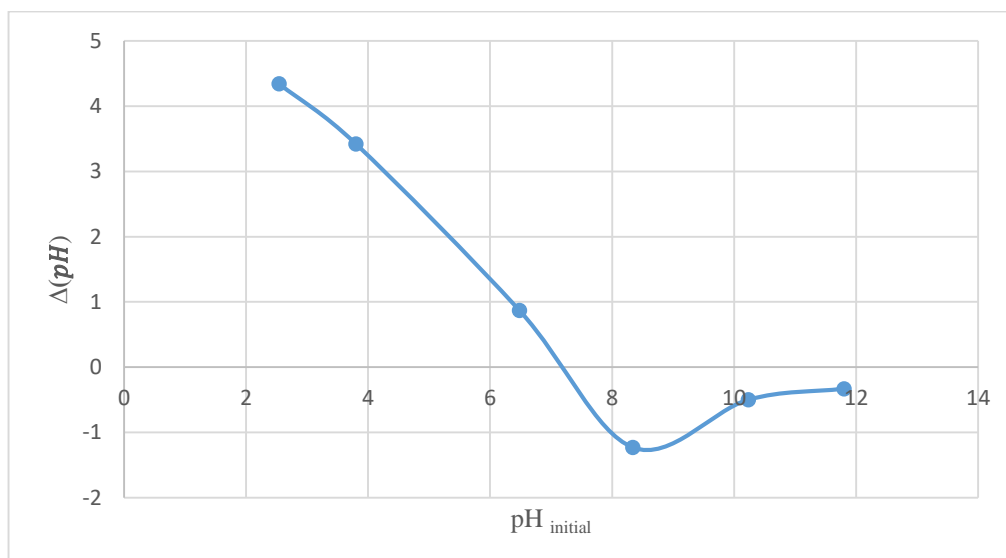


**Figure 3.16:** Plot of  $\Delta(\text{pH})$  vs.  $\text{pH}_{\text{initial}}$  for ZnO@KANT. Intercept shows value of  $\text{pH}_{\text{zcp}}$  for the solid. Results were taken at room temperature.

**Table 3.1: Zero charge points of different adsorbents measured using pH-drift method.**

Adsorbent	pH <sub>zpc</sub>
ZnO	9.8
MONT	4.5
KANT	7.5
ZnO@MONT	7.2
ZnO@KANT	7.2

Table 3.1 summarizes the pH<sub>zcp</sub> values for ZnO, MONT, KANT, ZnO@MONT and ZnO@KANT. The pH<sub>zcp</sub> of unsupported ZnO is ~9.8. At pH values lower than this pH, the surface of ZnO is positively charged. The surface is negatively charged at pH values higher than ~9.8.

For naked MONT, pH<sub>zcp</sub> is around 4.5. The surface charge of MONT at pH lower than ~4.5 is positive. At higher pH, it has a negatively surface charged.

The KANT has pH<sub>zcp</sub> around 7.5. At lower pH than 7.5, the surface charge of KANT is positive, and at pH values higher than 7.5 it has a negative surface charge.

The ZnO@MONT composite revealed pH<sub>zcp</sub> at ~7.2. The surface charge of the composite at pH values lower than ~7.2 is positive, and at higher values of pH (>~7.2), ZnO@MONT composite has a negatively surface charged.

The ZnO@KANT composite showed pH<sub>zcp</sub> at ~7.2. At pH lower than ~7.2, ZnO@KANT has positive surface charge, and at higher pH, it has negatively surface charged.

### 3.2.3 Effect of pH

TC adsorption onto the different adsorbents was studied in the pH range (3-11). Shaking process continued until reaching equilibrium (2 h). Figures (3.19-3.24) illustrate the effect of pH on TC adsorption process on different adsorbents.

#### 1. ZnO

Adsorption efficiency depends mainly on the  $\text{pH}_{\text{zcp}}$ , the surface charge of ZnO and equilibrium TC structure at the given pH. Figures 1.2, 3.17 and 3.18 illustrate how the surface charge of ZnO and TC (as a result of its varying structures) changes with different pH.

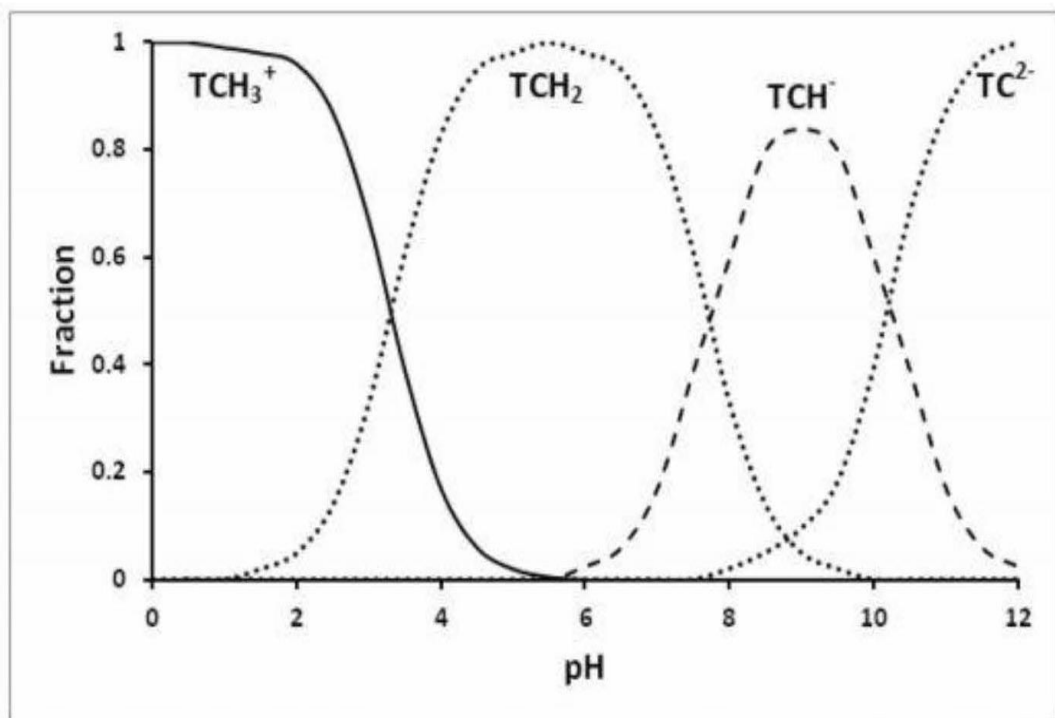


**Figure 3.17:** Effect of pH on TC structure (Zyoud et al., 2019).

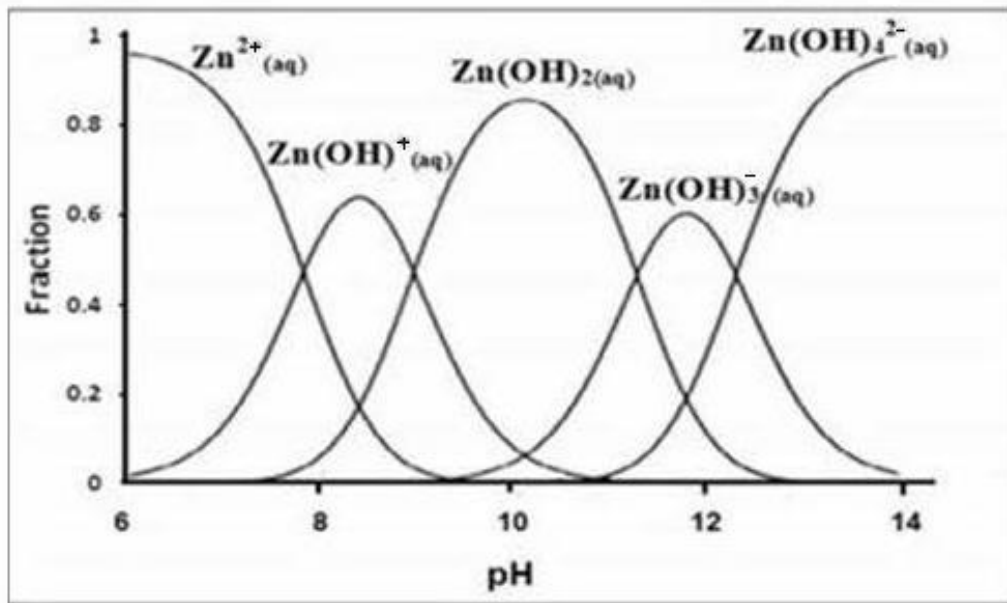


**Figure 3.18:** Effect of pH on ZnO surface structure (Zyoud et al., 2019).

Figure 3.19 shows that the best adsorption of ZnO was between pH 5 and 7. At lower or higher pH, the adsorption efficiency decreases.

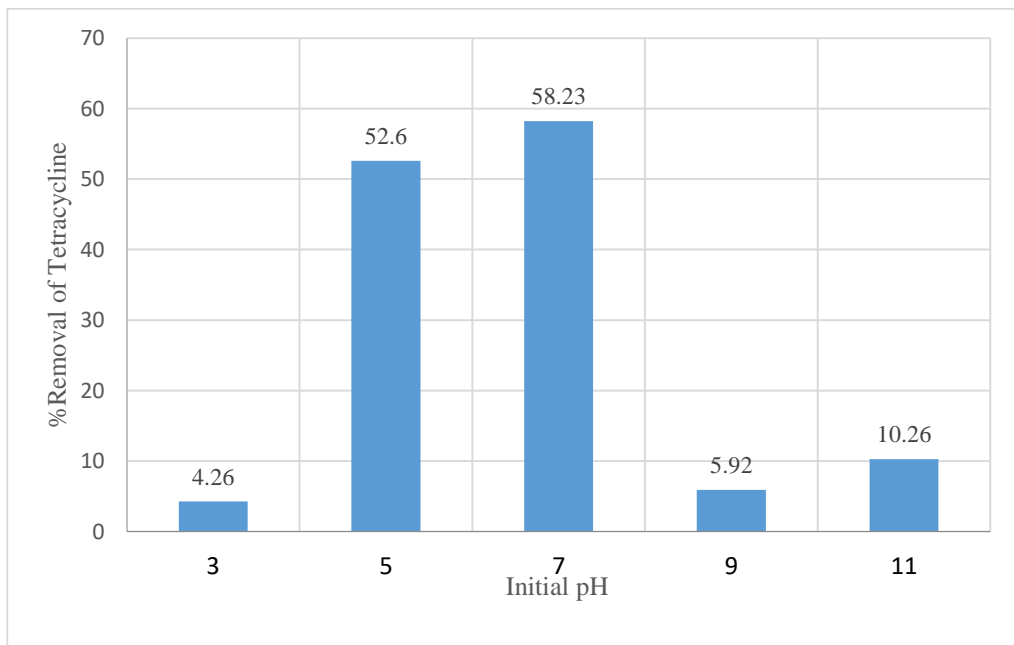


**Figure 3.19:** Effect of pH on TC percentage removal by adsorption onto ZnO adsorbent. Measurements are made using TC at (initial conc.: 100 mg/L, pH range from (3-11), temperature: 25 °C, contact time: 120 min and solid/liquid ratio: 0.1g/50 mL).

At pH  $\sim 7$ , ZnO has positive charge, and TC contains ions with negative charge. The opposite charges between the adsorbent and adsorbate increase the adsorption ability because of the electrostatic attraction between opposite ions.

At pH  $\sim 5$ , ZnO has positive charge, and TC is equilibrated as neutral to positive form. This means there is no electrostatic attraction. The high amount of removal in this case refers to the good attachment between the metal oxide (ZnO), and the ketol group at the TC structure (Zyoud et al., 2018). This attachment of neutral TC species shifts the positive ones towards the neutral, according to Le Chatelier's principle, and that increases the neutral species in the solution, which then attach with ZnO surface.

At pH  $\sim 3$ , ZnO surface charge is positive, Figure 3.18, and TC is equilibrated as neutral to positively charged species, Figures 3.17. This resemblance in surface charge causes repulsion between species. As a result, the adsorption ability decreases.

At pH  $\sim 9$ , ZnO surface has an equilibrium between positive and negative charge, as this pH value is very close to the zero point charge of ZnO ( $\text{pH}_{\text{zcp}}=9.8$ ), and TC surface is negatively charged. These negative ions at the surface of ZnO make repulsion with the similar TC charged species, which causes a clear decrease in the percentage removal of Tetracycline adsorbate.

At pH  $\sim 11$ , ZnO surface charge is negative, Figure 3.18, and TC has negatively charged equilibrium structure, Figure 3.17. This similarity in

charge of the ZnO surface and TC, make repulsion electrostatic. The adsorption efficiency thus decreases.

It is recommended that using pH between 5 and 7 is the best choice for ZnO adsorbent to get the optimum condition for TC adsorption.

## 2. Montmorillonite (MONT)

Figure 3.20 shows that MONT clay (0.1 g/50 mL) adsorbed the total amount of 100 mg/L TC at pH ~5. That means MONT is an excellent adsorbent of TC at different pH values. Thus, in order to study how pH affects the adsorption on MONT surface, a 200 mg/L TC solution was prepared and tested for pH factor.

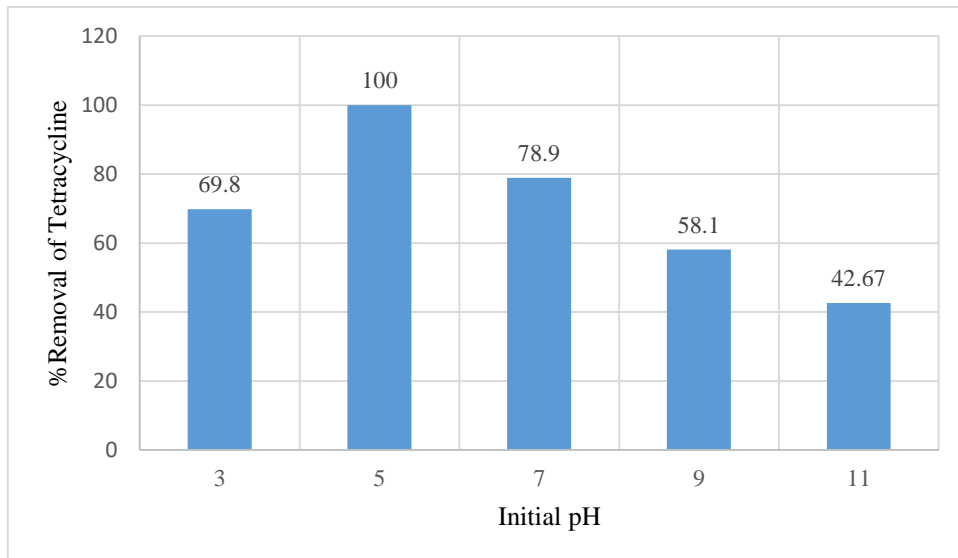


**Figure 3.20:** Effect of initial pH on the % removal of TC by adsorption onto MONT adsorbent. Measurements are made using TC at (initial conc.: 100 mg/L, pH range (3-11), temperature: 25 °C, contact time: 120 min and solid/liquid ratio: 0.1 g/50 mL).

Figure 3.21 shows that the best adsorption of TC was at pH 5. At pH ~5, MONT surface is negatively charged. TC is equilibrated as positive to neutral species. Thus, the positive ions are attracted to the negatively charged MONT clay. The opposite surface charges increase the adsorption efficiency to reach 74% (148 mg/L) from the 200 mg/L sample.

At pH ~3, also MONT makes high adsorption of TC. MONT has positive surface charge, and TC is equilibrated as neutral to positively charged species. The neutral species adsorbed at the MONT surface, because of the strong attachment between the metal oxide (at the surface of MONT clay) and the Ketol group of the TC. The other positive species are consequently shifted to convert to neutral ones, and so they have good adsorption at the surface of MONT clay.

At pH ~7 and 9, MONT clay makes a moderate adsorption of TC. MONT surface is negatively charged, and TC is equilibrated as neutral to negative species (small portion). Negative charges may cause a slightly repulsion between adsorbent and adsorbate, but the strong attachment between metal oxide in MONT clay and the ketol functional group at the surface of neutral TC species, causes shift of the equilibrium towards the neutral ions side, according to LeChatelier's principle. This increases the TC adsorption.

At pH ~11, MONT surface is negatively charged, and TC is equilibrated as totally negative charge. This similarity of charges repels TC

molecules far away from MONT surface. As a result, the adsorption efficiency is lowered.

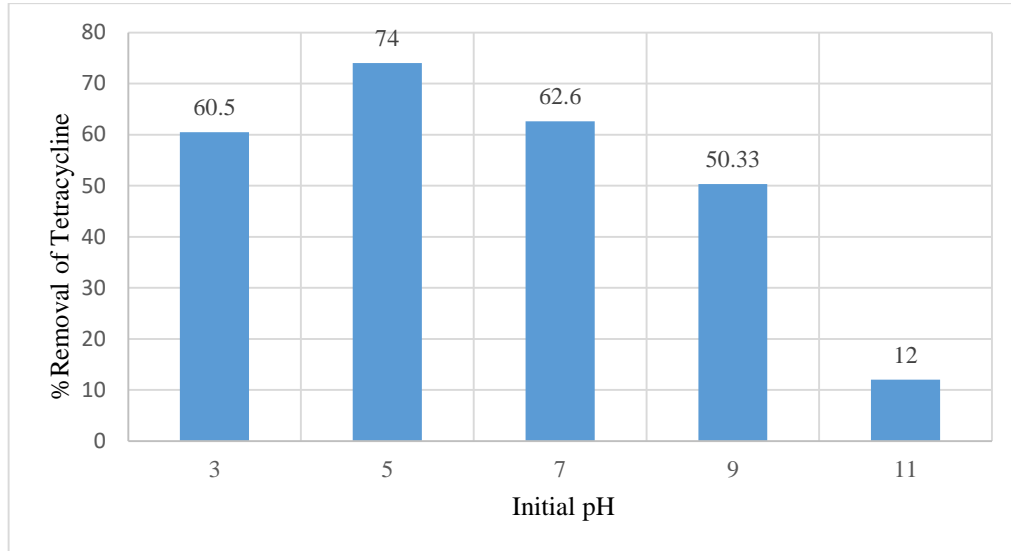


**Figure 3.21:** Effect of initial pH on the %removal of TC by adsorption onto MONT adsorbent. Measurements are made using TC at (initial conc.: 200 mg/L, pH range (3-11), temperature: 25 °C, contact time: 120 min, solid mass: 0.1g and volume of TC solution: 50 mL).

It is recommended that TC can be removed efficiently using MONT adsorbent at pH between 5 and 7 and get a maximum adsorption capacity.

### 3. Kaolinite (KANT)

KANT clay can be considered as bad adsorbent compared with MONT clay. This is referred to the large surface area of MONT (330 m<sup>2</sup>/g) compared to the KANT surfaces area (34 m<sup>2</sup>/g).

The highest adsorption that KANT has reached was 16% at pH 7, Figure 3.22.

At this pH, KANT surface charge is positive and TC is equilibrated as neutral to negative. The negative species is attracted to the positive surface of KANT as a result of electrostatic attraction. Thus,

the neutral species of TC shift to the negative side, and this increases the amount of adsorbed species.

At pH 3 to 5, KANT makes low adsorption, as it has positive surface charge and TC also has positive species. This similarity in surface charges causes repulsion between the adsorbent and adsorbate, which lowers the adsorption efficiency.

At pH ~9 and 11, KANT surface charge is negative and TC has negative charge species. This similarity in charges causes bad adsorption efficiency as a result of repulsion between the two negative surfaces of KANT and TC, which keeps them far away from each other.

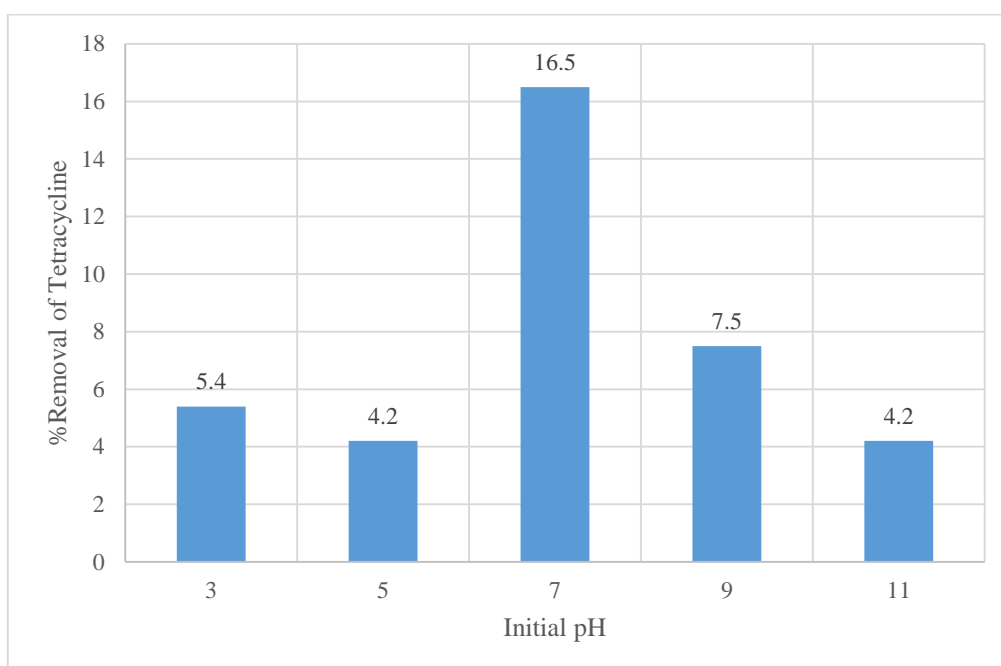


**Figure 3.22:** Effect of initial pH on the TC % removal by adsorption onto KANT adsorbent. Measurements are made using TC at (initial conc.: 100 mg/L, pH range (3-11), temperature: 25 °C, contact time: 120 min and solid/liquid ratio: 0.1 g/50 mL).

It is recommended that using pH ~7 is the best choice for KANT

#### 4. ZnO@MONT

ZnO@MONT was described as photocatalyst for removal of many contaminants (Fatimah et al., 2011; Zyoud et al., 2017). Effect of pH on TC adsorption on ZnO@MONT is useful for catalytic study. ZnO@MONT composite can be considered as good adsorbent. This is because MONT clay is an excellent adsorbent, which improves adsorption efficiency of ZnO@MONT.

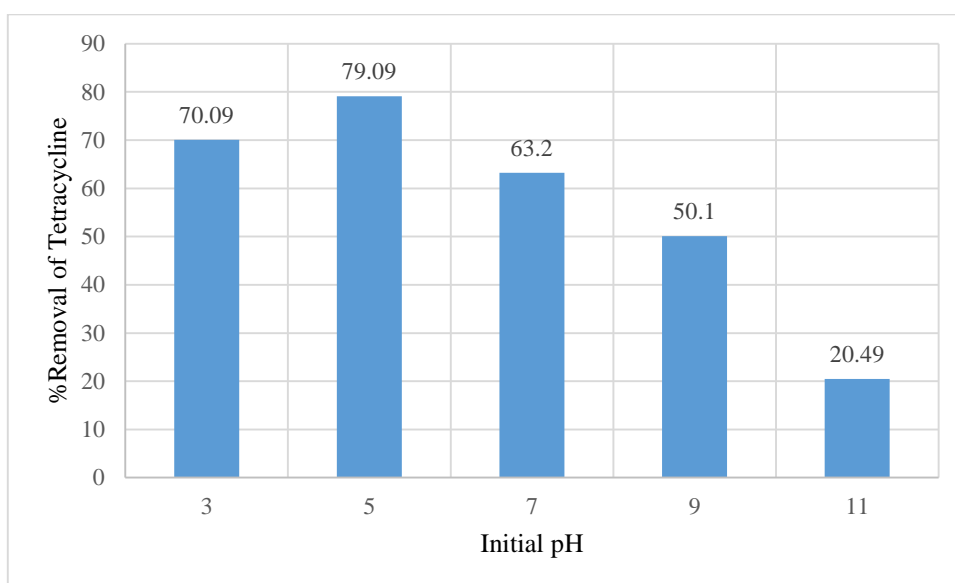


**Figure 3.23:** Effect of initial pH on the percentage removal by adsorption of TC onto ZnO@MONT composite adsorbent. Measurements are made using TC at (initial conc.: 100 mg/L, pH range from (3-11), temperature: 25 °C, contact time: 120 min and solid/liquid ratio: 0.1 g/50 mL).

Highest adsorption (79.09%) occurred at pH ~5, Figure 3.23. ZnO@MONT has positive surface charge at this pH, and TC is equilibrated as neutral to positive. Good attachment between ketol group at the neutral TC and the metal oxides of ZnO@MONT composite causes to equilibrium shift of TC positive species toward the neutral ones, resulting in increased adsorption.

At pH ~3, still a good adsorption (70.09%) occurred. ZnO@MONT surface charge is positive, and TC is equilibrated as neutral to positive. Neutral species make good attachment with ZnO@MONT (ketol group with metal oxides). Equilibrium shifts to the neutral side and increases the adsorption efficiency.

At pH ~9, ZnO@MONT clay makes a moderate adsorption of TC (50.1%) occurred. ZnO@MONT surface charge is negative and TC is equilibrated as neutral to negative (small portion). Negative charges may cause a slightly repulsion between adsorbent and adsorbate, but the ketol group at the surface of neutral TC makes good attachment with metal oxides in ZnO@MONT composite. This results in equilibrium shift of the TC negative species to become a neutral, and this, in turn, makes good adsorption with ZnO@MONT.

At pH ~7, a good adsorption (63.2%) occurred. The value less than other values.

ZnO@MONT is almost neutral, and TC is equilibrated as neutral to negative.

Neutral species of TC make good attachment on the neutral ZnO@MONT (ketol group with metal oxides). This shifts the equilibrium to the neutral side, and increases the adsorption efficiency.

At pH ~11, bad adsorption (20.49%) occurred. ZnO@MONT has a negative surface charge, and TC is equilibrated as negative. This similarity

between the charges causes an electrostatic repulsion, Thus, TC becomes far away from ZnO@MONT adsorbent.

It is recommended that TC can be removed efficiently using ZnO@MONT adsorbent at pH ~5 to get a maximum adsorption capacity.

## **5. ZnO@KANT**

ZnO@KANT was described as photocatalyst in light driven degradation of contaminants (Kutláková et al., 2015; Zyoud et al., 2019). Adsorption study of ZnO@KANT is therefore necessary.

ZnO@KANT can be considered as good adsorbent, compared with KANT clay. Figure 3.24 shows that the best adsorption (54.92%) was at pH ~7. ZnO@KANT is almost neutral, and TC is equilibrated as neutral to negative. The neutral species of TC make good attachment on the neutral ZnO@KANT (ketol group with metal oxides). Equilibrium of TC shifts it to the neutral side, which increases the adsorption efficiency.

At pH ~5, adsorption efficiency (53.6%) was high. At this pH, ZnO@KANT has positive surface charge, and TC is equilibrated as neutral to positive.

Neutral species of TC make good attachment with ZnO@KANT (ketol group with metal oxides). This equilibrium of TC shifts it to the neutral side, which increases the adsorption efficiency.

At pH ~3, adsorption (9.5%) was very low. At this pH, ZnO@KANT has positive surface charge, and TC has positive charge. Positive

charges make electrostatic repulsion, which decreases the adsorption process as the adsorbent surface and adsorbate become far away from each other.

At pH ~9, also adsorption (9.5%) was low. At this pH, ZnO@KANT surface charge is negative, and TC has negative charge. This similarity of surface charges causes electrostatic repulsion, which lowers the adsorption process.

At pH ~11, adsorption (8.5%) was also very low. At pH ~11, ZnO@KANT has negative surface charge, and TC is totally negative. Negative surface charges repel each other, which keeps the TC molecules far away from the adsorbent.

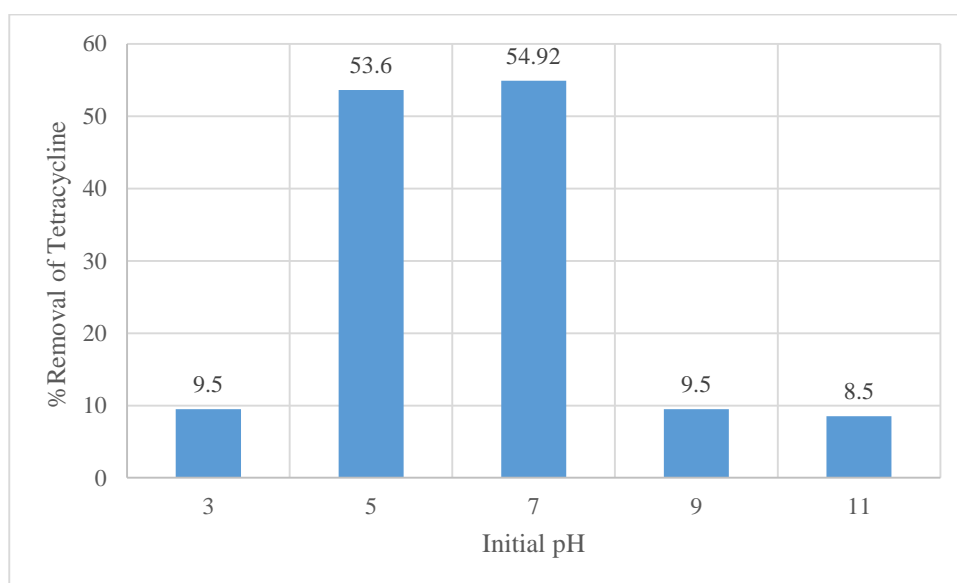


**Figure 3.24:** Effect of initial pH on the TC % removal by adsorption onto ZnO@KANT composite adsorbent. Measurements were taken using TC at (initial conc. : 100 mg/L, pH range (3-11), temperature: 25 °C, contact time: 120 min, adsorbent amount: 0.1 g and solution volume: 50mL).

It is recommended that using pH between 5 and 7 is the best choice for ZnO@KANT adsorbent to get the maximum adsorption capacity of TC.

### 3.2.4 Effect of TC concentration

Adsorption capacity of TC on the different adsorbents (ZnO, MONT, KANT, ZnO@MONT and ZnO@KANT) was studied using different initial concentrations, while using other conditions the same.

#### 1. ZnO

For ZnO, TC concentrations, 100, 130, 160 and 190 mg/L, were used. Figure 3.25 shows that the percentage of removal changes with changing concentration. At 190 mg/L, the highest percentage of removal was achieved (58%). %Removal is not best indicator about adsorption efficiency because of using different concentrations.

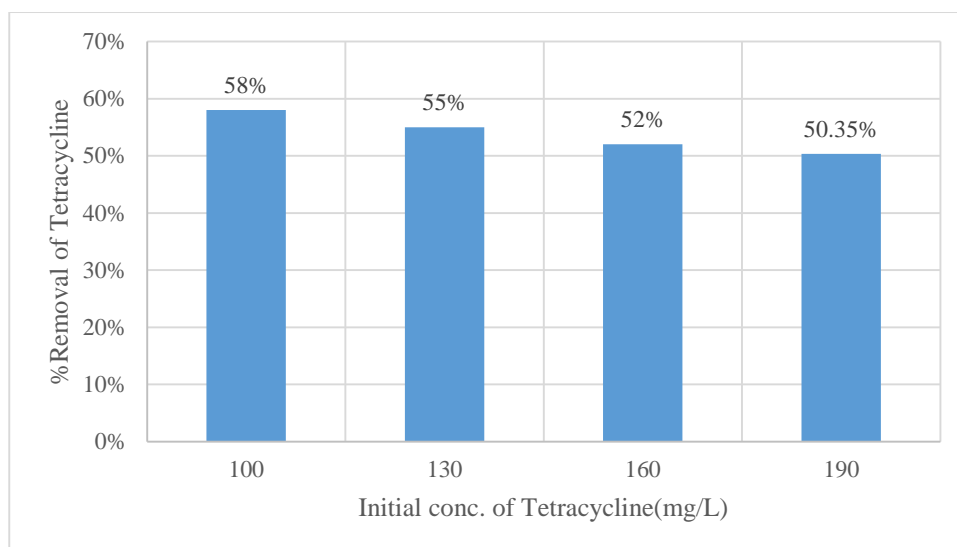


**Figure 3.25:** Effect of Tetracycline concentration on its % removal by adsorption onto the surface of ZnO adsorbent. Measurements were made using 100, 130, 160, 190 and 210 mg/L initial TC concentrations, natural pH, room temperature, contact time of 120 min and 0.1 g of ZnO in 50 mL of TC.

The amount of adsorbed TC molecules by ZnO was calculated. Figure 3.26 shows that increasing the concentration of TC results in increase in the amount of adsorbed TC.

The maximum adsorption was at 190 mg/L (96 mg/L, 58% Removal), and the lowest adsorption was at 100mg/L (58 mg/L, 58% Removal).

Therefore, amount of adsorbed TC increases with its nominal concentration, which indicates that the increase in TC concentration will equilibrate and increase the amount of adsorbed TC on the composite surface.

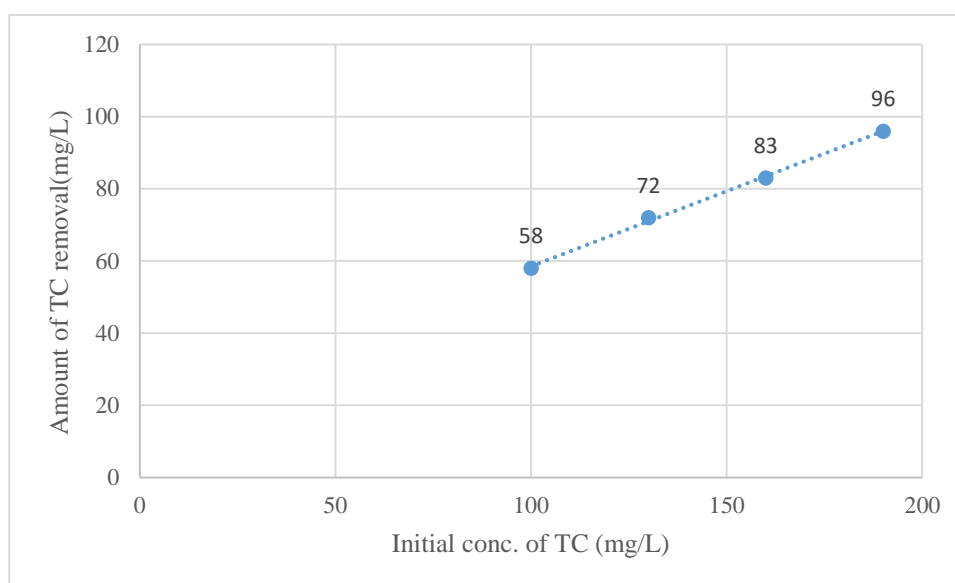


**Figure 3.26:** Effect of TC concentration on its removal amount (mg/L) onto the surface of ZnO adsorbent. Measurements were made using 100, 130, 160, 190 and 210 mg/L initial TC concentrations, natural pH, room temperature, contact time of 120 min and 0.1g /50mL solid/liquid ratio.

## 2. MONT

For MONT adsorbent, concentrations of TC that have been studied were 150, 250, 300 and 350 mg/L. Figure 3.27 shows that as the concentration of adsorbate increases, the percentage of removal decreases. The highest percentage of removal was at 150 mg/L concentration (89.48% Removal). But the percentage can't be good indicator about effect of concentration.

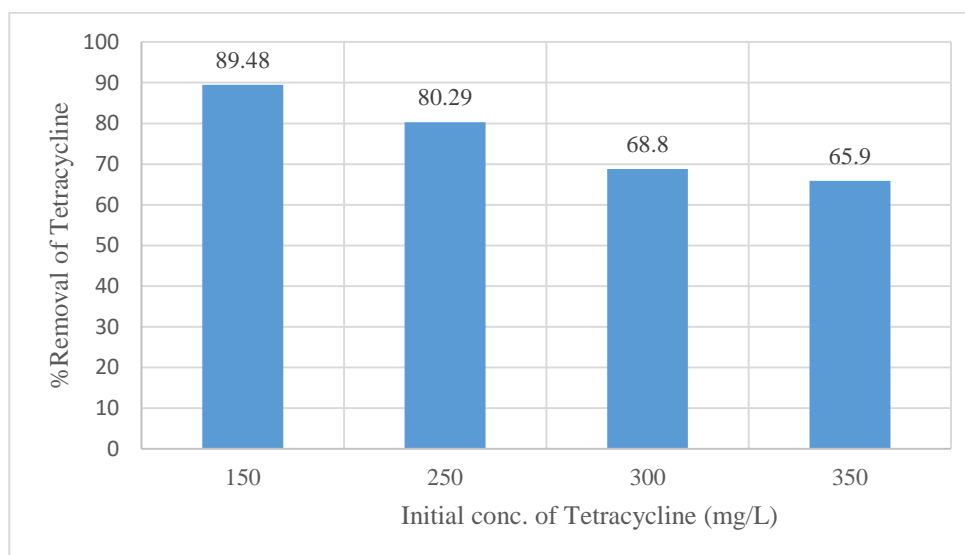


**Figure 3.27:** Effect of TC concentration on its % removal by adsorption onto the surface of MONT adsorbent. Measurements were made using 150, 250, 300 and 350 mg/L initial TC concentrations, natural pH, room temperature, 120 min contact time and 0.1 g of MONT in 50 mL of TC.

The amount of adsorbed TC molecules by MONT was calculated for each concentration. Figure 3.28 shows that when the concentration of TC increases, the adsorbed amount also increases. Which indicates that the increase in TC concentration will equilibrate and increase the amount of adsorbed TC on the composite surface.

The highest amount of adsorbate was (230.65 mg/L, 65.9% Removal) for initial concentration 350 mg/L, and the lowest amount was (134.22 mg/L, 89.48% Removal) for initial concentration 150 mg/L.

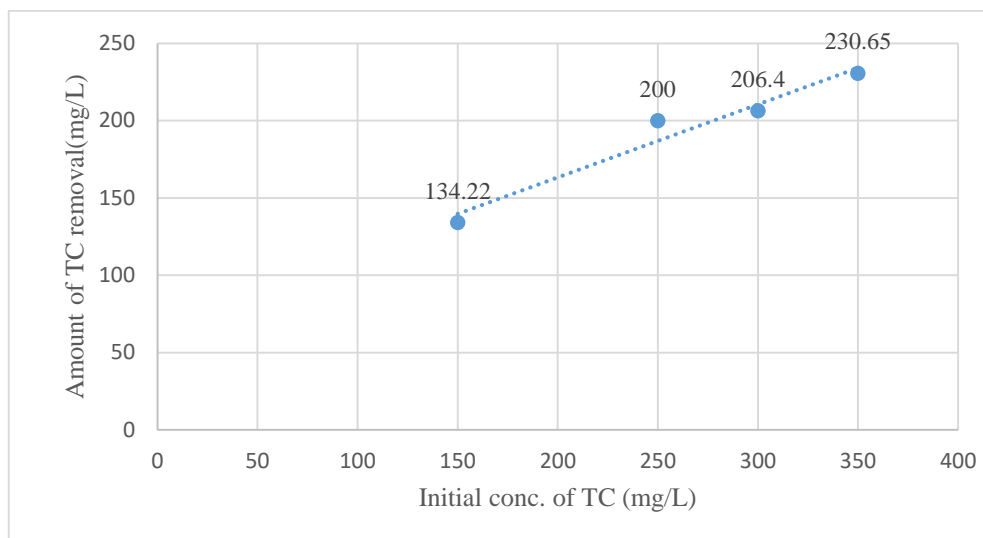


**Figure 3.28:** Effect of TC concentration on amount of adsorption onto the surface of MONT adsorbent. Measurements were made using 150, 250, 300 and 350 mg/L initial TC concentrations, natural pH, room temperature, 120 min contact time and 0.1 g/50 mL solid/liquid ratio.

### 3. KANT

For KANT solid, contaminant concentrations that have been investigated were 20, 40, 60 and 80 mg/L. Figure 3.29 shows that the highest percent of removal was at 20 mg/L concentration (32.15% Removal). But the percentage can't be good indicator about effect of concentration.

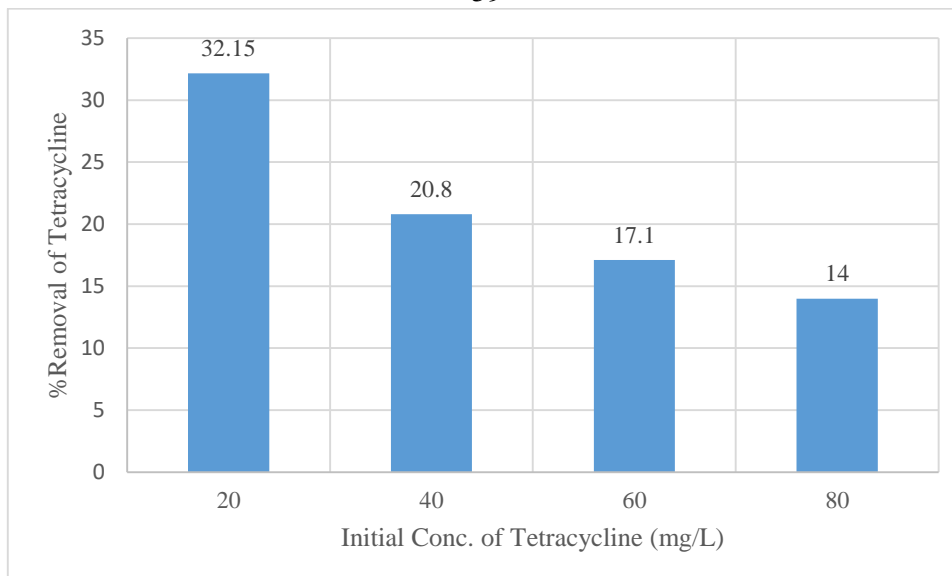


**Figure 3.29:** Effect of TC concentration on its % removal by adsorption onto KANT adsorbent surface. Measurements were made using 20, 40, 60 and 80 mg/L initial TC concentrations, natural pH, room temperature, 120 min contact time and 0.1 g of KANT in 50 mL of TC.

Amount of adsorbed TC molecules was calculated. Figure 3.30 shows that the adsorbed amount of TC increases with increasing TC concentration. Which indicates that the increase in TC concentration will equilibrate and increase the amount of adsorbed TC on the composite surface.

The maximum adsorbed amount was at 80 mg/L TC solution (11.2 mg/L, 14% Removal), and the lowest adsorbed amount was at 20 mg/L TC solution (6.43 mg/L, 32.15% Removal).

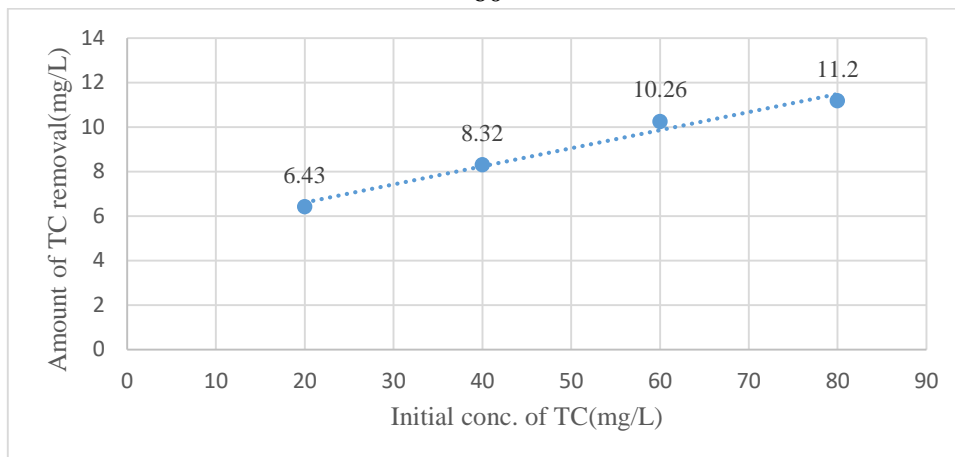


**Figure 3.30:** Effect of TC concentration on its removal by adsorption onto KANT adsorbent. Measurements were made using 20, 40, 60 and 80 mg/L initial concentrations, natural pH, room temperature, 120 min contact time and solid/liquid ratio of 0.1g/50 mL.

#### 4. ZnO@MONT

For ZnO@MONT adsorbent, TC concentrations that have been studied were 130, 160, 190 and 210 mg/L. Figure 3.31 shows that the highest percentage of removal was at 160 mg/L TC solution (68.7% Removal). The percentage can't be real indicator about the adsorption efficiency.

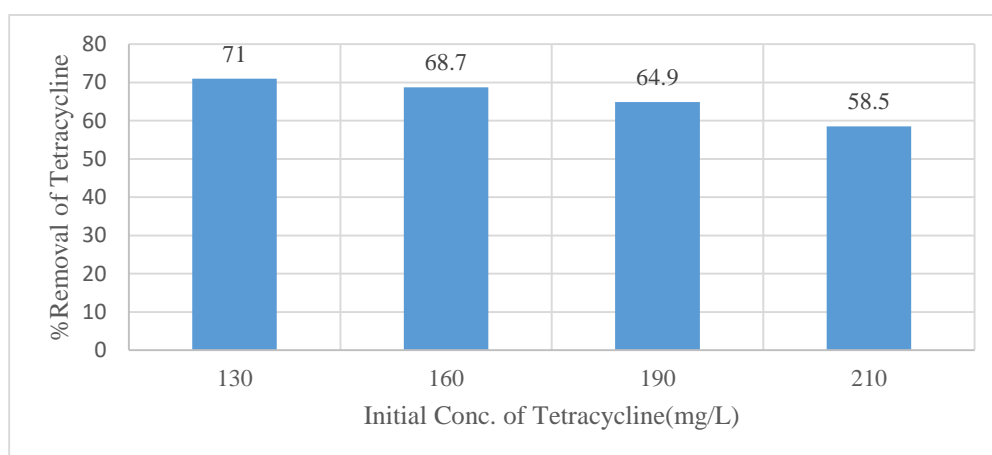


**Figure 3.31:** Effect of TC concentration on its % removal by adsorption onto the surface of ZnO@MONT adsorbent. Measurements were made using 130, 160, 190 and 210 mg/L initial TC concentrations, natural pH, room temperature, 120 min contact time and 0.1 g of ZnO@MONT in 50 mL of TC.

Amount of adsorbed TC was calculated. Figure 3.32 shows that at higher concentration of TC, its adsorbed amount becomes higher. Which indicates that the increase in TC concentration will equilibrate and increase the amount of adsorbed TC on the composite surface. The maximum adsorbed amount was (122.85 mg/L, 58.5% Removal) for initial TC 210mg/L. The minimum adsorbed amount for initial TC 130 mg/L solution was (92.3 mg/L, 71% Removal).

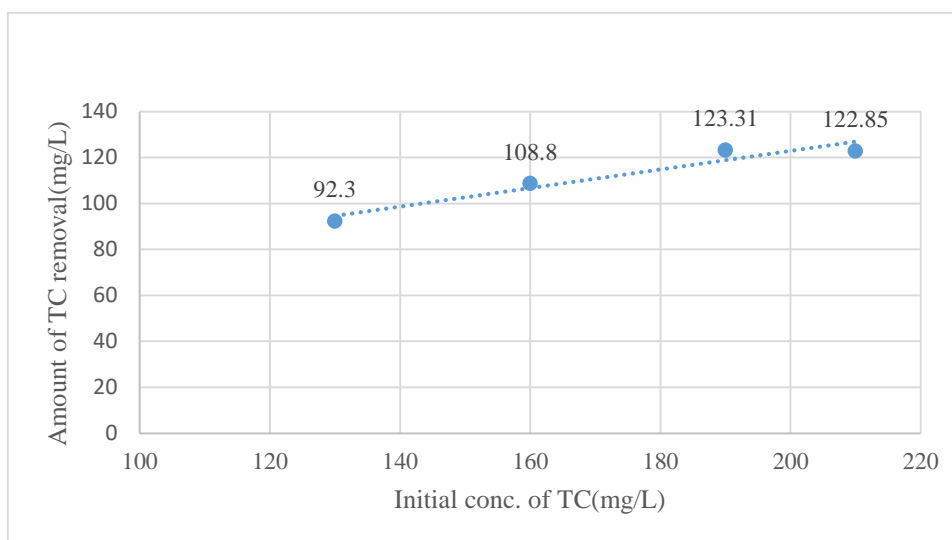


**Figure 3.32:** Effect of TC concentration on amount of adsorption onto the surface of ZnO@MONT adsorbent. Measurements were made using 130, 160, 190 and 210 mg/L initial TC concentrations, natural pH, room temperature, 120 min contact time and 0.1 g/50 mL solid/liquid ratio.

## 5. ZnO@KANT

For ZnO@KANT, TC initial concentrations that have been used were 70, 130, 160 and 190 mg/L. Figure 33 shows that their small differences between results of adsorption. The highest percentage of removal (68%) was at 70 mg/L TC concentration. The percentage of removal can't be good indicator about the effect of concentration.

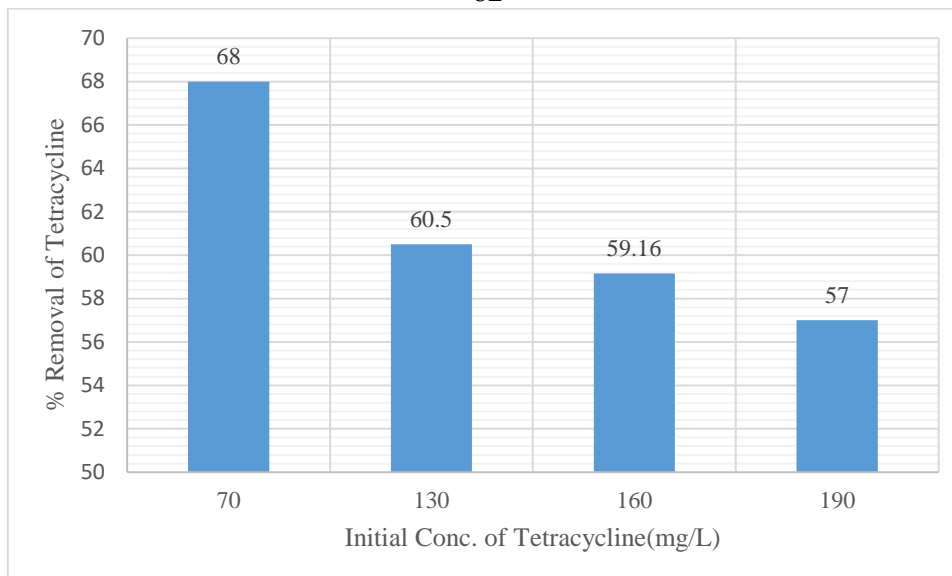


**Figure 3.33:** Effect of TC concentration on its % removal onto the ZnO@KANT adsorbent surface. Measurements were made using 70, 130, 160 and 190 mg/L initial TC concentrations, natural pH, room temperature, 120 min contact time and 0.1 g/50 mL solid/liquid ratio.

Amount of adsorbed TC contaminant was calculated. Figure 3.34 shows that increasing in the TC initial concentration, gives higher adsorption of this adsorbate. Which indicates that the increase in TC concentration will equilibrate and increase the amount of adsorbed TC on the composite surface. The TC initial concentration 190 mg/L showed highest adsorption (108.5 mg/L, 57% Removal), and the lowest adsorbed amount of was (47 mg/L, 68% Removal) occurred for TC initial concentration 70 mg/L.

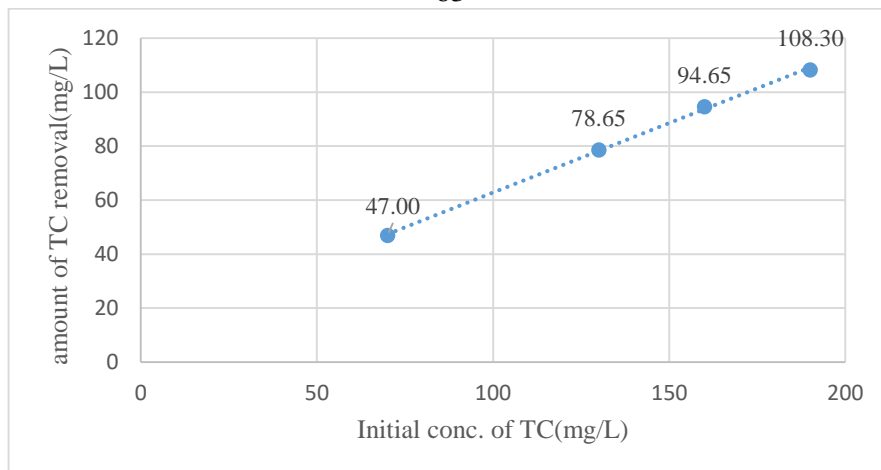


**Figure 3.34:** Effect of TC concentration on its removal amount by adsorption onto the surface of ZnO@KANT adsorbent. Measurements were made using 70, 130, 160 and 190 mg/L initial concentrations, natural pH, room temperature, 120 min contact time and 0.1 g ZnO@KANT in 50 mL TC.

### 3.2.5 Effect of contact time

Effects of contact time on % removal of TC by different adsorbents are shown in Figure 3.35.

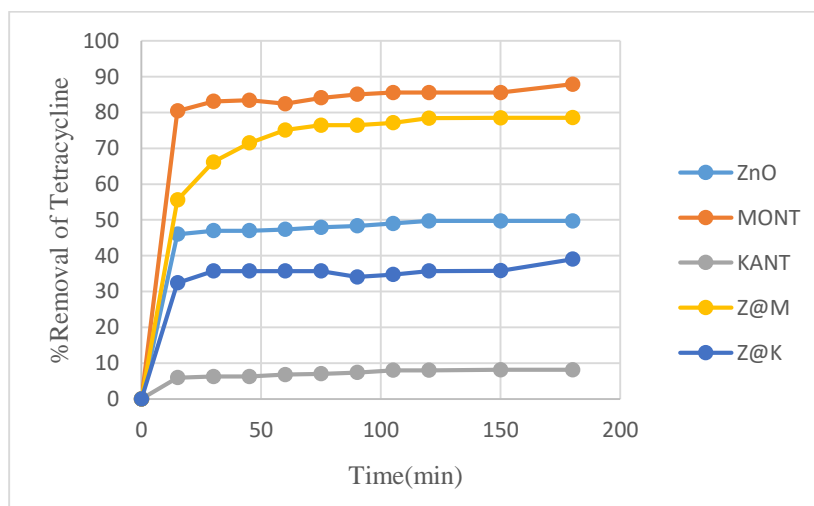


**Figure 3.35:** Effect of contact time on the % removal of TC by adsorption onto different adsorbents. Measurements were made using initial TC concentration: 100 mg/L, natural pH, room temperature and solid/liquid ratio: 0.1 g/50 mL. For MONT, 200 mg/L TC was used.

Maximum TC removal for ZnO, MONT, KANT, ZnO@MONT and ZnO@KANT were 45.9%, 87.8%, 7.2%, 78.4% and 39.02% respectively, adsorbent amount 0.1g/50 mL, initial natural pH, 25 °C and initial concentration 100 mg/L in approximately 2 hours. For MONT, 200 mg/L TC was used. TC removal is fast for the first 15 min, and then it was slowed down until equilibrium.

Based on Figure 3.35, equilibrium adsorption values were taken after ~120 min time.

### 3.2.6 Adsorption isotherms

Adsorption isotherms are good tools to describe how the adsorption process happen (B. B. Mohammed et al., 2019). It also gives an indication about the adsorption capacity.

Adsorption isotherms of TC onto ZnO, MONT, KANT, ZnO@MONT and ZnO@KANT at room temperature are shown in figures (3.36-3.40).

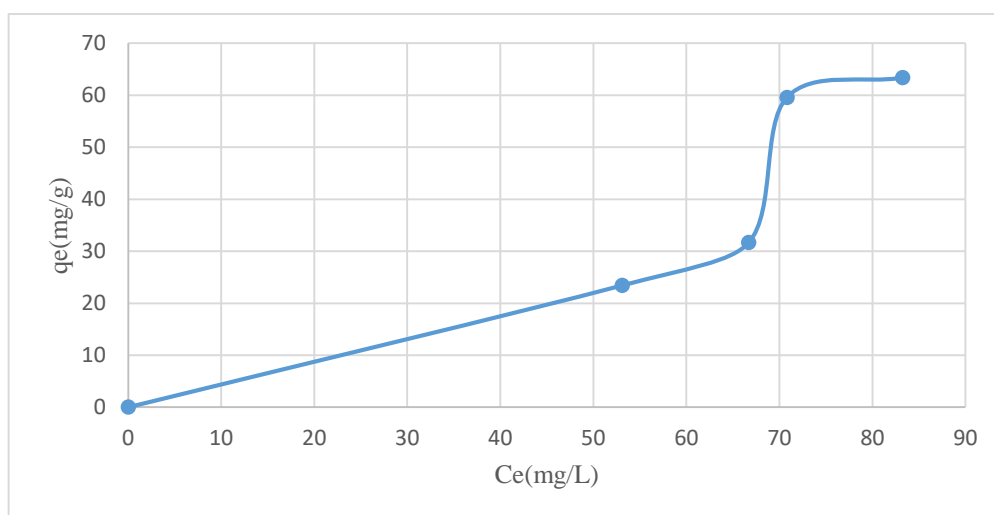


**Figure 3.36:** Equilibrium adsorption isotherm of TC onto ZnO. Measurements were made using 100, 130, 190 and 210 mg/L initial TC concentrations, room temperature, natural pH, contact time: 120 min and solid/liquid ratio: 0.1 g/50 mL.

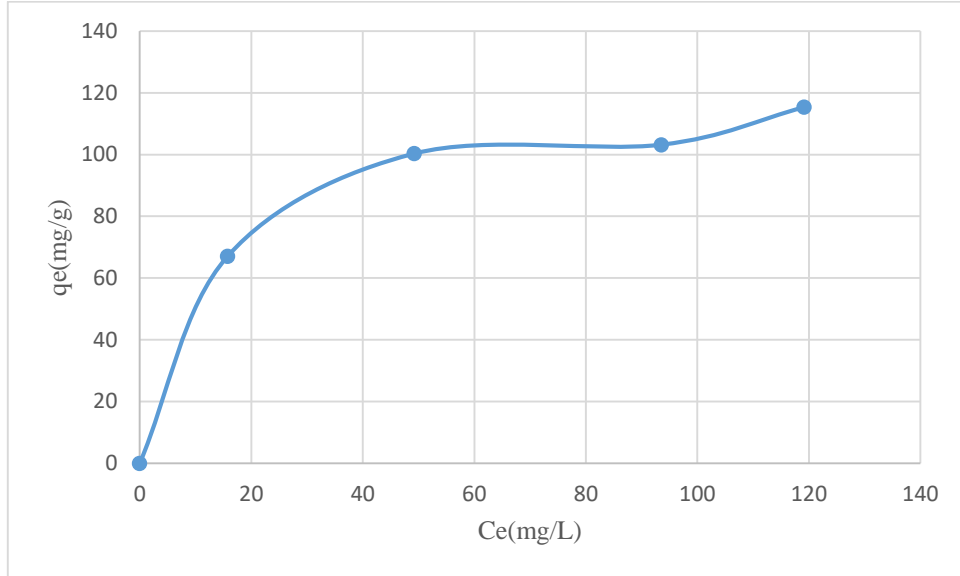


**Figure 3.37:** Equilibrium adsorption isotherm of TC onto MONT. Measurements were made using 150, 250, 300 and 350 mg/L initial TC concentrations, natural pH, contact time: 120 min and solid/liquid ratio: 0.1 g/50 mL.

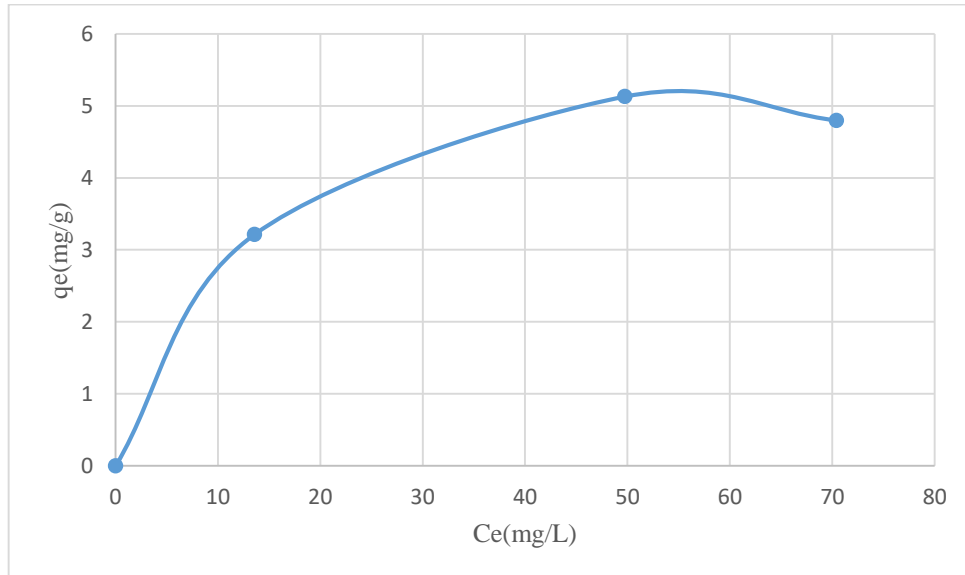


**Figure 3.38:** Equilibrium adsorption isotherm of TC onto KANT. Measurements were made using 20, 60 and 80 mg/L initial TC concentrations, room temperature, natural pH, contact time: 120 min and solid/liquid ratio: 0.1 g/50 mL.

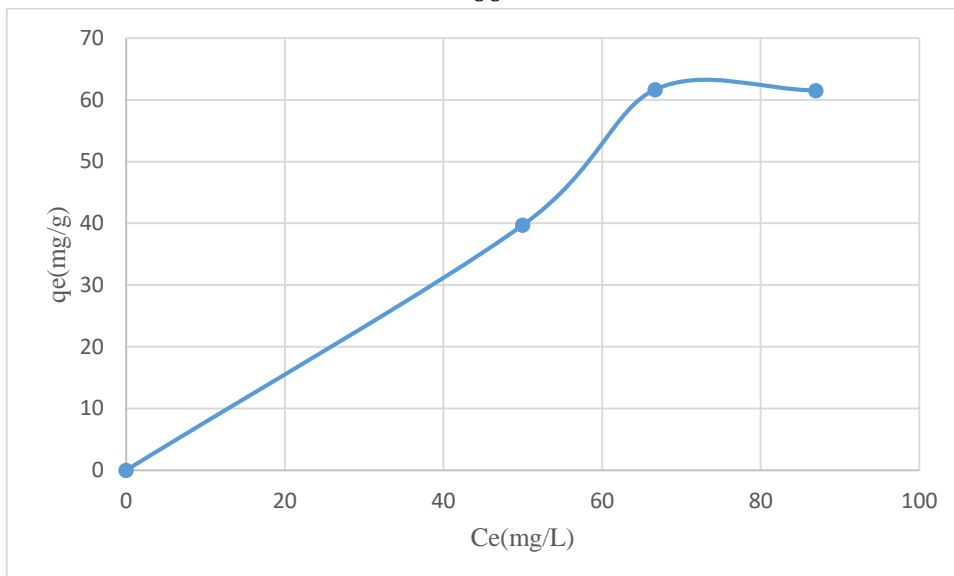


**Figure 3.39:** Equilibrium adsorption isotherm of TC onto ZnO@MONT. Measurements were made using 130, 190 and 210 mg/L initial TC concentrations, room temperature, natural pH, contact time: 120 min and solid/liquid ratio: 0.1 g/50 mL.

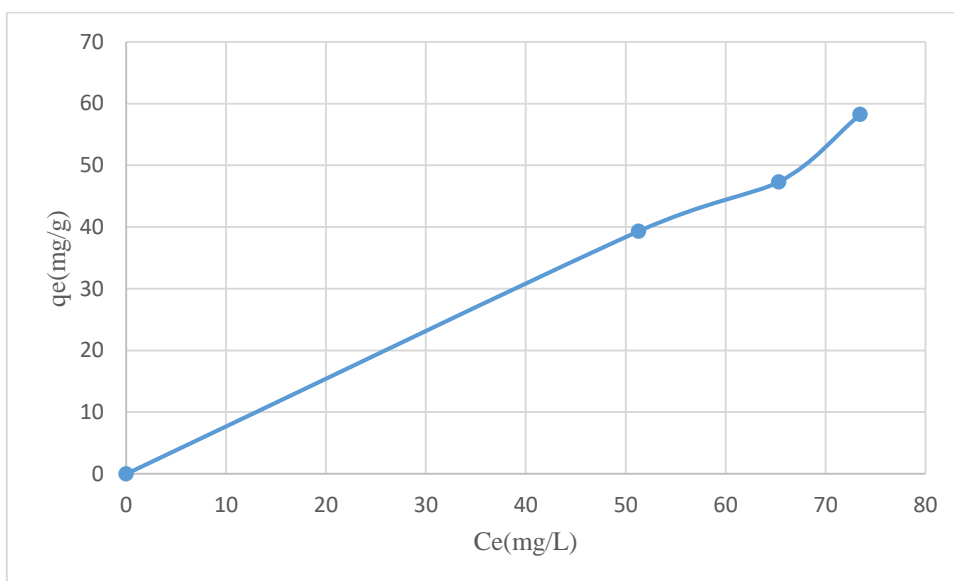


**Figure 3.40:** Equilibrium adsorption isotherm of TC onto ZnO@KANT. Measurements were made using 130, 160 and 190 mg/L initial TC concentrations, room temperature, natural pH, 120 min and solid/liquid ratio: 0.1 g/50mL.

Langmuir and Freundlich isotherm models were examined in this work in order to describe the relation between the amounts of TC adsorbed on the different adsorbents and equilibrium concentration 25 °C.

The adsorption data were fitted to Langmuir by plotting  $C_e/q_e$  versus  $C_e$ , Figures (3.41-3.45) for each adsorbent.

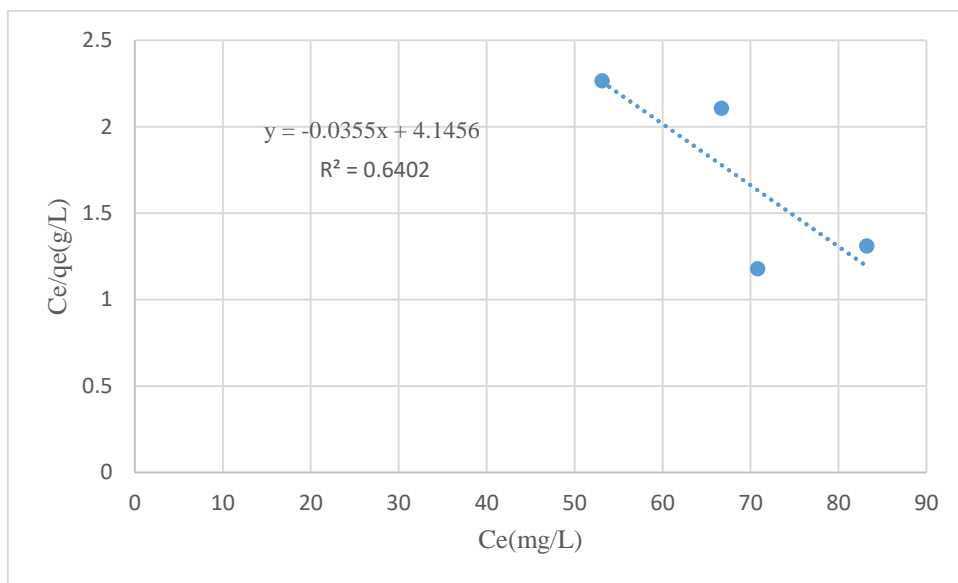


**Figure 3.41:** Langmuir plot for TC adsorption onto ZnO. Measurements were made using 100, 130, 190 and 210 mg/L initial TC concentrations, room temperature, natural pH, contact time: 120 min and solid/liquid ratio 0.1 g/50 mL.

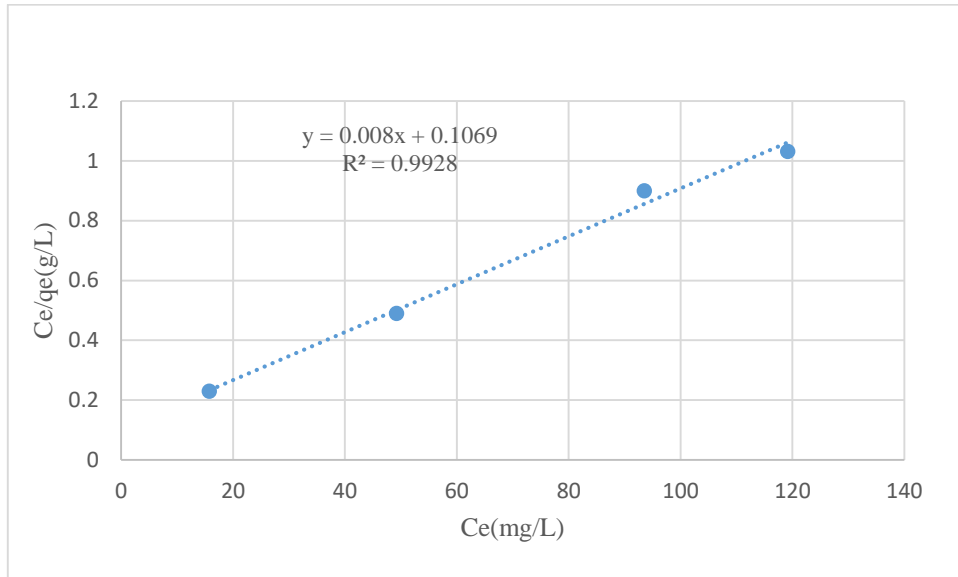


**Figure 3.42:** Langmuir plot for TC adsorption onto MONT. Measurements were made using 150, 250, 300 and 350 mg/L initial TC concentrations, room temperature, natural pH, contact time: 120 min and solid/liquid ratio 0.1 g/50 mL.

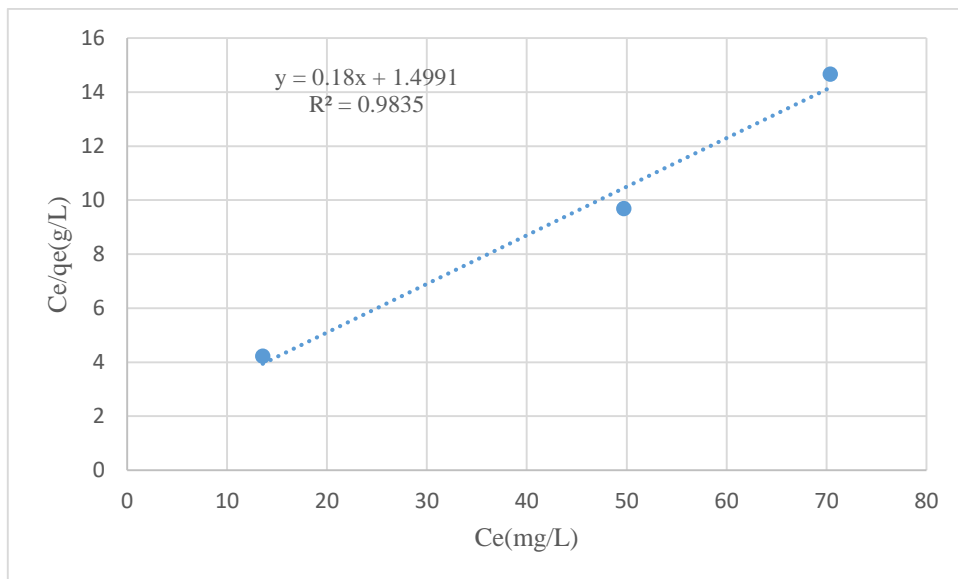


**Figure 3.43:** Langmuir plot for TC adsorption onto KANT. Measurements were made using 20, 60 and 80 mg/L initial TC concentrations, room temperature, natural pH, contact time: 120 min and solid/liquid ratio 0.1 g/50 mL.

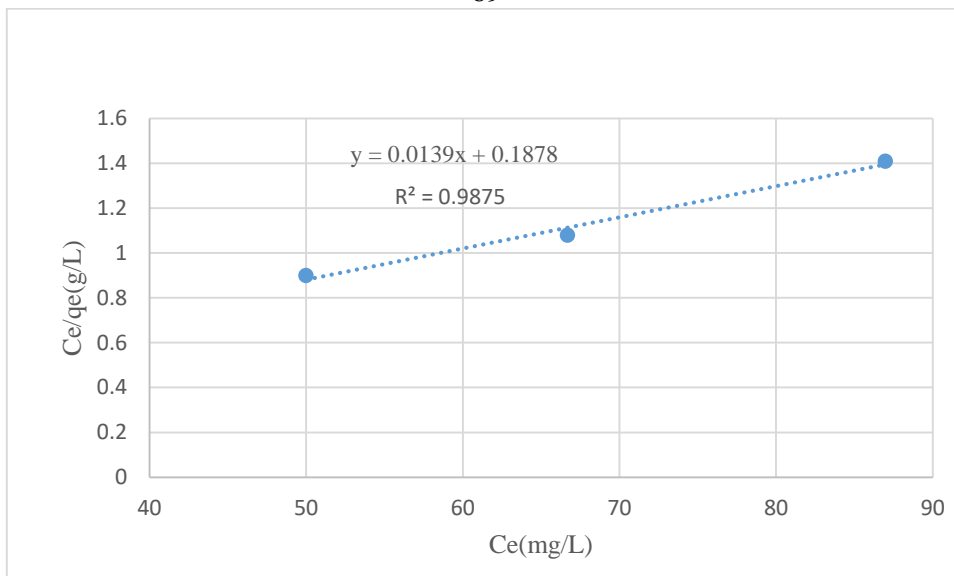


**Figure 3.44:** Langmuir plot for TC adsorption onto ZnO@MONT. Measurements were made using 130, 190 and 210 mg/L initial TC concentrations, room temperature, natural pH, contact time: 120 min and solid/liquid ratio 0.1 g/50 mL.

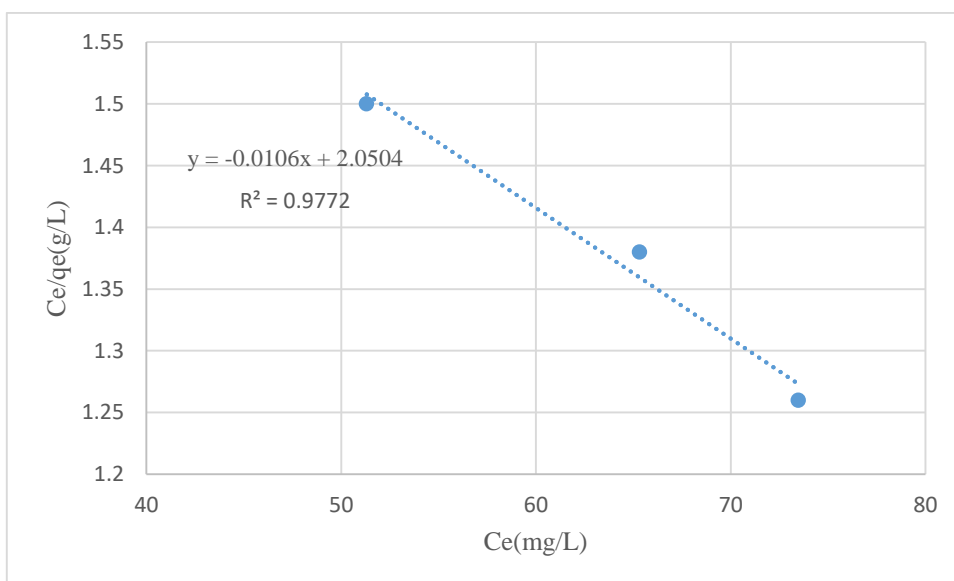


**Figure 3.45:** Langmuir plot for TC adsorption onto ZnO@KANT. Measurements were made using 130, 160 and 190 mg/L initial TC concentrations, room temperature, natural pH, contact time: 120 min and solid/liquid ratio 0.1 g/50 mL.

Adsorption data were also fitted to Freundlich equations by plotting  $\log q_e$  versus  $\log C_e$ , Figures (3.46-3.50) for each adsorbent.

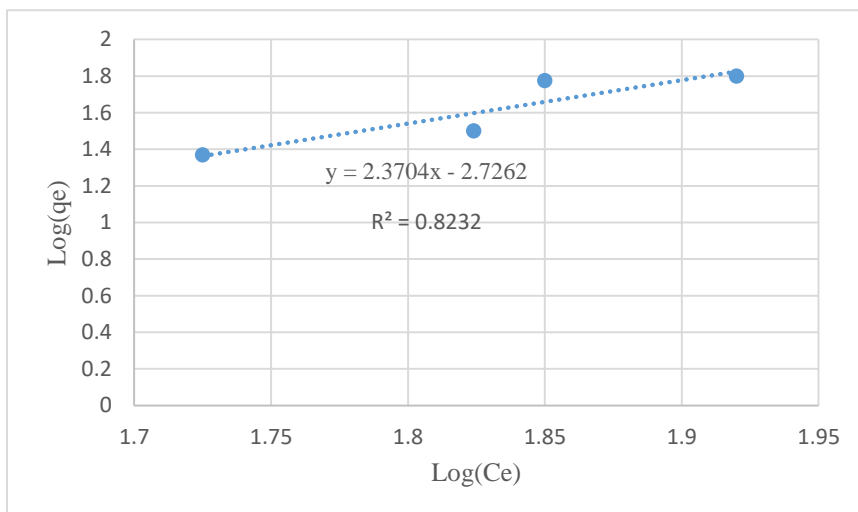


**Figure 3.46:** Freundlich plot for TC adsorption onto ZnO. Measurements were made using 100, 130, 190 and 210 mg/L initial TC concentrations, room temperature, natural pH, contact time: 120 min and solid/liquid ratio 0.1 g/50 mL.

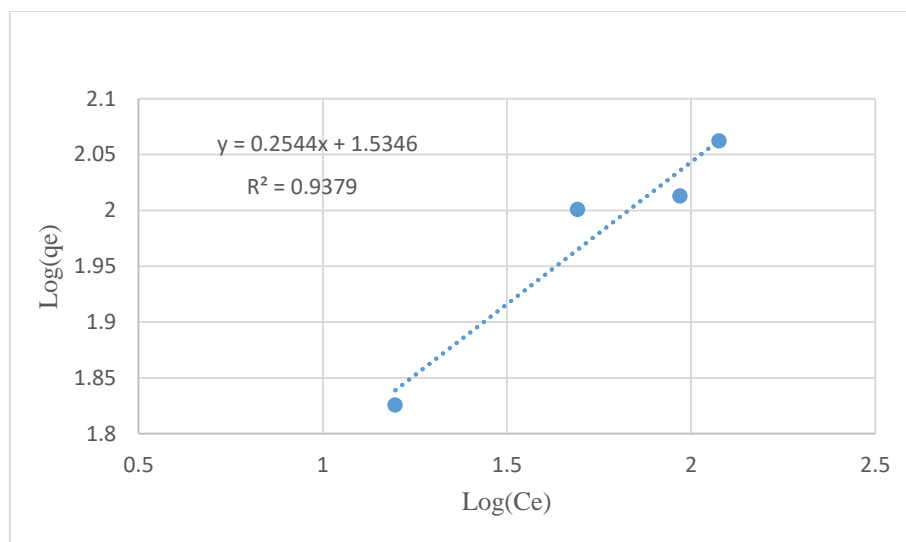


**Figure 3.47:** Freundlich plot for TC adsorption onto MONT. Measurements were made using 150, 250, 300 and 350 mg/L initial TC concentrations, room temperature, natural pH, contact time: 120 min and solid/liquid ratio 0.1 g/50 mL.

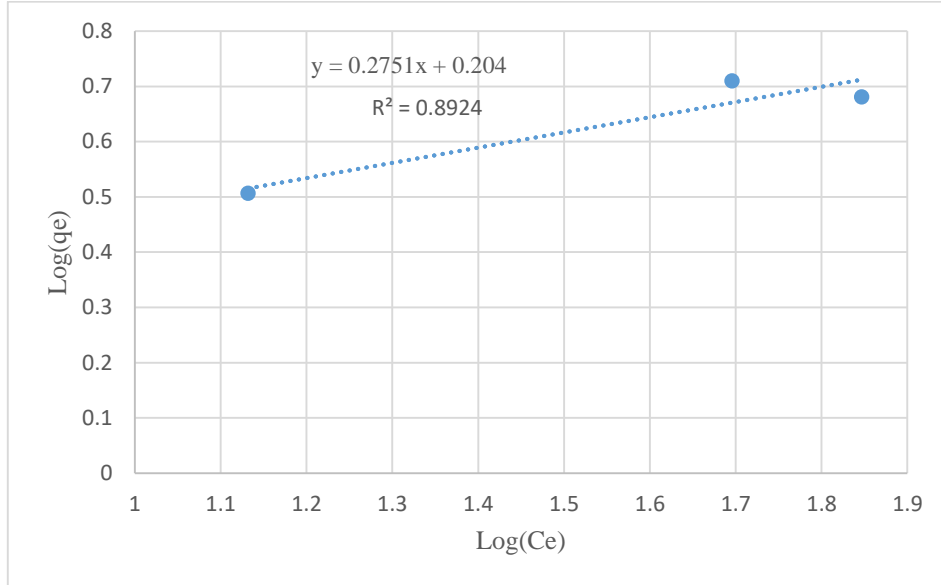


**Figure 3.48:** Freundlich plot for TC adsorption onto KANT. Measurements were made using 20, 60 and 80 mg/L initial TC concentrations, room temperature, natural pH, contact time: 120 min and solid/liquid ratio 0.1 g/50 mL.

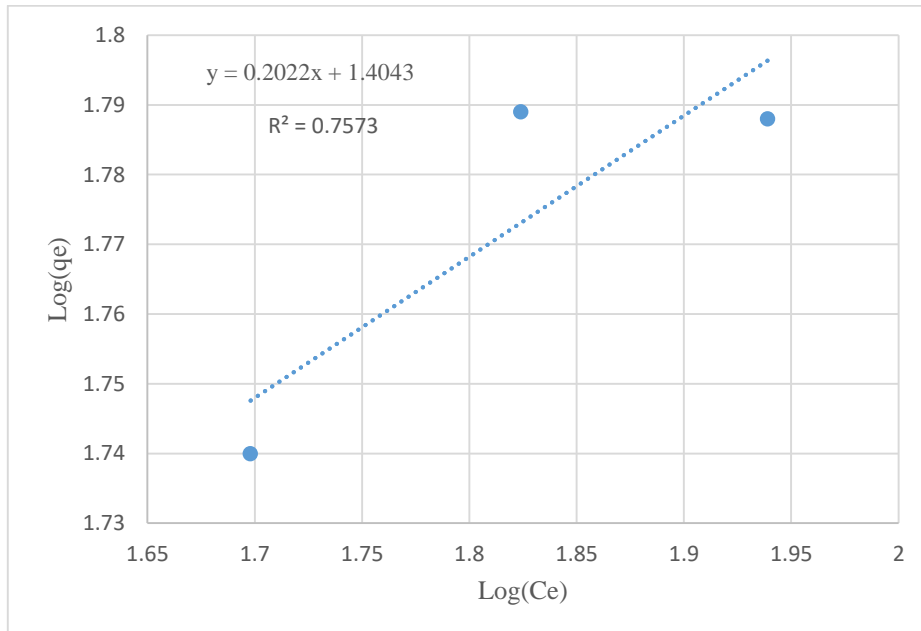


**Figure 3.49:** Freundlich plot for TC adsorption onto ZnO@MONT. Measurements were made using 130, 190 and 210 mg/L initial TC concentrations, room temperature, natural pH, contact time: 120 min and solid/liquid ratio 0.1 g/50 mL.

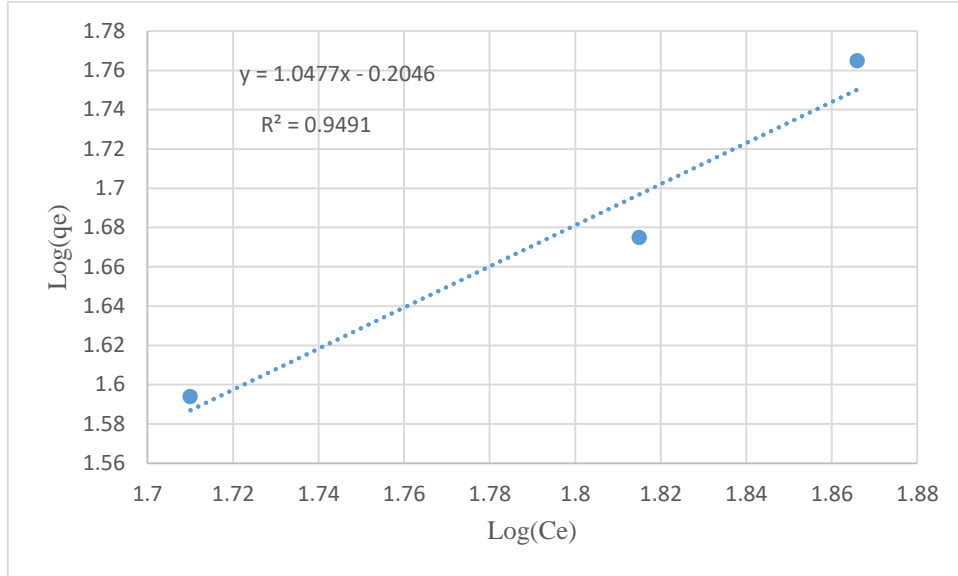


**Figure 3.50:** Freundlich plot for TC adsorption onto ZnO@KANT. Measurements were made using 130, 160 and 190 mg/L initial TC concentrations, room temperature, natural pH, contact time: 120 min and solid/liquid ratio 0.1 g/50 mL.

From the graphs above, Langmuir and Freundlich isotherm parameters were calculated using the slope and intercept by applying the Langmuir and Freundlich equations (2.2 and 2.3). The values and the correlation coefficients of the TC adsorption on different adsorbents are shown in Table 3.2.

**Table 3.2: Langmuir and Freundlich isotherm parameters and correlation coefficients for TC adsorption onto different adsorbents.**

Isotherm	Langmuir			Freundlich		
Adsorbent	Parameters			Parameters		
	$Q_0$ (mg/g)	$b$ (L/mg)	$R^2$	$K_f$ ((mg/g)(L/mg) <sup>1/n</sup> )	$n$	$R^2$
ZnO	-28.57	-0.008	0.640	0.0019	0.421	0.8232
MONT	125	0.074	0.992	34.24	3.93	0.9379
KANT	7.39	0.020	0.983	1.599	3.63	0.8924
ZnO@MONT	71.9	0.074	0.987	25.11	4.949	0.7575
ZnO@KANT	-94.33	-0.005	0.977	0.624	0.954	0.949

From table 3.2, each different adsorbent fit a different isotherm, depending on their properties. For ZnO and ZnO@KANT, adsorption capacity values have a negative sign; which means that these adsorbents don't obey the Langmuir isotherm, while the Freundlich isotherm was more suitable adsorption isotherm module (Banerjee & Chattopadhyaya, 2017). However, those adsorbents are not good enough for TC adsorption, as concluded from the results of  $K_F$  and  $(n)$  in the Table 3.2.  $K_F$  Freundlich constant gives an idea about the adsorption capacity,  $(n)$  can be considered as an indicator for the adsorption process efficiency; when  $n$  has a value between 1 and 10, we can see that the adsorption process is effective.  $K_F$  values of ZnO and ZnO@KANT are 0.0019 and 0.624, respectively. The  $(n)$  values are 0.421 and 0.95 for ZnO and ZnO@KANT, respectively. These values indicate that ZnO@KANT is better than naked ZnO, but both adsorbents don't have a high adsorption capacity.

In contrast, Langmuir isotherm better fits for MONT, KANT and ZnO@MONT adsorbents. For these adsorbents,  $R^2$  values in the Langmuir model graphs are higher than those for the Freundlich isotherm, which indicates a better linearity in the Langmuir graphs.  $Q_0$  values are 125, 7.39 and 71.9 mg/g for MONT, KANT and ZnO@MONT, respectively. From these results, MONT can be considered the best adsorbent as it has the maximum adsorption capacity.

### **3.2.7 Kinetic of TC Adsorption**

In general, Kinetic study is applied to determine the optimum operating conditions and the rate determining step (Meroufel et al., 2013). In this work, the mechanism of TC adsorption on ZnO, MONT, KANT, ZnO@MONT and ZnO@KANT was determined using three kinetic models; the pseudo-first-order model, the pseudo second order and the intra-particle diffusion model.

In order to check the applicability of these models, linear plots of  $\log(q_e - q_t)$  versus  $t$  were used to check the suitability of the pseudo-first-order model, Figures (3.51-3.55).

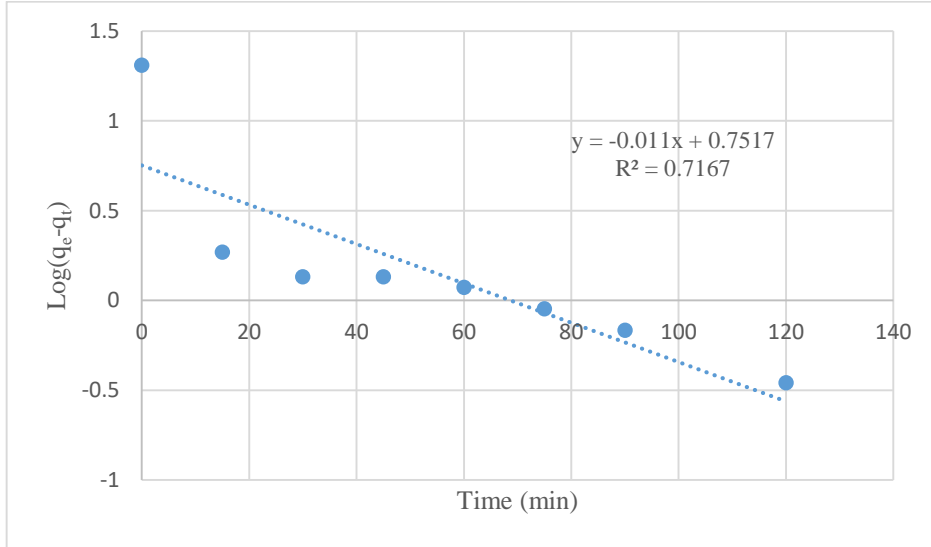


**Figure 3.51:** Kinetics of TC adsorption onto ZnO adsorbent according to pseudo-first-order model at (initial concentration:100 mg/L, contact time:150 min, natural pH, room temperature and solid/liquid ratio: 0.1g/50 mL).

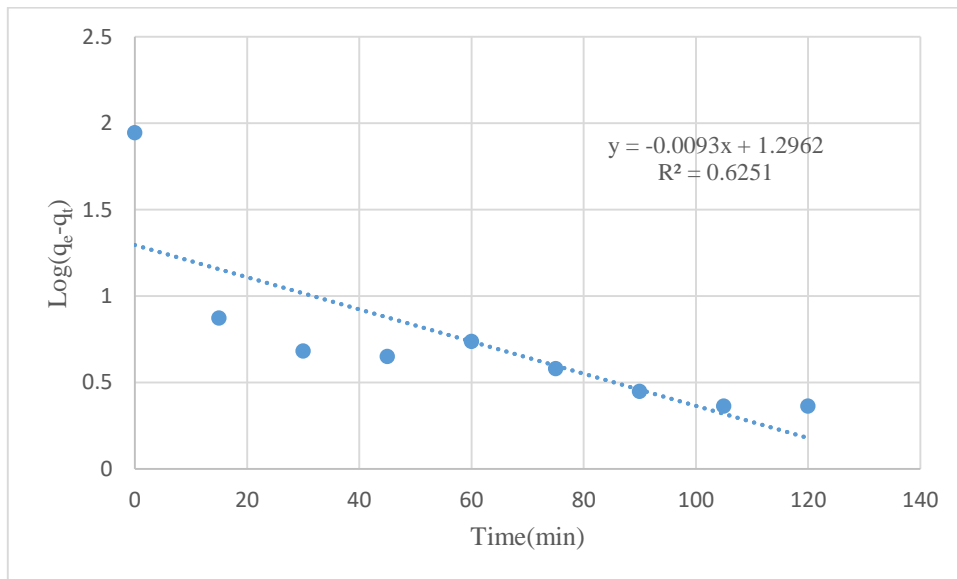


**Figure 3.52:** Kinetics of TC adsorption onto MONT adsorbent according to pseudo-first-order model at (initial concentration: 200 mg/L, contact time: 180 min, natural pH, room temperature and solid/liquid ratio: 0.1g/50 mL).

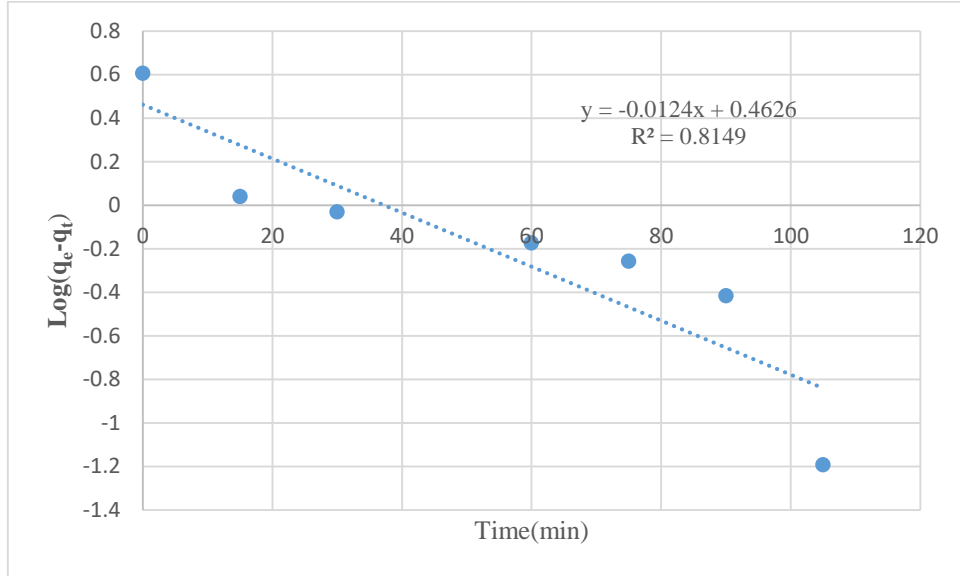


**Figure 3.53:** Kinetics of TC adsorption onto KANT adsorbent according to pseudo-first-order model at (initial concentration: 100 mg/L, contact time: 150 min, natural pH, room temperature and solid/liquid ratio: 0.1g/50 mL).

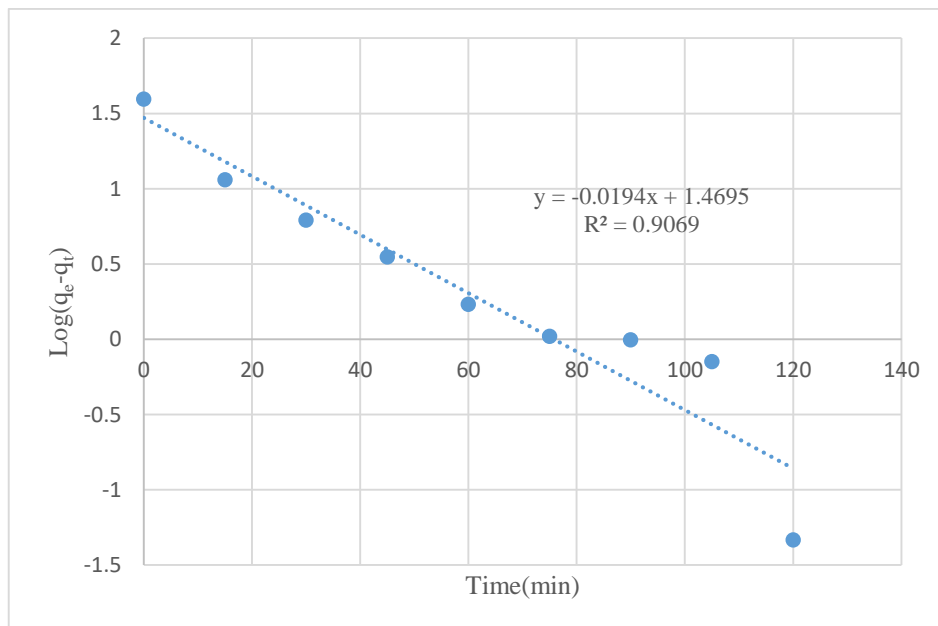


**Figure 3.54:** Kinetics of TC adsorption onto ZnO@MONT adsorbent according to pseudo-first-order model at (initial concentration: 100 mg/L, contact time: 180 min, natural pH, room temperature and solid/liquid ratio: 0.1g/50 mL).

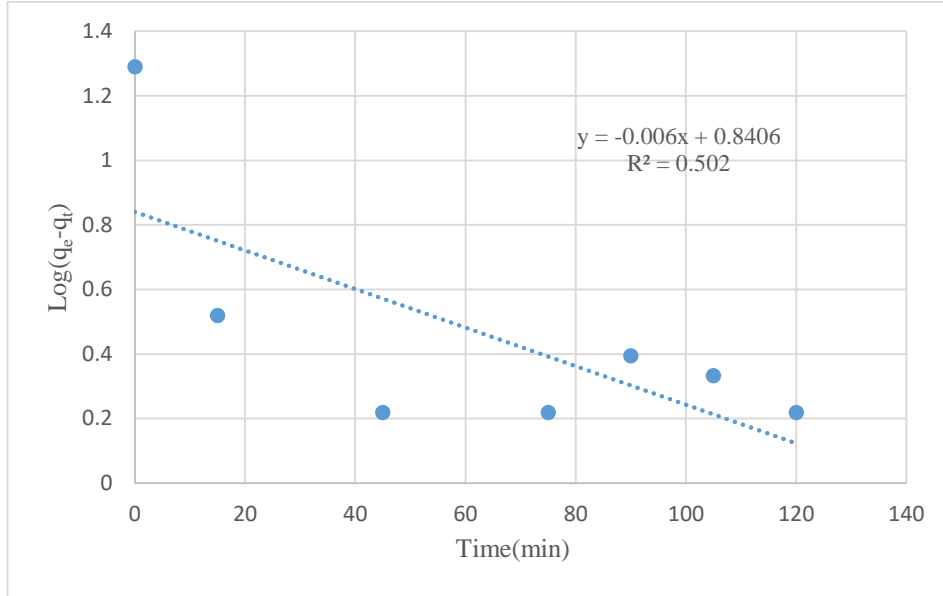


**Figure 3.55:** Kinetics of TC adsorption onto ZnO@KANT adsorbent according to pseudo-first-order model at (initial concentration: 100 mg/L, contact time: 180 min, natural pH, room temperature and solid/liquid ratio: 0.1g/50 mL).

For the pseudo-second-order model, ( $t/q_t$ ) values were plotted versus ( $t$ ), Figures (3.56-3.60).

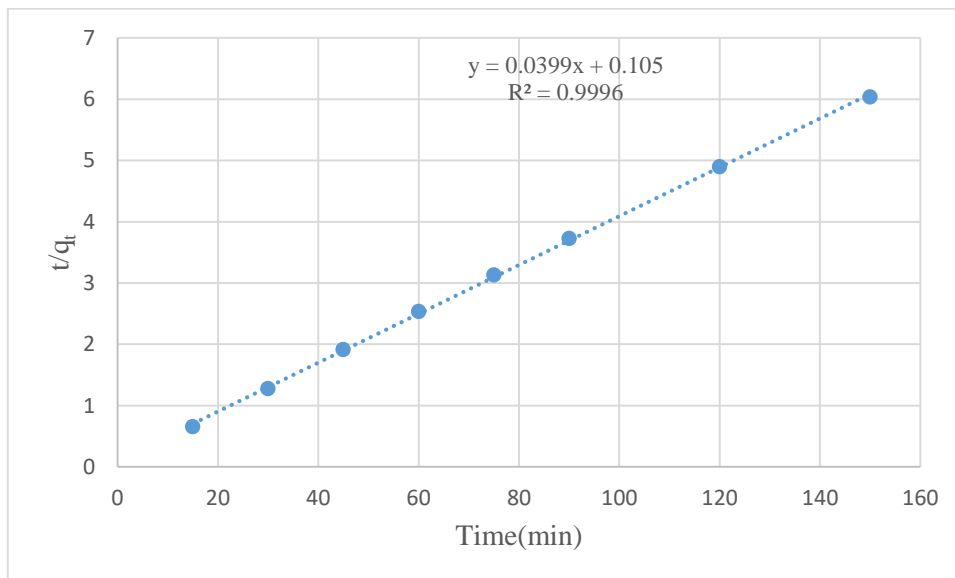


**Figure 3.56:** Kinetics of TC adsorption onto ZnO adsorbent according to pseudo-second-order model at (initial concentration: 100 mg/L, contact time: 150 min, natural pH, room temperature and solid/liquid ratio: 0.1g/50 mL).

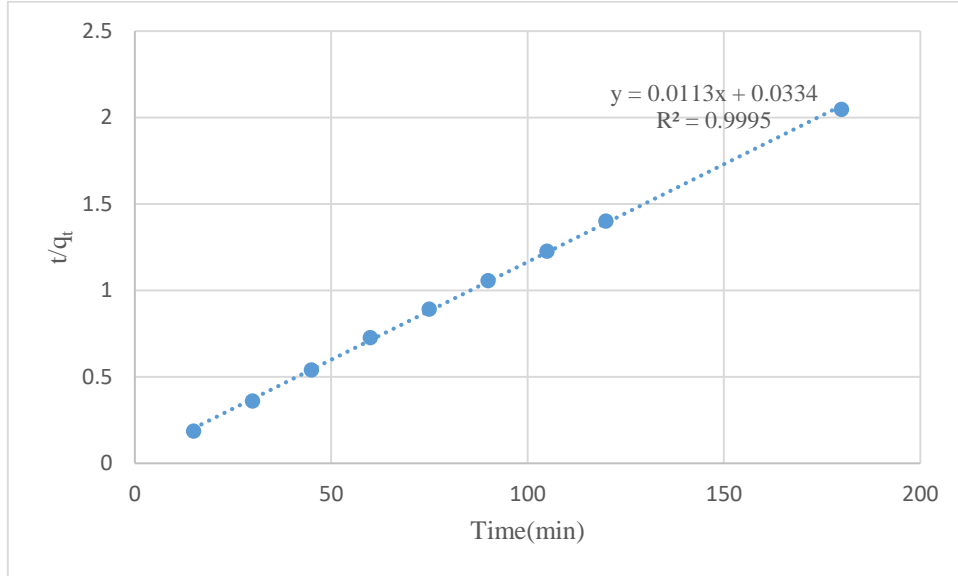


**Figure 3.57:** Kinetics of TC adsorption onto MONT adsorbent according to pseudo-second-order model at (initial concentration: 200 mg/L, contact time: 180 min, natural pH, room temperature and solid/liquid ratio: 0.1g/50 mL).

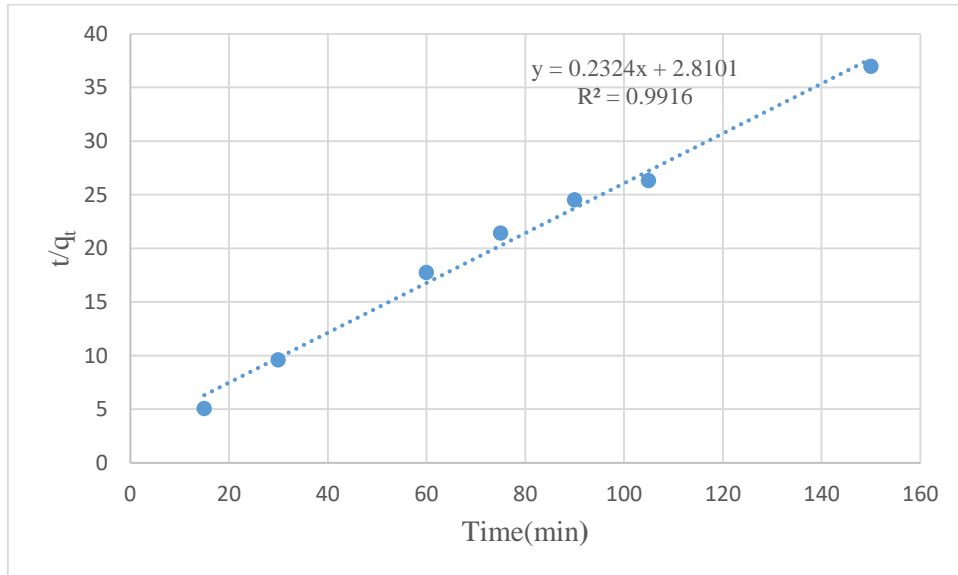


**Figure 3.58:** Kinetics of TC adsorption onto KANT adsorbent according to pseudo-second-order model at (initial concentration: 100 mg/L, contact time: 150 min, natural pH, room temperature and solid/liquid ratio: 0.1g/50 mL).

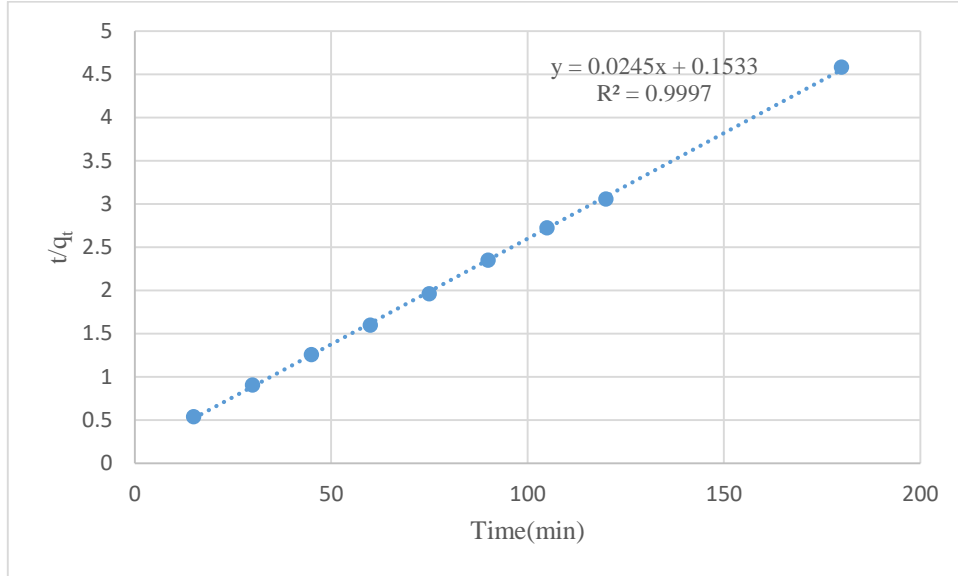


**Figure 3.59:** Kinetics of TC adsorption onto ZnO@MONT adsorbent according to pseudo-second-order model at (initial concentration: 100 mg/L, contact time: 180 min, natural pH, room temperature and solid/liquid ratio: 0.1g/50 mL).

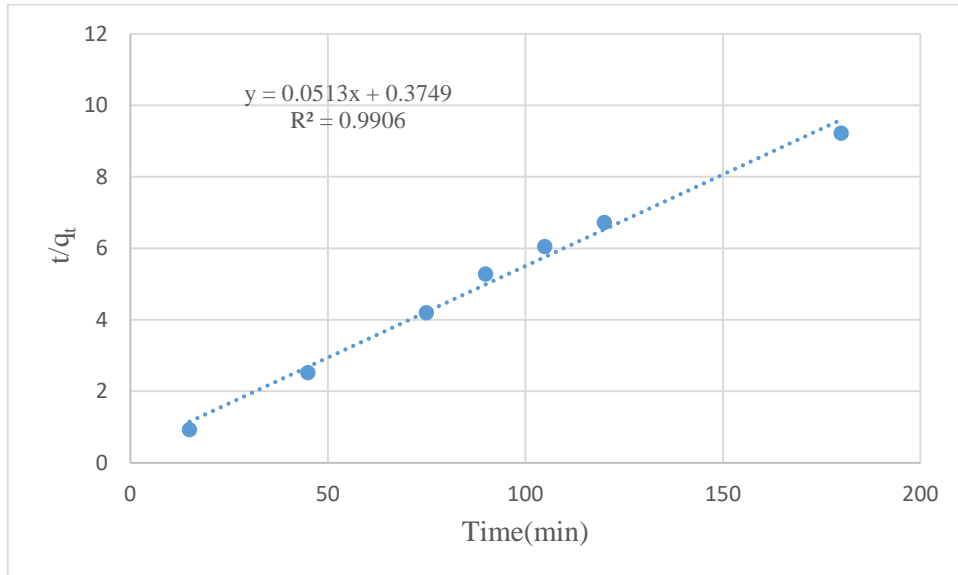


**Figure 3.60:** Kinetics of TC adsorption onto ZnO@KANT adsorbent according to pseudo-second-order model at (initial concentration: 100 mg/L, contact time: 180 min, natural pH, room temperature and solid/liquid ratio: 0.1g/50 mL).

For the intra-particle diffusion model, ( $q_t$ ) values were plotted against ( $t^{1/2}$ ) was used, Figures (3.61-3.65).

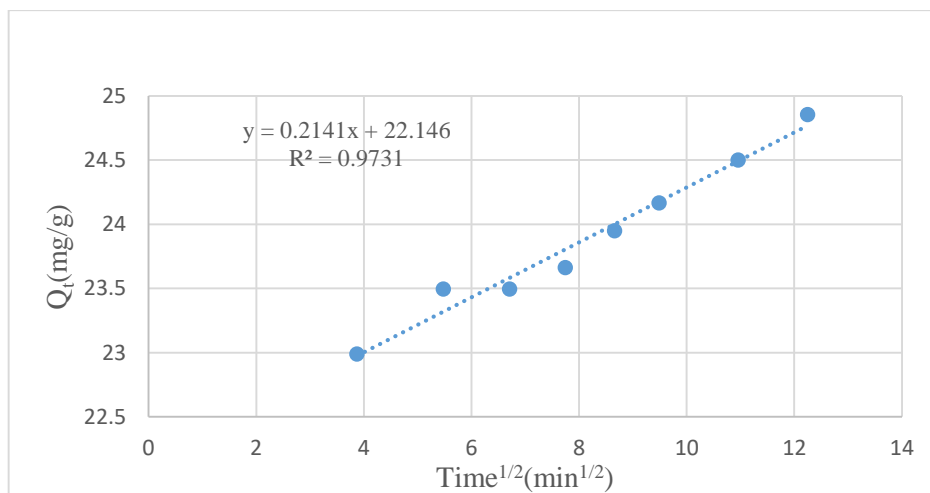


**Figure 3.61:** Kinetics of TC adsorption by ZnO adsorbent according to the intra-particle diffusion model at (initial concentration: 100 mg/L, contact time: 150 min, natural pH, room temperature and solid/liquid ratio: 0.1g/50 mL).

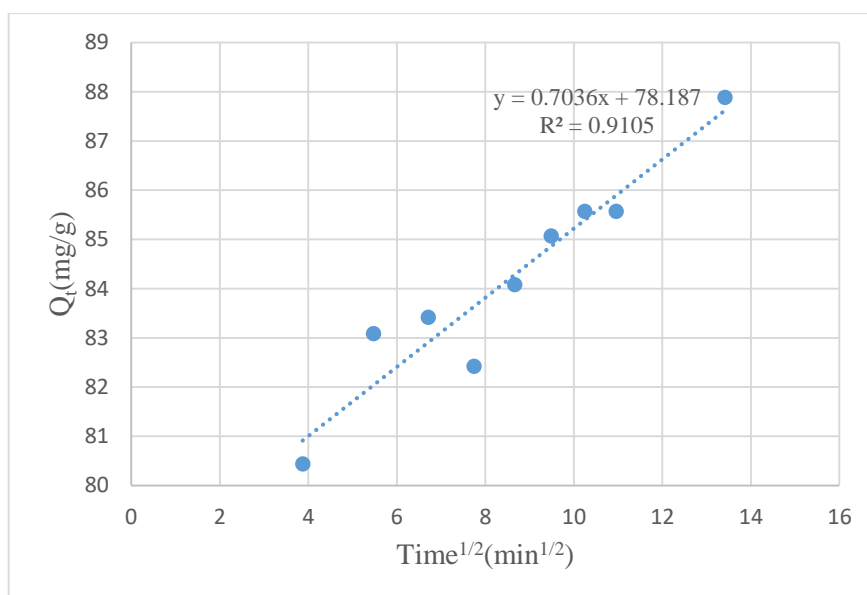


**Figure 3.62:** Kinetics of TC adsorption by MONT adsorbent according to the intra-particle diffusion model at (initial concentration: 200 mg/L, contact time: 180 min, natural pH, room temperature and solid/liquid ratio: 0.1g/50 mL).

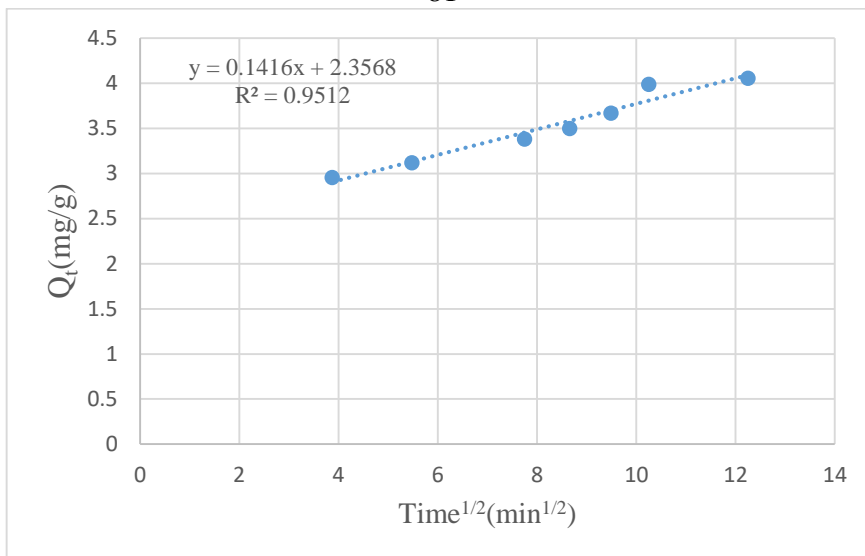


**Figure 3.63:** Kinetics of TC removal by KANT adsorbent according to the intra-particle diffusion model at (initial concentration: 100 mg/L, contact time: 150 min, natural pH, room temperature and solid/liquid ratio: 0.1g/50 mL).

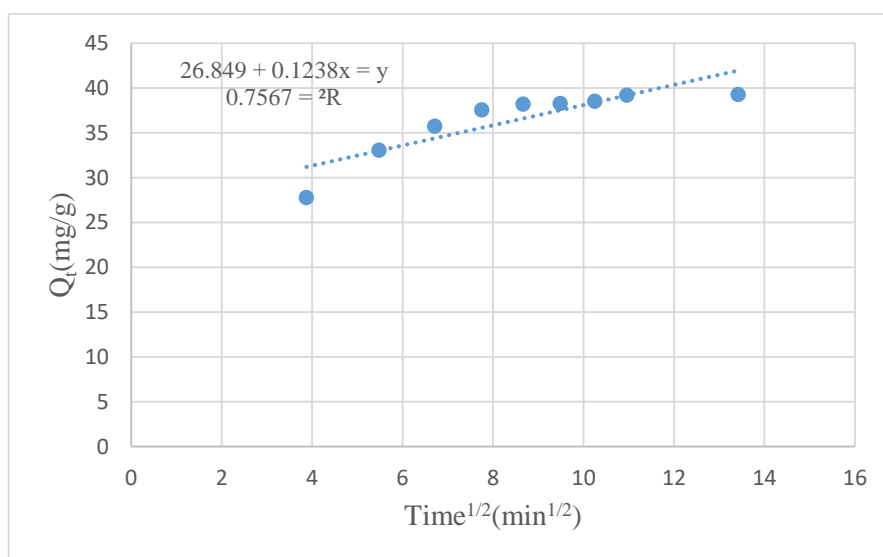


**Figure 3.64:** Kinetics of TC adsorption by ZnO@MONT adsorbent according to the intra-particle diffusion model at (initial concentration: 100 mg/L, contact time: 180 min, natural pH, room temperature and solid/liquid ratio: 0.1g/50 mL).

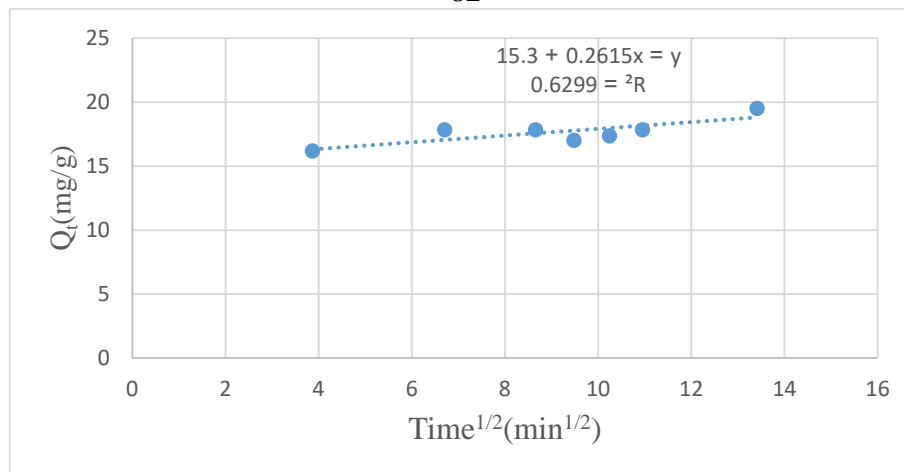


**Figure 3.65:** Kinetics of TC adsorption onto ZnO@KANT composite adsorbent according to the intra-particle diffusion model at (initial concentration: 100 mg/L, contact time: 180 min, natural pH, room temperature and solid/liquid ratio: 0.1g/50 mL).

The correlation coefficients and parameters are shown in table 3.3 for the pseudo first order and the second order model. For the intra particle diffusion model, results are presented in table 3.4.

**Table 3.3: Pseudo-first-order and pseudo-second-order kinetic model parameters and correlation coefficients for TC adsorption onto different adsorbents.**

Adsorbent	$q_e(\text{exp})$ (mg/g)	Pseudo-first-order model			Pseudo-second-order model		
		$K_1$ ( $\text{min}^{-1}$ ) ( $10^2$ )	$q_e$ (calc) (mg/g)	$R^2$	$K_2$ (g/mg min) ( $10^3$ )	$q_e$ (calc) (mg/g)	$R^2$
ZnO	24.85	2.53	5.6437	0.7167	15.16	25	0.9996
MONT	87.88	2.141	19.7788	0.6251	3.8	88.495	0.9995
KANT	4.0553	2.8	2.901	0.8149	19.21	4.302	0.9916
ZnO@MONT	39.26	4.4	29.47	0.9069	3.915	40.816	0.9997
ZnO@KANT	19.511	1.38	6.927	0.502	7.019	19.493	0.9906

Table 3.3 shows that the pseudo second order model is more suitable for describing adsorption mechanism on each adsorbent. By comparing the correlation coefficients for the two models, we can see that the  $R^2$  values are

closer to 1 in pseudo second order. In contrast, the correlation coefficients of all the adsorbents in the pseudo first order are low which means that there is no good linearity in the plot. In addition, in the pseudo second order model, the  $q_e$  (calc) values for each adsorbent is very close to the experimental one. On the other hand, there is a clear distance between the  $q_e$  (calc) and  $q_e$  (exp) in the pseudo first order model. This confirms that the pseudo second order model is more suitable to successfully describe the mechanism of TC adsorption on the different adsorbents used in this study. In conclusion, this adsorption depends on the adsorbent and adsorbate chemical properties. In other words, there is a chemisorption relation between TC and the solid adsorbents.

**Table 3.4: Intra-particle diffusion kinetic model parameters and correlation coefficients for TC adsorption onto different adsorbents.**

Adsorbent	$K_p(\text{mg/g min}^{1/2})$	C	$R^2$
ZnO	0.2141	22.146	0.9731
MONT	0.7036	78.187	0.9105
KANT	0.1416	2.3568	0.9512
ZnO@MONT	1.1238	26.849	0.7567
ZnO@KANT	0.2615	15.3	0.6299

Table 3.4 summarizes correlation coefficients,  $K_p$  values and the y-intercept for TC adsorption according to intra-particle diffusion model.

Figures (3.51-3.55) show that the straight line does not pass via the origin, this means that the rate is limited by mass transfer across the boundary layer.

### 3.3 Adsorption capacity

Adsorption capacity of several adsorbents were calculated at different pH, using the following equation:

$$q_e = \%R \times C_o \times V \div W \quad (3.1)$$

where  $q_e$  (mg/g) is the maximum adsorbed amount of the adsorbate at equilibrium per unit mass of adsorbent (adsorption capacity),  $\%R$  is the percentage of removed amount,  $C_o$  (mg/L) is the initial concentration of the adsorbate,  $V$  (L) is the volume of the solution and  $W$  (g) is the weight of the adsorbent.

**Table 3.5: Adsorption capacity of different solid systems in mg/g at different pH values.**

Solid system TC concentration, mg/L	pH				
	3	5	7	9	11
ZnO 100 mg/L	2.13 mg/g	26.3 mg/g	29.115 mg/g	2.96 mg/g	5.13 mg/g
MONT 100 mg/L	34.9 mg/g	50 mg/g	39.45 mg/g	29.05 mg/g	21.33 mg/g
MONT 200 mg/L	60.5 mg/g	74 mg/g	62.6 mg/g	50.33 mg/g	12 mg/g
KANT 100 mg/L	2.7 mg/g	2.1 mg/g	8.25 mg/g	3.75 mg/g	2.1 mg/g
ZnO@MONT 100 mg/L	35.045 mg/g	39.545 mg/g	31.6 mg/g	25.05 mg/g	10.245 mg/g
ZnO@KANT 100 mg/L	4.75 mg/g	26.8 mg/g	27.46 mg/g	4.75 mg/g	4.25 mg/g

By comparing the results, the maximum adsorption capacity was for MONT with initial concentration of 200 mg/L, at pH 5. This emphasizes that MONT is the best choice for TC adsorption.

## Conclusions

1. Among the different solids studied, Montmorillonite (MONT) clay was the best adsorbent for TC removal compared with the other adsorbents.
2. Zero charge point (ZCP) for ZnO, MONT, KANT, ZnO@MONT and ZnO@KANT was determined (9.8, 4.5, 7.5, 7.2 and 7.2, respectively) using pH drift method.
3. Surface area for ZnO, MONT, KANT, ZnO@MONT and ZnO@KANT was measured using BET method and found to be 27, 330, 34, 310 and 35 m<sup>2</sup>/g, respectively.
4. Adsorption of TC on each adsorbent was affected by solution pH, surface charge of TC and surface charge of the adsorbent (ZCP), the opposite charges cause a higher adsorption.
5. The optimal pH value was ~7 for ZnO, KANT and ZnO@KANT, and ~5 for MONT and ZnO@MONT adsorbents.
6. Experimental data showed that increasing in TC concentration causes increase in the amount of its removal by different adsorbents.
7. Experimental data showed that equilibrium time of TC adsorption by any adsorbent can be taken after ~120 min.
8. Kinetic study showed that the pseudo-second-order model is more suitable for describing adsorption mechanism on each adsorbent.

9. Adsorption of TC on ZnO and ZnO@KANT followed Freundlich isotherm, while MONT, KANT and ZnO@MONT followed Langmuir isotherm.
10. MONT had the maximum adsorption capacity (125 mg/g) compared to others, so it is considered the best adsorbent.

## **Recommendations for future work**

1. Application of the optimum conditions of TC adsorption on photo-degradation process by adsorbents used in this work.
2. Using zero charge point values for the different adsorbents (ZnO, MONT, KANT, ZnO@MONT and ZnO@KANT) as a references in removal of other pollutants by adsorption and photo-degradation.
3. Studying the effect of pH on TC adsorption using smaller pH scale.
4. Studying the effect of other factors that may affect the TC adsorption, such as: temperature, ionic strength and adsorbent concentration.
5. Studying of the possibility of recovery and reuse of the adsorbents and effect of that on their activity.
6. More characterization of adsorbents as measuring their porosity and using atomic absorption spectroscopy for performing their elemental analysis.
7. Applying kinetic data on other adsorption kinetic models like: Pseudo n order model for n different from zero, First-order reversible reaction model and Elovich model.

## References

- Appel, C., Ma, L. Q., Rhue, R. D., & Kennelley, E. (2003). *Point of zero charge determination in soils and minerals via traditional methods and detection of electroacoustic mobility*. *Geoderma*, 113(1-2), 77-93.
- Arefi, M. R., & Rezaei-Zarchi, S. (2012). *Synthesis of zinc oxide nanoparticles and their effect on the compressive strength and setting time of self-compacted concrete paste as cementitious composites*. *International journal of molecular sciences*, 13(4), 4340-4350.
- Banerjee, S., & Chattopadhyaya, M. (2017). *Adsorption characteristics for the removal of a toxic dye, tartrazine from aqueous solutions by a low cost agricultural by-product*. *Arabian Journal of Chemistry*, 10, S1629-S1638.
- Bangari, R. S., & Sinha, N. (2019). *Adsorption of tetracycline, ofloxacin and cephalixin antibiotics on boron nitride nanosheets from aqueous solution*. *Journal of Molecular Liquids*, 293, 111376.
- Bhatia, P., & Nath, M. (2020). *Green synthesis of p-NiO/n-ZnO nanocomposites: Excellent adsorbent for removal of congo red and efficient catalyst for reduction of 4-nitrophenol present in wastewater*. *Journal of Water Process Engineering*, 33, 101017.
- Bushra, R., Ahmed, A., & Shahadat, M. (2016). *Mechanism of adsorption on nanomaterials*. In *Advanced Environmental Analysis* (pp. 90-111).

- Choi, A. E. S., Roces, S., Dugos, N., & Wan, M.-W. (2017). *Adsorption of benzothiophene sulfone over clay mineral adsorbents in the frame of oxidative desulfurization*. **Fuel**, 205, 153-160.
- Chopra, I., & Roberts, M. (2001). *Tetracycline antibiotics: mode of action, applications, molecular biology, and epidemiology of bacterial resistance*. **Microbiol. Mol. Biol. Rev.**, 65(2), 232-260.
- Sridev, K. R. (2009). *Synthesis and Optical Characteristics of ZnO Nanocrystals*. **Bulletin of Material Science**, 32, 165-168.
- Dąbrowski, A., & science, i. (2001). *Adsorption—from theory to practice*. **Advances in colloid**, 93(1-3), 135-224.
- Danner, M.-C., Robertson, A., Behrends, V., & Reiss, J. (2019). *Antibiotic pollution in surface fresh waters: occurrence and effects*. **Science of The Total Environment**.
- de Sá, A., Abreu, A. S., Moura, I., & Machado, A. V. (2017). *Polymeric materials for metal sorption from hydric resources*. In **Water purification** (pp. 289-322): Elsevier.
- Djurišić, A. B., Chen, X., Leung, Y. H., & Ng, A. M. C. (2012). *ZnO nanostructures: growth, properties and applications*. **Journal of Materials Chemistry**, 22(14), 6526-6535.
- Nguta, J. M. (2014). **TETRACYCLINES**. **Pharmacology/Toxicology**.

- Duarte-Silva, R., Villa-García, M., Rendueles, M., & Díaz, M. (2014). *Structural, textural and protein adsorption properties of kaolinite and surface modified kaolinite adsorbents*. **Applied Clay Science**, 90, 73-80.
- Dumont, F., Warlus, J., Watillon, A., & science, i. (1990). *Influence of the point of zero charge of titanium dioxide hydrosols on the ionic adsorption sequences*. **Journal of colloid**, 138(2), 543-554.
- Fatimah, I., Wang, S., & Wulandari, D. (2011). *ZnO/montmorillonite for photocatalytic and photochemical degradation of methylene blue*. **Applied Clay Science**, 53(4), 553-560.
- Gatabi, M. P., Moghaddam, H. M., & Ghorbani, M. (2016). *Point of zero charge of maghemite decorated multiwalled carbon nanotubes fabricated by chemical precipitation method*. **Journal of Molecular Liquids**, 216, 117-125.
- Guo, B., Jiang, J., Serem, W., Sharma, V. K., & Ma, X. (2019). *Attachment of cerium oxide nanoparticles of different surface charges to kaolinite: Molecular and atomic mechanisms*. **Environmental research**, 177, 108645.
- Guo, X., Mu, Q., Zhong, H., Li, P., Zhang, C., Wei, D., & Zhao, T. (2019). *Rapid removal of tetracycline by *Myriophyllum aquaticum*: Evaluation of the role and mechanisms of adsorption*. **Environmental Pollution**, 254, 113101.

- Han, T., Liang, Y., Wu, Z., Zhang, L., Liu, Z., Li, Q., . . . Pan, F. J. J. o. h. m. (2019). **Effects of tetracycline on growth, oxidative stress response, and metabolite pattern of ryegrass.** *380*, 120885.
- Hocaoglu, S., Wakui, Y., & Suzuki, T. (2019). *Separation of arsenic (V) by composite adsorbents of metal oxide nanoparticles immobilized on silica flakes and use of adsorbent coated alumina tubes as an alternative method.* **Journal of water process engineering**, *27*, 134-142.
- <http://www.zzm.umcs.lublin.pl/Wyklad/FGF-Ang/4A.F.G.F.Ads.S-G.%20Interface.pdf>.
- [https://nptel.ac.in/content/storage2/courses/103104045/pdf\\_version/lecture25.pdf](https://nptel.ac.in/content/storage2/courses/103104045/pdf_version/lecture25.pdf).
- [https://shodhganga.inflibnet.ac.in/bitstream/10603/22665/8/08\\_chapter3.pdf](https://shodhganga.inflibnet.ac.in/bitstream/10603/22665/8/08_chapter3.pdf).
- [https://www.researchgate.net/figure/Structure-of-graphene-oxide-a-Structure-of-tetracycline-and-pKa-values-b\\_fig22\\_259155862](https://www.researchgate.net/figure/Structure-of-graphene-oxide-a-Structure-of-tetracycline-and-pKa-values-b_fig22_259155862).
- [https://www.scripps.edu/baran/images/grpmtgpdf/Lin\\_Mar\\_05revised.pdf](https://www.scripps.edu/baran/images/grpmtgpdf/Lin_Mar_05revised.pdf).
- [https://www.srs.fs.usda.gov/pubs/ja/ja\\_barton002.pdf](https://www.srs.fs.usda.gov/pubs/ja/ja_barton002.pdf).
- Hu, Y., Zhu, Y., Zhang, Y., Lin, T., Zeng, G., Zhang, S., . . . Long, H. (2019). *An efficient adsorbent: Simultaneous activated and magnetic ZnO doped biochar derived from camphor leaves for ciprofloxacin adsorption.* **Bioresource technology**, *288*, 121511.

- Isah, M., Asraf, M. H., Malek, N. A. N. N., Jemon, K., Sani, N. S., Muhammad, M. S., . . . Saidin, M. A. R. (2019). *Preparation and characterization of chlorhexidine modified zinc-kaolinite and its antibacterial activity against bacteria isolated from water vending machine*. **Journal of Environmental Chemical Engineering**, 103545.
- Jemutai-Kimosop, S., Orata, F., Shikuku, V. O., Okello, V. A., & Getenga, Z. M. (2020). *Insights on adsorption of carbamazepine onto iron oxide modified diatomaceous earth: Kinetics, isotherms, thermodynamics, and mechanisms*. **Environmental research**, 180, 108898.
- K. Fytianos, E. V. a. E. K. (2000). *Sorption–desorption behavior of 2, 4-dichlorophenol by marine sediments*. **Chemosphere**, 40, 3-6.
- Kamaraj, M., Srinivasan, N., Assefa, G., Adugna, A. T., Kebede, M., & Innovation. (2020). *Facile development of sunlit ZnO nanoparticles-activated carbon hybrid from pernicious weed as an operative nano-adsorbent for removal of methylene blue and chromium from aqueous solution: Extended application in tannery industrial wastewater*. **Environmental Technology**, 17, 100540.
- Kamaraj, M., Srinivasan, N., Assefa, G., Adugna, A. T., Kebede, M., & Innovation. (2020). *Facile development of sunlit ZnO nanoparticles-activated carbon hybrid from pernicious weed as an operative nano-adsorbent for removal of methylene blue and chromium from*

*aqueous solution: Extended application in tannery industrial wastewater. Environmental Technology, 17, 100540.*

- Kang, S., Zhao, Y., Wang, W., Zhang, T., Chen, T., Yi, H., . . . Song, S. (2018). *Removal of methylene blue from water with montmorillonite nanosheets/chitosan hydrogels as adsorbent. Applied Surface Science, 448, 203-211.*
- Kenane, A., Galca, A.-C., Matei, E., Yahyaoui, A., Hachemaoui, A., Benkouider, A. M., . . . Rasoga, O. (2020). *Synthesis and characterization of conducting aniline and o-anisidine nanocomposites based on montmorillonite modified clay. Applied Clay Science, 184, 105395.*
- Khan, T. A., Dahiya, S., & Ali, I. (2012). *Use of kaolinite as adsorbent: Equilibrium, dynamics and thermodynamic studies on the adsorption of Rhodamine B from aqueous solution. Applied Clay Science, 69, 58-66.*
- Kłosek-Wawrzyn, E., Małolepszy, J., & Murzyn, P. (2013). *Sintering behavior of kaolin with calcite. Procedia Engineering, 57, 572-582.*
- Kong, Y., Zhuang, Y., Han, K., Shi, B., Physicochemical, S. A., & Aspects, E. (2020). *Enhanced tetracycline adsorption using alginate-graphene-ZIF67 aerogel. Colloids, 588, 124360.*
- Kragović, M. M., Stojmenović, M., Petrović, J. T., Loredó, J., Pašalić, S., Nedeljković, A., & Ristović, I. (2019). *Influence of Alginate Encapsulation on Point of Zero Charge (pHpzc) and Thermodynamic*

*Properties of the Natural and Fe (III)-Modified Zeolite. Procedia Manufacturing, 32, 286-293.*

- Kumar, A., & Lingfa, P. (2019). *Sodium bentonite and kaolin clays: Comparative study on their FT-IR, XRF, and XRD. Materials Today: Proceedings.*
- KutlÁková, K. M., Tokarský, J., & Peikertová, P. (2015). *Functional and eco-friendly nanocomposite kaolinite/ZnO with high photocatalytic activity. Applied Catalysis B: Environmental, 162, 392-400.*
- Lazaratou, C., Vayenas, D., & Papoulis, D. (2019). *The role of clays, clay minerals and clay-based materials for nitrate removal from water systems: A review. Applied Clay Science, 105377.*
- Li, X., & Yang, H. (2014). *Pd hybridizing ZnO/kaolinite nanocomposites: Synthesis, microstructure, and enhanced photocatalytic property. Applied Clay Science, 100, 43-49.*
- Li, Z., Schulz, L., Ackley, C., Fenske, N., & science, i. (2010). *Adsorption of tetracycline on kaolinite with pH-dependent surface charges. Journal of colloid, 351(1), 254-260.*
- Liu, C.-X., Xu, Q.-M., Yu, S.-C., Cheng, J.-S., & Yuan, Y.-J. (2020). *Bio-removal of tetracycline antibiotics under the consortium with probiotics Bacillus clausii T and Bacillus amyloliquefaciens producing biosurfactants. Science of The Total Environment, 710, 136329.*

- Liu, J., Zhou, B., Zhang, H., Ma, J., Mu, B., & Zhang, W. (2019). ***A novel Biochar modified by Chitosan-Fe/S for tetracycline adsorption and studies on site energy distribution.*** *Bioresource technology*, 294, 122152.
- Liu, L., Luo, X.-B., Ding, L., & Luo, S.-L. (2019). ***Application of nanotechnology in the removal of heavy metal from water.*** In ***Nanomaterials for the Removal of Pollutants and Resource Reutilization*** (pp. 83-147): Elsevier.
- Liu, X., Huang, D., Lai, C., Zeng, G., Qin, L., Zhang, C., . . . Liu, S. (2018). ***Recent advances in sensors for tetracycline antibiotics and their applications.*** *TrAC Trends in Analytical Chemistry*, 109, 260-274.
- Lu, F. H. a. G. (1998). ***Adsorption characteristics of phenolic compounds onto coal-reject-derived adsorbents.*** *Energy Fuels*, 12, 1100-1107.
- Lv, G., Li, Z., Elliott, L., Schmidt, M. J., MacWilliams, M. P., & Zhang, B. (2019). ***Impact of tetracycline-clay interactions on bacterial growth.*** *Journal of Hazardous Materials*, 370, 91-97.
- Maged, A., Iqbal, J., Kharbish, S., Ismael, I. S., & Bhatnagar, A. (2020). ***Tuning tetracycline removal from aqueous solution onto activated 2: 1 layered clay mineral: characterization, sorption and mechanistic studies.*** *Journal of Hazardous Materials*, 384, 121320.
- Meroufel, B., Benali, O., Benyahia, M., Benmoussa, Y., & Zenasni, M. (2013). ***Adsorptive removal of anionic dye from aqueous solutions by***

- Algerian kaolin: Characteristics, isotherm, kinetic and thermodynamic studies. J. Mater. Environ. Sci*, 4(3), 482-491.
- Mohammed, A. A., & Kareem, S. L. (2019). *Adsorption of tetracycline fom wastewater by using Pistachio shell coated with ZnO nanoparticles: Equilibrium, kinetic and isotherm studies. Alexandria Engineering Journal*, 58(3), 917-928.
  - Mohammed, B. B., Yamni, K., Tijani, N., Alrashdi, A. A., Zouihri, H., Dehmani, Y., . . . Lgaz, H. (2019). *Adsorptive removal of phenol using faujasite-type Y zeolite: Adsorption isotherms, kinetics and grand canonical Monte Carlo simulation studies. Journal of Molecular Liquids*, 296, 111997.
  - Mu, T.-H., & Sun, H.-N. (2019). *Sweet Potato Leaf Polyphenols: Preparation, Individual Phenolic Compound Composition and Antioxidant Activity. In Polyphenols in Plants* (pp. 365-380): Elsevier.
  - Murray, H. H. (1991). *Overview—clay mineral applications. Applied Clay Science*, 5(5-6), 379-395.
  - Murray, H. H. (2006). *Structure and composition of the clay minerals and their physical and chemical properties. Developments in clay science*, 2, 7-31.
  - Nguyen, F., Starosta, A. L., Arenz, S., Sohmen, D., Dönhöfer, A., & Wilson, D. N. (2014). *Tetracycline antibiotics and resistance mechanisms. Biological chemistry*, 395(5), 559-575.

- Parolo, M., Avena, M., Pettinari, G., Zajonkovsky, I., Valles, J., & Baschini, M. (2010). *Antimicrobial properties of tetracycline and minocycline-montmorillonites*. **Applied Clay Science**, 49(3), 194-199.
- Parsa, P., Paydayesh, A., & Davachi, S. M. (2019). *Investigating the effect of tetracycline addition on nanocomposite hydrogels based on polyvinyl alcohol and chitosan nanoparticles for specific medical applications*. **International journal of biological macromolecules**, 121, 1061-1069.
- Pasquale, T. R., & Tan, J. S. (2005). *Nonantimicrobial effects of antibacterial agents*. **Clinical infectious diseases**, 40(1), 127-135.
- Prasad, M., Reid, K., & Murray, H. (1991). *Kaolin: processing, properties and applications*. **Applied Clay Science**, 6(2), 87-119.
- Qiu, H., Lv, L., Pan, B.-c., Zhang, Q.-j., Zhang, W.-m., & Zhang, Q.-x. (2009). *Critical review in adsorption kinetic models*. **Journal of Zhejiang University-Science A**, 10(5), 716-724.
- Rocky, K. A., Islam, M. A., Pal, A., Ghosh, S., Thu, K., & Saha, B. B. (2020). *Experimental investigation of the specific heat capacity of parent materials and composite adsorbents for adsorption heat pumps*. **Applied Thermal Engineering**, 164, 114431.
- Sahu, O., & Singh, N. (2019). *Significance of bioadsorption process on textile industry wastewater*. In **The Impact and Prospects of Green Chemistry for Textile Technology** (pp. 367-416): Elsevier.
- Sani, H. A., Ahmad, M. B., Hussein, M. Z., Ibrahim, N. A., Musa, A., Saleh, T. A., & Protection, E. (2017). *Nanocomposite of ZnO with*

*montmorillonite for removal of lead and copper ions from aqueous solutions. Process Safety, 109, 97-105.*

- Sarma, J., Mahiuddin, S., Physicochemical, S. A., & Aspects, E. (2014). *Specific ion effect on the point of zero charge of  $\alpha$ -alumina and on the adsorption of 3, 4-dihydroxybenzoic acid onto  $\alpha$ -alumina surface. Colloids, 457, 419-424.*
- Silva, D. T., Fonseca, M. G., Borrego-Sánchez, A., Soares, M. F., Viseras, C., Sainz-Díaz, C. I., . . . Materials, M. (2020). *Adsorption of tamoxifen on montmorillonite surface. Microporous, 110012.*
- Silvy, R. P., Lopez, F., Romero, Y., Reyes, E., León, V., & Galiasso, R. (1995). *Influence of titania loading on tungsten adsorption capacity, dispersion, acidic and zero point of charge properties of W/TiO<sub>2</sub>-Al<sub>2</sub>O<sub>3</sub> catalysts. In Studies in Surface Science and Catalysis (Vol. 91, pp. 281-290): Elsevier.*
- Song, C., Liu, H.-Y., Guo, S., & Wang, S.-G. (2020). *Photolysis mechanisms of tetracycline under UV irradiation in simulated aquatic environment surrounding limestone. Chemosphere, 244, 125582.*
- Tu, Y., Ren, L.-F., Lin, Y., Shao, J., He, Y., Gao, X., & Shen, Z. (2020). *Adsorption of antimonite and antimonate from aqueous solution using modified polyacrylonitrile with an ultrahigh percentage of amidoxime groups. Journal of Hazardous Materials, 388, 121997.*
- Turner, W., & Merriman, L. M. (2005). **Clinical Skills in Treating the Foot E-Book: Elsevier Health Sciences.**

- Uriarte, D., Domini, C., & Garrido, M. (2019). *New carbon dots based on glycerol and urea and its application in the determination of tetracycline in urine samples*. **Talanta**, 201, 143-148.
- Vikrant, K., Kim, K.-H., Peng, W., Ge, S., & Ok, Y. S. (2020). *Adsorption performance of standard biochar materials against volatile organic compounds in air: A case study using benzene and methyl ethyl ketone*. **Chemical Engineering Journal**, 387, 123943.
- Villanueva, M. E., Salinas, A., Copello, G. J., Diaz, L. E., & Technology, C. (2014). *Point of zero charge as a factor to control biofilm formation of Pseudomonas aeruginosa in sol-gel derivatized aluminum alloy plates*. **Surface**, 254, 145-150.
- Wang, G., Lian, C., Xi, Y., Sun, Z., Zheng, S., & science, i. (2018). *Evaluation of nonionic surfactant modified montmorillonite as mycotoxins adsorbent for aflatoxin B1 and zearalenone*. **Journal of colloid**, 518, 48-56.
- Wu, M., Zhao, S., Tang, M., Jing, R., Shao, Y., Liu, X., . . . Aspects, E. (2019). *Adsorption of sulfamethoxazole and tetracycline on montmorillonite in single and binary systems*. **Colloids**, 575, 264-270.
- Zhang, X., Lin, X., He, Y., Chen, Y., Luo, X., & Shang, R. (2019). *Study on adsorption of tetracycline by Cu-immobilized alginate adsorbent from water environment*. **International journal of biological macromolecules**, 124, 418-428.
- Zhang, X., Lin, X., He, Y., & Luo, X. (2019). *Phenolic hydroxyl derived copper alginate microspheres as superior adsorbent for*

*effective adsorption of tetracycline. International journal of biological macromolecules*, 136, 445-459.

- Zhao, Z., Nie, T., & Zhou, W. (2019). *Enhanced biochar stabilities and adsorption properties for tetracycline by synthesizing silica-composited biochar. Environmental Pollution*, 254, 113015.
- Zhou, W., Wang, J., He, J., Yang, X., Shi, Y., Wang, X., . . . Aspects, E. (2019). *Adsorption of U (VI) on montmorillonite in the presence of ethylenediaminetetraacetic acid. Colloids*, 583, 123929.
- Zhu, B.-L., Qi, C.-L., Zhang, Y.-H., Bisson, T., Xu, Z., Fan, Y.-J., & Sun, Z.-X. (2019). *Synthesis, characterization and acid-base properties of kaolinite and metal (Fe, Mn, Co) doped kaolinite. Applied Clay Science*, 179, 105138.
- Zhu, R., Chen, Q., Zhou, Q., Xi, Y., Zhu, J., & He, H. (2016). *Adsorbents Based on Montmorillonite for Contaminant Removal from Water: A Review. Applied Clay Science*, 123, 239-258.
- Zyoud, A., Jondi, W., AlDaqqah, N., Asaad, S., Qamhieh, N., Hajamohideen, A., . . . Hilal, H. (2017). *Self-Sensitization of Tetracycline Degradation with Simulated Solar Light Catalyzed by Zno@ Montmorillonite. Solid State Sciences*, 74, 131-143.
- Zyoud, A. H., Saleh, F., Helal, M. H., Shawahna, R., & Hilal, H. S. (2018). *Anthocyanin-Sensitized Tio2 Nanoparticles for Phenazopyridine Photodegradation Under Solar Simulated Light. Journal of Nanomaterials*, 2018.

- Zyoud, A. H., Zubi, A., Zyoud, S. H., Hilal, M. H., Zyoud, S., Qamhieh, N., . . . Hilal, H. S. (2019). *Kaolin-Supported Zno Nanoparticle Catalysts in Self-Sensitized Tetracycline Photodegradation: Zero-Point Charge and Ph Effects*. *Applied Clay Science*, 182, 105294.

جامعة النجاح الوطنية

كلية الدراسات العليا

دراسة امتزاز الملوث تتراسايكلين من الماء  
باستخدام أكسيد الزنك المثبت على السطوح الصلبة  
بطريقة قياس شحنة السطح المتعادلة

إعداد

رولا فتحي محمد طوير

إشراف

أ.د. حكمت هلال

د. عاهد زيود

قدمت هذه الأطروحة استكمالاً لمتطلبات الحصول على درجة الماجستير في الكيمياء بكلية الدراسات العليا في جامعة النجاح الوطنية في نابلس، فلسطين.

2020

ب  
دراسة امتزاز الملوث تتراسايكلين من الماء باستخدام أكسيد الزنك المثبت على السطوح الصلبة  
بطريقة قياس شحنة السطح المتعادلة

إعداد

رولا فتحي محمد طوير

إشراف

أ.د. حكمت هلال

د. عاهد زيود

## المخلص

يشكل تلوث المياه تحديًا صعبًا يواجهه العالم في الوقت الحاضر. وقد يكون سبب هذا التلوث هو مبيدات الآفات والأسمدة الزراعية والتصريف الصناعي والنفايات المنزلية وبقايا الأدوية. يعتبر تلوث المياه السطحية بواسطة المستحضرات الصيدلانية تهديدًا بيئيًا خطيرًا ، مما يجعل إزالتها من المياه قضية حيوية في الأبحاث. وطريقة الامتزاز (عملية بسيطة واقتصادية وآمنة وفعالة ) هي واحدة من أكثر الطرق الشائعة التي تستخدم في معالجة المياه.

في هذا العمل، تمت دراسة امتزاز المضاد الحيوي المستخدم على نطاق واسع وهو (التيتراساكيلين) باستخدام أكسيد الزنك وسطوح المونتموريلونيت والكولينييت، واستخدام أكسيد الزنك المثبت على سطح المونتموريلونيت والكولينييت، وهي مواد منخفضة التكلفة وصديقة للبيئة وفعالة.

وقد تم تثبيت أكسيد الزنك (بحجم النانو) على سطح المونتموريلونيت (وهي أحد الوحول المتوفرة طبيعيًا) ذات مساحة سطح عالية ، والكولينييت (وهي مادة وحل أيضا لها ثبات عال)، لتحسين الامتزاز للتيتراسايكلين وتحسين عملية استخراج أكسيد الزنك من المياه بعد عملية الامتزاز.

وقد تمت دراسة خصائص المواد المستخدمة المحضرة منها والتجارية باستخدام الأشعة السينية والمجهر الإلكتروني الماسح. وتم قياس قيم شحنة النقطة الصفيرية لأكسيد الزنك المثبت على السطوح الصلبة في الوسط المائي بواسطة التغير الحرج لدرجة الحموضة. كما تمت دراسة أثر العوامل المختلفة على عملية الامتزاز، مثل : درجة الحموضة ( 3-11)، ونوع المادة الممتزة، ووقت الخلط، وتركيز مادة التيتراسايكلين الملوثة. كانت نتائج قيم الشحنة الصفيرية كالتالي: 9.8

لأكسيد الزنك، 4.5 للمونتموريلونيت، 7.5 للكولينيت التجاريات، و7.2 للمواد المحضرة (أكسيد الزنك المثبت على سطح المونتموريلونيت، وأكسيد الزنك المثبت على سطح الكولينيت).

أثبتت النتائج التجريبية أن المونتموريلونيت هو أفضل مادة ممتزة من بين المواد التي تم دراستها في هذا البحث، والذي يتبع لنموذج فريندليخ مع سعة امتزاز 125 ملغم/غم في الوسط المائي المتعادل. وتبين أن مادة الكولينيت والمونتموريلونيت المثبت على سطحها مادة أكسيد الزنك تتبع أيضا نموذج فريندليخ. أما مادة أكسيد الزنك والكولينيت المثبت عليها أكسيد الزنك فتتبع نموذج لانجمير.

وأظهرت دراسة الخواص الحركية للمواد الممتزة أنها جميعا تتبع نموذج (الرتبة الثانية الكاذبة). هذا وقد تم قياس وقت الاتزان للامتزاز بعد 120 دقيقة في كافة القياسات. وقد كان الامتزاز الافضل عند درجة الحموضة بين 5 و7 لكافة المواد (حيث يتأثر الامتزاز بقيم الشحنة الصغرية للمادة الممتزة، وشحنة سطح التيتراسايكلين) حيث أن الشحنات المتضادة أنتجت أعلى قيم امتزاز بسبب التجاذب الإلكتروستاتيكي بين الطرفين. وقد أدت زيادة تركيز التيتراسايكلين الملوث إلى زيادة كمية الامتزاز.